THE HONG KONG
POLYTECHNIC UNIVERSITY
香港理工大學
Pao Yue-kong Library
包玉剛圖書館

Copyright Undertaking

This thesis is protected by copyright, with all rights reserved.

By reading and using the thesis, the reader understands and agrees to the following terms:

1. The reader will abide by the rules and legal ordinances governing copyright regarding the use of the thesis.
2. The reader will use the thesis for the purpose of research or private study only and not for distribution or further reproduction or any other purpose.
3. The reader agrees to indemnify and hold the University harmless from and against any loss, damage, cost, liability or expenses arising from copyright infringement or unauthorized usage.

IMPORTANT

If you have reasons to believe that any materials in this thesis are deemed not suitable to be distributed in this form, or a copyright owner having difficulty with the material being included in our database, please contact lbsys@polyu.edu.hk providing details. The Library will look into your claim and consider taking remedial action upon receipt of the written requests.

Pao Yue-kong Library, The Hong Kong Polytechnic University, Hung Hom, Kowloon, Hong Kong

http://www.lib.polyu.edu.hk

MODELLING WOODY VEGETATION IN SUDANO-SAHELIAN ZONE OF NIGERIA USING REMOTE SENSING

MUHAMMAD USMAN

PhD

The Hong Kong Polytechnic University

2018

The Hong Kong Polytechnic University

Department of Land Surveying and Geo-Informatics

Modelling Woody Vegetation in Sudano-Sahelian Zone of Nigeria Using Remote Sensing

Muhammad USMAN

A thesis submitted in partial fulfillment of the

requirements for the degree of Doctor of Philosophy

November 2017

Certification of Originality

I hereby declare that this thesis is my own work and that, to the best of my knowledge and belief, it reproduces no material previously published or written, nor material that has been accepted for the award of any other degree or diploma, except where due acknowledgement has been made in the text.

_____ (Signed)

Muhammad USMAN _____ (Name of Student)

Dedication

To my beloved parents

Abstract

Rural areas surrounding Nigeria's second largest city, Kano, in the northern Nigeria, have some of the highest rural population densities in the world, and these have been increasing rapidly in recent decades, with as yet, no signs of stabilising. The subsistence nature of livelihoods in this semi-arid region bordering the African Sahel zone, where rainfall is known to be highly variable, introduces considerable risk for crop and woody vegetation productivity. A scenario of recent high rural and urban population growth in and around the city of Kano, set in context of predicted temperature increase and greater rainfall variability due to climate change, may give cause for concern. As almost all rural, and the vast majority of urban households still use wood fuel for cooking, lighting and heating (although Nigeria is the world's 6th largest oil producer), a return to the rainfall amounts of the drought decades of the 1970s and 80s could cause widespread economic and social distress. There are many accounts of rainfall trends in the northern Nigeria, many observing severe declines, and others a decline in recent decades followed by a return to normal. Almost all studies report great spatial variation in rainfall amounts and trends, with large differences in nearby areas, or conflicting results for the same regions. Furthermore, these reported statistics appear in many cases to be conflicting with farmers' perceptions of rainfall trends and its effects on their lives and livelihood. This study evaluates the available sources of rainfall data over recent decades in the northern Nigeria, using both climate station data and satellite-based rainfall products, as satellite rainfall variables are spatially superior to point-based ground stations. These rainfall data are first compared with satellite-based vegetation indices NDVI products such as GIMMS 3g and MODIS, extending back several decades to the early 1980s. They are also compared with several satellite-based rainfall products such as ARC, CHIRPS, TARCAT and TRMM, covering the same decades.

The second part of the study evaluates climatic impacts on the rural landscape and thus on the agricultural economy, specifically on farmland trees, which are used by farmers for fuelwood for own use as well as for sale to supplement farm incomes. This part of the study focuses on the "Kano Close Settled Zone", due to

its high rural population density as a case study example for savanna Africa. It evaluates high resolution remotely sensed images for tree inventory and changes in woody biomass, in terms of tree density and species composition, in the intensively farmed parklands surrounding Kano City. The objective is to observe trends in the woody vegetation surrounding Kano City from the 1960s onwards, which may be related to climatic trends.

The last part of the study evaluates the use of Geographic Object Based Image Analysis (GEOBIA) for delineation of tree crown cover in the agroforestry landscape of the Kano Close-Settled Zone (KCSZ) using high resolution WorldView-2 image and modelling of above ground biomass (AGB) using tree crown cover.

Results of the study indicate a recovery of rainfall across northern Nigeria in the past three decades, although not back to 1960s levels. This recovery is observed from both ground station and CHIRPS satellite data, to be due to a longer rainy season, with higher rainfall amounts toward the end of the growing season in August to October. Vegetation indices from AVHRR GIMMS 3g and MODIS satellite products across the West African Sahel and Sudan zones confirm this recovery in terms of increased biomass. To evaluate the impacts of rainfall trends on the rural landscape and economy at local level, trends in farmland tree stocks around Kano, were determined from field data and high resolution images including archived aerial photographs and recent satellite images. Field survey was conducted in 1981 and 2016, and the images covered the 1960s pre-drought period, the 1970s to 80s drought period, and recent period of 2013-15. Contrary to other work on woody vegetation in West Africa, mostly from the Sahel Zone, a substantial increase in tree densities was observed since the 1960s and continuing through the drought decades, with at least a doubling of farmland tree densities at the present time. This observed increase is surprising in view of high population growth and reports of increased temperatures due to global warming. This increase in tree densities around Kano is attributed to continued reliance on wood as the main energy source, by a still rapidly growing population, with a more than doubling of Kano city's population in the 15 years up to the last population census in 2006. This growth would not have been possible without a

parallel increase in the main energy source. Observations of a decline in a wide range of traditional tree species and replacement by fewer fast-growing and drought-tolerant species parallel recent reports from other parts of West Africa.

The overall finding of the study is that trends in farmland tree stocks are less related to long term climatic trends, than to the Nigerian socio-economy, as farmers make decisions about the numbers and species of trees on their farms according to their own domestic needs and from sale of wood. The continued overwhelming dependence on biomass for fuel by a still rapidly growing population across northern Nigeria may be a cause for concern. Return to the drought conditions of previous decades coupled with tree death due to climate change may have serious consequences for rural households for whom the longevity of woody vegetation offers security against rainfall variability and crop failure.

Key Words: *Northern Nigeria, Sudano-Sahelian zone, Woody Biomass, Tree density, Species composition, Rainfall variability, Vegetation trends, Remote Sensing.*

Publications Arising from the Thesis

Journal

Usman, M., Nichol, J.E. (2018). Remarkable increase in tree density and fuelwood production in the croplands of northern Nigeria, ***Land Use Policy***.

Conference

Nichol, J.E. and Usman, M. (2016). Rural energy trends in northern Nigeria: Response to population growth. In: Royal Geographical Society with IBG Annual International Conference 2016. London, United Kingdom, August 30- September 2.

Nichol, J.E., Usman, M., and Wong M. S. (2017). The changing role of trees in the agroforestry landscape of northern Nigeria. In: Royal Geographical Society with IBG Annual International Conference 2017. London, United Kingdom, August 30- September 1.

Acknowledgements

All praises to Almighty Allah, the creator of the universe, who blessed me with the knowledge, and enabled me to complete this thesis. All respects to the Holy Prophet Muhammad (May Allah grant peace and honor to him and his family), who is the last messenger, and whose life is a perfect model for the whole humanity.

I would like to express my highest respect and profound thanks to my supervisor, Prof. Janet E. Nichol, for her kind supervision, patience, correction of drafts, and encouragement throughout my study period. Apart from my research, she also encouraged and trained me to play squash.

I also extend my gratitude to Dr. Man Sing Wong Charles, for being my supervisor the last year of my studies, after Prof. Janet E. Nichol retired. He was always helpful and available for discussion.

I am also thankful to Dr. Luka F. Buba for being my co-supervisor and providing me with climate data from the Nigerian Meterological Agency (NIMET).

I am very grateful to the Head of LSGI, Chair of Departmental Research Committee, and all the faculty members for their support. I am sincerely thankful to the General Office (GO), the Research Office (RO), the Finance Office (FO), and the Student Affair Office (SAO) for their continuous support during the academic period.

I am thankful to The Hong Kong Polytechnic University for awarding funding for a Research Attachment Programme for conducting field survey in Northern Nigeria. Thanks to Prof. Maharazu A. Yusuf, Head of Department of Geography, Bayero University of Kano (BUK), for inviting me as visiting fellow to Nigeria, in order to conduct field survey and collect aerial photographs and climate data from different organizations. Thanks to everyone who helped in Nigeria, the faculty members of department of geography, especially Prof. A.I. Tanko, Dr Salisu Muhammad, Dr Murtala M. Badamasi. I am also truly grateful to Muhammad Zikirullah Aliyu, Incharge of Cartography Lab, who helped me for organizing field trips. I would also acknowledge to Jasper Tomlinson and

Prof. Mike Mortimore (Late) for providing past records of climate and insights about my research. I would also acknowledge Umar Lawal Mashi from KTARDA and Abdul Bashir Bawale from KAZP, Katsina for providing information about past droughts.

I am very grateful to my Pakistani friends in Nigeria, especially families of Mufti Shafique and Dr Furrukh Mahmood for welcoming me and regularly inviting me for lunch and dinner, I had a very good time with Bilal Shafique, Mohsin Shafique, Muhammad Afzal and Saad Furrukh.

A warm gratitude goes to my field assistants in Kano and Daura, Particularly Isa Sani from Centre for Dryland Agriculture and Aliyu Mani from ICRISAT; without their kind help this study was not possible. Special thanks to Dr. Abdulhakim M. Abdi from Lund Univeristy, for providing R scripts for processing and analyzing remote sensing data.

Special thanks to Dr Asma Turadu Ibrhaim and Aminu Tukur Hadiza, my host in the Federal Capital Terriority Abuja. I am also thankful to Prof. M. D. Magaji for helping me to draft official letters and providing personal contacts of officials of IAR Zaria and ICRISAT Kano for obtaining climate data. I sincerely appreciate the kind response of local farmers in all the three study areas in Kano, Minjibir and Daura LGA of Katsiana.

Special mention goes to Dr Stéphanie Horion, my host during my visit to Copenhagen University, Denmark. I am also grateful to Martin Brandt, Feng Tian and Prof. Rasmus Fensholt for their great input for my research. I am also thankful to the Pakistani community in Copenhangen, especially Irfan Sakhawat, Kashif Tufail and Tanveer Ahamad, for providing me with accommodation during my stay.

I am greatly indebted to departmental colleagues Dr. Majid Nazeer, Mr. Syed Muhammad Irteza Naqvi, Mr. Waleed Umer, Mr. Ivan Elias, Ms. Ester Nervino, Ms. Shamsa Kanwal, Ms. Sarah Hassan and Ms. Sidra Hafeez for their kind help. Special thanks to Dr. Muhammad Bilal and Dr. Sawaid Abbas, who was always available for discussion.

I express my indebtedness and deepest sense of gratitude to all of my family members, especially my parents, for their endless love, moral support, encouragement, and prayers for successful completion of this study.

Lastly, I am very thankful to Research Grants Council (RGC), Hong Kong, for awarding me with the Hong Kong Ph.D. Fellowship, which supported me during my studies, and gave me such a wonderful opportunity for cultural and personal engagement.

Muhammad USMAN

Table of Content

List of Tables

List of Figures

List of Abbreviations

Abbr	Abbreviation
AGB	Aboveground Biomass
AP	Aerial Photograph
AR5	Fifth Assessment Report
ARC	African Rainfall Climatology
AVHRR	Advanced Very High Resolution Radiometer
CHIRPS	Climate Hazards group Infrared Precipitation with Stations
CA	Crown Area
cm	Centimeter
CoV	Coefficient of Variation
CCD	Cold Cloud Duration
DBH	Diameter at Breast Height
Elv	Elevation
EUMETSAT	European Organisation for the Exploitation of Meteorological Satellites
FAO	Food and Agricultue Organization
FEWS	Famines Early Warning System
GCP	Ground Control Point
GEOBIA	Geographic Object Based Image Analysis
GIMMS 3G	Global Inventory Mapping and Monitoring 3rd Generation
GIS	Geographic Information System
GPS	Global Positioning System
GTS	Global Telecommunication System
H	Height
ha	Hectare
HCS	Hyperspherical Color Space
HRS	High Resolution Satellite Images
IAR	Institute of Agricultural Research
IITA	International Institute for Tropical Agriculture
IPCC	International Panel on Climate Change
IVI	Importance Value Index
JAXA	Japan Aerospace Exploration Agency
KAZP	Katsina Arid Zone Programme
KCSZ	Kano Close-Settled Zone
km	Kilometer
km^2	Square kilometers
LIDAR	Light Detection and Ranging
m	Meter

m^2	Square meter
mm	Millimeter
MB	Mean Bias
ME	Mean Error
MK	Mann-Kendall
MODIS	Moderate Resolution Imaging Spectroradiometer
NASA	National Aeronautics and Space Administration
NDVI	Normalised Difference Vefetation Index
NIMET	Nigerian Meteorological Agency
NN	Northern Nigeria
NOAA	National Oceanic and Atmospheric Administration
PMW	Passive Microwave
PR	Precipitation Radar
r	Pearson product-moment coefficient of linear correlation
RADAR	RAdio Detection And Ranging
RFE	African Rainfall Estimate
RMSE	Root Mean Square Error
RS	Remote Sensing
SPI	Standardized Rainfall Index
SPOT	Satellite Pour l'Observation de la Terre
SS	Sudano-Sahelian
SSA	Sub-Saharan Africa
TAMSAT	Tropical Applications of Meteorolody using SATellites
TARCAT	TAMSAT African Rainfall Climatology and Timse series
TCC	Tree Crown Cover
TIR	Thermal Infrared
TMI	TRMM Microwave Mmager
TPA	TMM Multi-satellite Precipitation Analysis
TRMM	Tropical Rainfall Measuring Mission
TS	Theil-Sen
UN	United Nation
UNEP	United Nation' Environment Program
UNICEF	United Nations International Children's Emergency Fund
USGS	United State Geological Survey
WA	West Africa
WV	WorldView 2

Chapter 01

Introduction

1.1. Introduction

More than 50% of the African continent is classified as dryland and a large portion of the population in sub-Saharan Africa lives in rural drylands where agriculture is the primary source of livelihoods (Abdi, 2017). According to Behnke and Mortimore (2016), dryland is characterized by low precipitation and high potential evapotranspiration and having an aridity index value of <0.65. The aridity index is a measure of the ratio between average annual precipitation and annual potential evapotranspiration (Behnke and Mortimore, 2016). Climate change is predicted to affect all parts of the world by the end of the 21st century, but sub-Saharan Africa is likely to be one of the hardest-hit regions due to its marginal climate and high rural population densities. The Fifth Assessment Report (AR5) of the International Panel on Climate Change (IPCC) predicts that temperatures in dryland Africa will rise faster than the global average during the 21st century (IPCC, 2014). Predicted changes in the rainfall regime suggest up to 20% decline in the length of growing season across the arid Sudan and Sahel zones of West Africa (Thornton et al., 2006). Furthermore, increasing temperatures and changes in precipitation along with a projected increase in crop pests and weeds, are very likely to reduce cereal crop production. These climatic impacts are expected to endanger food security of both urban and rural households. In this region where rainfall is already highly variable on both annual and decadal timescales, peoples' livelihoods are still closely tied to biomass production. Therefore such predictions need to be considered in the context of social and economic trends. At national level, these trends cannot be divorced from government policies which, whether intended or incidental, often have repercussions at village level.

West Africa south of the Sahara experiences decreasing rainfall northwards, from the tropical rain forest, through the Guinea and Sudan savanna zones, to the

Sahel zone where rainfall declines to 100 mm at its northern edge (Figure 1.1). The Sudan zone, with mean annual rainfall of 500-1000 mm is densely populated, with rural population densities up to 300-500 persons per square kilometre (km^2) surrounding Kano, Nigeria's second city, and the largest city in savanna Africa.

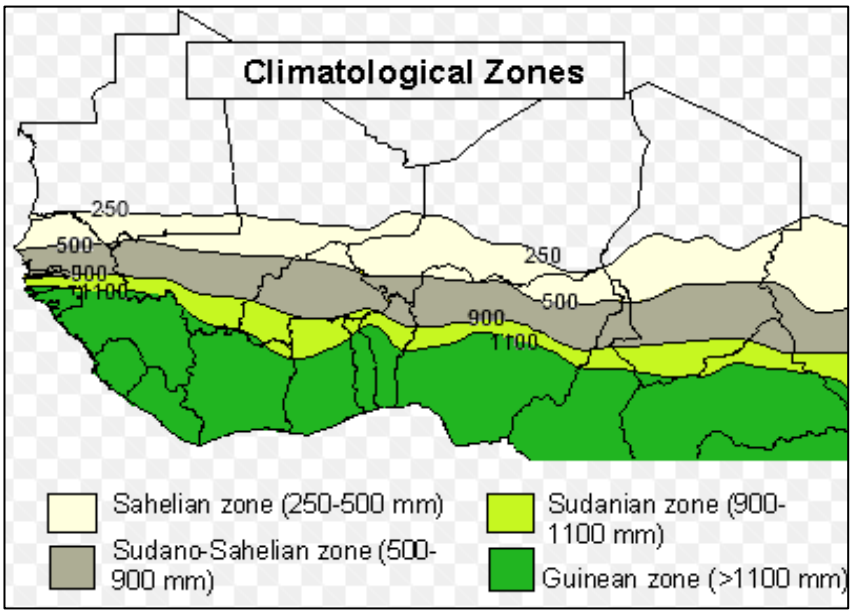

Figure 1.1 West Africa climatological zones based on mean annual rainfall 1961-90 [Source: http://www.fao.org/giews/en/]

Kano has some of the highest rural population densities in the world. The number of persons per km^2 almost doubled from 169 in 1991 (Tiffen, 2001) to 308 in 2006 (National Population Commission, 2006). Kano city itself grew rapidly from the late 1950s, with annual growth rates rising to approximately 6% from 2% in earlier decades. The city's population grew from 0.13 million in 1952, saw a tenfold increase over the next 40 years to 1.36 million in 1991 and then more than doubled to 2.83 million over the next 15 years up to 2006 (National Population Commission, 2006). The rural population has increased correspondingly though there are few reliable data. Since 47% of the population of Kano region was below 15 years of age in 2006 (National Population Commission, 2006), there is potential for further rapid growth. Indeed, by 2050 Nigeria's population is expected to be 2.5 times its current size, reaching 440 million, and to account for 10% of all births in the world (UNICEF, 2014).

Many studies have examined the relationship between biomass and climate in arid West Africa over the last three decades since satellite images were available, and certain trends are now recognised. Following many reports of rapid human-induced desertification which was being reported as recently as 2007 (UNEP, 2007), satellite observations suggest a greening trend originating in the 1980s decade, and continuing to present. This greening is seen as a response to increasing rainfall after severe droughts in the 1970s and 1980s (Anyamba & Tucker, 2005; Brandt et al., (2014a, 2014b); Hiernaux et al., 2009; Mishra et al., 2015; Olsson et al., 2005; Tappan et al., 2004), rather than to human land use pressures. But how this satellite-observed greening based on the Normalised Difference Vegetation Index (NDVI) is related to ground conditions and to local household economies has not been rigorously examined. Furthermore, it is acknowledged that the NDVI's ability to represent biomass is more representative of the green herbaceous layer than the mainly non-green biomass of woody vegetation, and the short-approximately 3-decade record of satellite images is shorter than the lifespan of many trees (Gonzalez et al., 2012).

By far the majority of studies of biomass trends in West Africa have been in Sahelian countries, where mean annual rainfall is around 400-500 mm and grazing of perennial grasses and woody shrubs is the main land use activity. Few studies are available for the moister and more densely populated Sudan zone. In a review of remotely sensed vegetation dynamics in West Africa (Karlson & Ostwald, 2016; Knauer et al., 2014), only three of over 100 studies were of Africa's most populous country, Nigeria, where over 40% of land area lies within the Sudan zone (Figure 1.1). Moreover, it is likely that climate-controlled biomass impacts on local economies will be country-specific due to differing government policies, particularly those relating to energy distribution and energy subsidies, and particularly in Nigeria where government energy policies determine fuel options (Cline-Cole and Maconachie, 2016).

In spite of Nigeria's position as the world's 6th largest oil producer, wood remains by far the most common energy source for cooking and heating, even in major cities. Nigeria's northwestern states with 37% of the national population receive only 6% of Nigeria's fossil fuel supply (Naibbi and Healey, 2013), thus

urban areas experience frequent blackouts and electricity supply is rare in rural areas. Due to the unreliability or absence of electricity in Kano, and fluctuating price of kerosene, 95% of energy used for cooking is from wood (National Bureau of Statistics, 2011).

Wood fuel in Kano has traditionally been derived from trees grown and maintained by farmers in the farmed parklands surrounding the city (Figure 1.2). Rural households derive a large variety of other basic necessities and additional income from farmland trees, which provide food, fodder, medicines, fibre and building materials (Boffa, 1999; Timberlake et al, 2010). Thus the current scenario of high and still increasing population growth combined with predictions of higher temperatures and decreased rainfall, may pose a major challenge to food security in coming decades.

Figure 1.2 A fallow agricultural field with different tree species in the Kano Close Settled Zone, Northern Nigeria during the dry season (January 2016). Photo: Muhammad Usman

A few more recent studies have specifically examined trends in woody vegetation (Brandt, et al., 2014a; Gonzalez et al., 2012; Hänke et al., 2016; Hiernaux et al., 2009) using time-series of images combining archived aerial

photographs and recent high resolution satellite images. Such higher resolution datasets have enabled the estimation of tree cover and density. As with satellite-based NDVI, trends in tree cover and tree density appear to be aligned with climatic trends. Gonzalez et al. (2012), working in three Sahelian villages in Senegal and Mauritania found an overall long term decline in tree cover in the second half of the twentieth century, and Audu (2013) gives similar warnings for northern Nigeria, although no recent research has been done. Brandt et al. (2014a) and Hänke et al. (2016), report similar declines in Sahelian tree cover in the later twentieth century. However, while Brandt et al. (2014a) note that tree densities are still far below the levels of the 1960s, Hänke et al. (2016) and Brandt et al. (2017) observe recovery back to 1960s levels by 2006 and 2015, respectively.

Recognising that tree densities alone may not fully represent social-ecological interactions, several studies have also considered trends in tree species composition, comparing recent field inventory with past field inventory (Herrmann and Tappan, 2013) or with informant recollection (Gonzalez et al., 2012; Brandt et al., 2014a; Hänke et al., 2016; Tappan et al., 2004; Vincke et al., 2010). Overall, a decline and shift in species diversity related to increasing aridity is reported, entailing a trend to fewer, and more drought-tolerant species at the expense of those with more southerly distributions.

The aim of this study is firstly to evaluate the available sources of rainfall data over recent decades in northern Nigeria using both climate station rainfall data and satellite-based rainfall products to study inter-annual variability and temporal trends in rainfall. Secondly to evaluate high resolution remotely sensed images for changes in woody biomass, in terms of tree density and species composition, in the intensively farmed parklands surrounding "Kano Close-Settled Zone (KCSZ)", due to its high rural population density as a case study for savanna Africa. Finally, to evaluate the use of Geographic Object Based Image Analysis (GEOBIA) for delineation of tree crown cover in the agroforestry landscape of the KCSZ and modelling of above ground biomass (AGB) using tree crown cover.

1.2. Research objectives

There are many accounts of rainfall trends in northern Nigeria (Buba, 2010; Hess et al., 1995; Mortimore, 2000; Olaniran, 1991, 1988; Tarhule and Woo, 1998; Tomlinson, 2010), many observing severe declines, and others decline in recent decades followed by a return to normal. Almost all studies of rainfall in northern Nigeria report great spatial variation in rainfall amounts and trends, with large differences in nearby areas, or conflicting results (Buba, 2010; Mortimore, 2000; Tomlinson, 2010) for the same regions. Additionally, previous studies have been confined to data from a few climate stations, and are therefore spatially incomplete. Furthermore, these reported statistics appear in many cases to be conflicting with farmers' perceptions of rainfall trends and its effects on their lives and livelihood. Local farmers in Nigeria perceive a long term decreasing rainfall trends (Bose et al., 2014; Falaki et al., 2011; West et al., 20018), while rainfall analysis based on gauge and satellite data over the last three decades show recovery in rainfall after the severe droughts of 1970s and 1980s. This study aims to evaluate available sources of rainfall data over recent decades in the Kano region of northern Nigeria, and to assess their impacts on the rural landscape and thus on the agricultural economy. The specific objectives are:

1. To evaluate rainfall data from ground stations compared to satellite-based estimates at daily, dekadal, monthly and annual time scales, and to analyse inter-annual variability and temporal trends over a 30-year period (1984-2013).
2. To calculate vegetation trends across the drylands of northern Nigeria using MODIS (2000-2015) and AVHRR GIMMS 3g (1982-2015).
3. To examine trends in woody biomass, in terms of farmland tree density and species composition in the 'Kano Closed Settled Zone' of northern Nigeria as a case study, due to its high rural population density. This is based on historical data from archived aerial photographs and satellite images, as well as field data collected in the early 1980s and 2016.

4. To delineate tree crown cover through GEOBIA using high resolution WorldView-2 image and modelling of above ground biomass using tree crown cover.

1.3. Dissertation Overview

The dissertation consists of following chapters.

Chapter 1 is an introductory chapter, with brief literature review and objectives.

Chapter 2 describes the ecological zones of Africa and gives a brief overview of the geography of Northern Nigeria.

Chapter 3 is a brief overview of the overall methodology.

Chapter 4 examines relationship between gauge rainfall and satellite rainfall products from daily to annual scale and long term trends of rainfall and vegetation.

Chapter 5 deals with the use high resolution remotely sensed images along with field survey for tree inventory and changes in woody biomass, in terms of tree density and species composition, in the intensively farmed parklands surrounding Kano City.

Chapter 6 is about delineation tree crown cover through GEOBIA using high resolution WV-2 images and modelling above ground biomas using tree crown cover.

Chapter 7 deals with overall conclusion and limitations of this study.

Chapter 02

Characteristics of the Study area and Methodology

2.1. Ecological Zones of West Africa

In West Africa, decreasing rainfall and increasing temperature northward differentiates vegetation into three latitudinal ecological zones: the Guinea, the Sudan and Sahel zones. Figure 1.1 shows these three major ecological zones of West Africa, within which the vegetation and economy are largely determined by rainfall. The most southerly, Guinea zone is forested, grading into tree savanna at its northern edge. Shifting cultivation is the main traditional land use and land cover type, with crops and economic trees planted in clearings.

The Sudan Zone, with mean annual rainfall of approximately 500 to 1000 mm, supports a tree savanna vegetation with flat-topped trees browsed extensively by the savanna fauna and domestic livestock, when the grassy ground cover dries during the winter dry season.

The Sahel Zone is the most northerly ecological zone and borders the Sahara Desert on its northern edge. The rainfall from 100 to 500 mm annually is only adequate to support a low and discontinuous shrub canopy and herbaceous ground flora of dry grasses. The region supports less fixed cultivation, but the native shrubs and grasses are browsed by cattle owned by the Fulani nomadic pastoralists.

2.2. Study Area

The study area covers the Sudano-Sahelian savanna ecological zone of northern Nigeria between latitude 8°-16° N and longitude 1°-17° E. This zone covers the northern states and the Federal Capital Territory Abuja of Nigeria (Figure 2.1). The landscape comprises rolling or gently undulating plains often referred to as the "High Plains of Hausaland" (Mortimore, 1962). The 'Kano Close-Settled Zone' (KCSZ) of northern Nigeria (Mortimore and Wilson, 1965) surrounds Nigeria's second largest city, Kano, is situated in the northern part of the Sudan zone. The

KCSZ describes the densely populated agricultural region influenced by the proximity of Kano and serving as its hinterland in terms of interdependency of products and trade, good and services. In this zone over 80 % of the land is cultivated in the April to September rainy season. The main crops are cereals of Maize (Guinea corn), Millet and Sorghum, which are grown for subsistence, along with a few field crops of root vegetables, beans, and a few vegetables. Green vegetables are grown along valleys such as the Jakara valley to the east of Kano city using river water, as well as on irrigation schemes. The 'parkland' landscape is defined by the large variety of trees grown and maintained on farmland, which are used for a very wide variety of purposes including medicinal, food, fiber, construction and as fuelwood (Boffa, 1999; Timberlake et al., 2010). Three study areas were selected within Kano's hinterland to examine long term trends in tree density and species composition (Figure 2.1).

Most rainfall in Nigeria comes from southwesterly winds from the tropical Atlantic Ocean, thus the annual rainfall amount and duration of rainy season decreases from south to north, with greater variability northward (Anyadike, 1993; Hess et al., 1995). Rainfall is highly variable both inter-annually and on a decadal timescale. The most southerly Guinea zone receives more than 1500 mm rainfall falling to 250 mm at the northern boundary. Severe drought in the 1970s and 80s was experienced throughout West Africa.

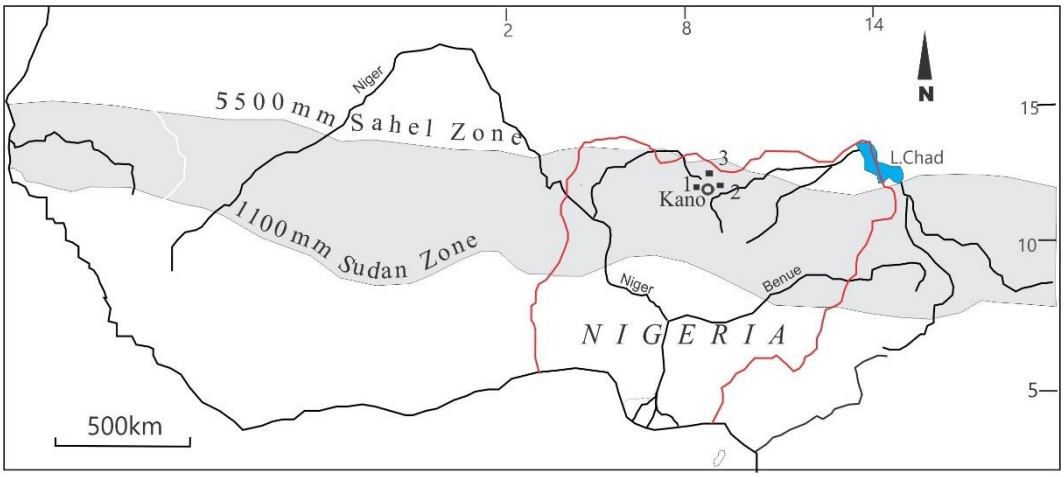

Figure 2.1 Climatological zones of West Africa showing location of study areas.

2.3. Overall Methodology

This chapter describes the overall methodology used for this study. As it is not convenient to explain all of the methodological steps used to fulfil all three objectives, a schematic diagram of the overall methodology is presented (Figure 2.2). However, details of the processing steps of each sub-study are described in respective sections.

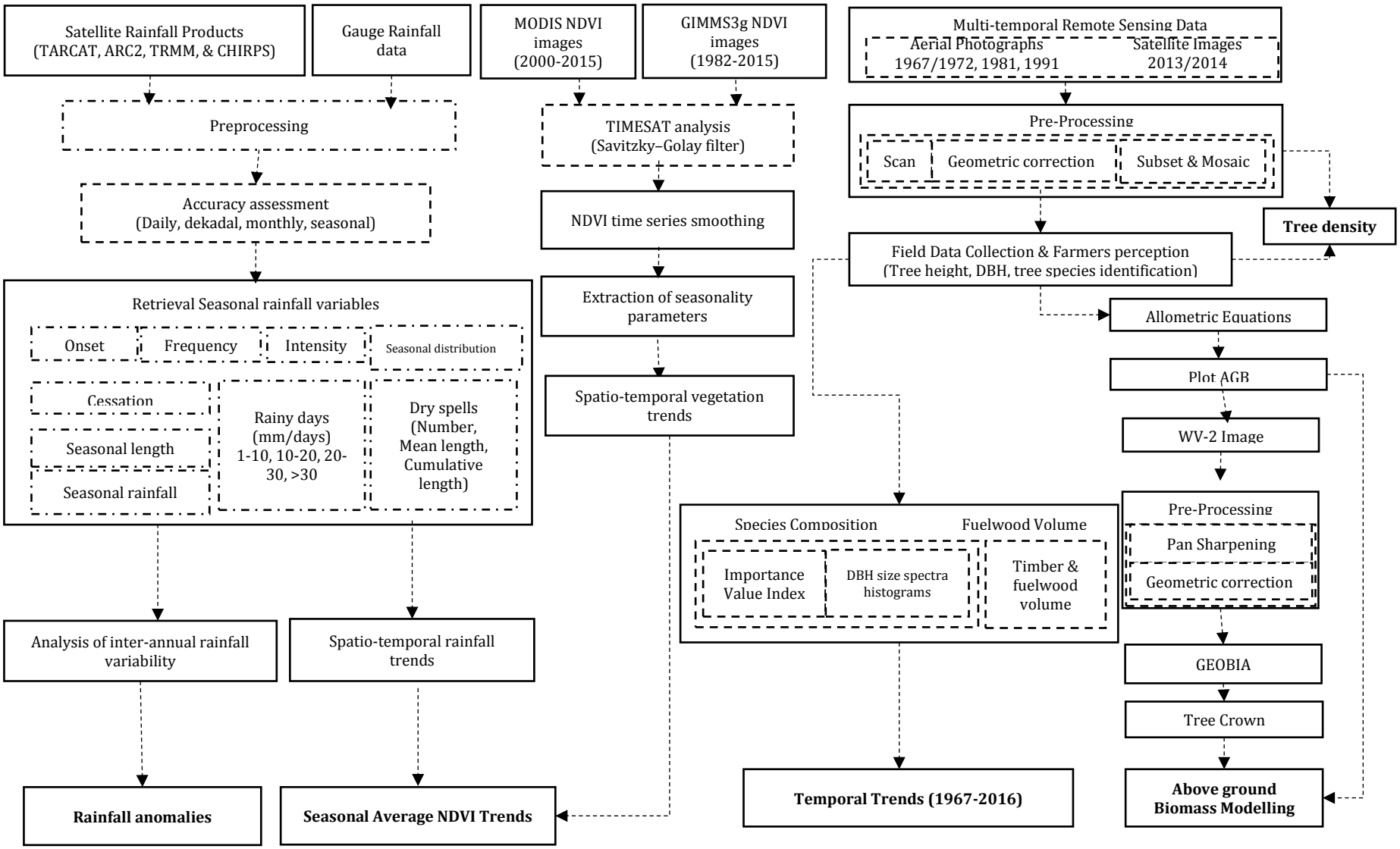

Figure 2.2 Flowchart of overall methodology.

Chapter 03

Spatio-temporal analysis of changes in rainfall regime using long term satellite based rainfall and NDVI data in the Sudano Sahelian zone of Nigeria

3.1. Introduction

The Sudano-Sahelian ecological zone of Sub-Saharan Africa at Latitude (12°-20° N), is well known for its variable climate, where rainfall variability in the last three decades of the 20th century exceeded that in other parts of the world (Sanogo et al., 2015). The period 1931-1960 was considered to have above average rainfall, but an abrupt change occurred in the late 1960s, with up to 30% decline in average rainfall between 1961 and 1990 (Hulme, 1992; Fink et al., 2010). Severe droughts occurred during the 1970-1990 period (Nicholson, 2000), and those of 1972-1974 and 1983-1985 entailed severe food shortages, and loss of human life and livestock (Mortimore, 2000). After several decades of dry conditions, farmers in drought-hit areas appear to have adapted to the general increase in rainfall variability (Mortimore and Adams, 2001).

Northern Nigeria's climate is semi-arid, and rural livelihoods depend mainly on rain-fed agriculture (Hess et al., 1995; Tarhule and Woo, 1998), thus rainfall variability, which increases northwards, and changes in rainfall threaten the livelihoods of local people (Mortimore, 2000, Zhang et al., 2017). Variability of rainfall appears to be inversely proportional to the total amount of rainfall, with the lesser the amount, the greater the variability (Buba, 2010). As rainfall in Nigeria decreases northwards, there is much rainfall variability in the northern Nigerian states. Timing of the start of the rainy season is important, as farmers make decisions about cropping and livestock movement which affect productivity, based on the first rains (Ingram et al., 2002). The major determinant of crop production is soil moisture, but the region's variable rainfall makes prediction of drought stress difficult. Drought stress during the seedling

stage of the main cereal staples millet and sorghum results in reduced grain yield. For millet, a drought period of 15 to 20 days in mid-season, which extends to the post-flowering period, would cause severe reduction in grain yield, and drought just before the flowering period may reduce yields by up to 70% (Seetharama et al, 1984). Sorghum in particular is sensitive to late season rainfall, as sorghum does not enter the high water use period during its life cycle until August. Thus in addition to total seasonal rainfall and timing of rainy season onset, other important rainfall variables include the number, timing and length of dry spells, and seasonal distribution of rainfall is also an important variable.

There are many accounts of rainfall trends in northern Nigeria (Buba, 2010; Mortimore, 2000; Tomlinson, 2010), mainly observing severe declines in the last decades of the 20th century, followed by a return to normal (Hess et al., 1995; Olaniran, 1991, 1988; Tarhule and Woo, 1998). However, none provide a detailed study of the last 2 decades for different rainfall variables specific to crop production and rural livelihoods. For this, accurate rainfall data with high temporal, as well as spatial resolution is required.

Most of the rainfall in Africa is formed by convective clouds, thus rainfall amount can vary over a few tens of km (Nicholson, 2000). However, the spatial distribution of rain gauge stations in West Africa is very sparse and these were significantly reduced over the last 3-4 decades (Sanogo et al., 2015). Also, as the number of rain gauge stations in Nigeria has decreased significantly over the last 3-4 decades, the spatial inadequacy has increased. For example the number of gauges returning rainfall records in northern Kaduna state (now Katsina state) diminished from about 50 in 1941-70 to only 12 by 1999 (Tomlinson, 2010).

Satellite based precipitation estimates provide an alternative to sparse, traditional gauge-based rainfall measurements. They are at continental and global scale and have high spatial and -temporal resolution. Thus they provide timely, repetitve and cost effective information about rainfall at different time scales from daily to annual for applications in climate change, Famine Early Warning Systems (FEWS), and hydrological studies (Maidment et al., 2014). It is therefore necessary to assess the accuracy of different satellite based rainfall products compared to gauge rainfall, before they can be considered operational

for local crop production forecasting and rural productivity assessments. A few previous studies have evaluated satellite-based rainfall products at continental scale: for West Africa (Sanogo et al., 2015), and for three different river basins in Africa (Thiemig et al., 2012). Also there are some studies at country level including Burkina Faso (Dembélé and Zwart, 2016), Ethiopia (Bayissa et al., 2017) and Mozambique (Toté et al., 2015).

However, evaluation of satellite based rainfall products show large differences in algorithm performances depending on location, local climate, season and topography (Maidment et al., 2013; Toté et al., 2015). Also choice of the best rainfall product depends on the specific application. For drought monitoring studies, the accuracy of low rainfall is the main requirement, and for hydrological and flood forecasting application, the accuracy of high rainfall events is crucial (Toté et al., 2015).

Dembélé and Zwart (2016) evaluated rainfall estimates from seven different operational satellites with rainfall from gauges in Burkina Faso for the period 2001-2014 at daily to annual time scales. Poor performance was observed at daily scale, with best performance of r=0.47, for the Climate Hazards group Infra-red Precipitation with Stations (CHIRPS), but performance improved as the time scale increase from monthly to seasonal. Bayissa et al (2017) assessed meteorological droughts at dekadal to seasonal scales, and also found best performance for CHIRPS, compared to four other satellite-based rainfall products (ARC, PERSIANN, TARCAT and TRMM) in the Upper Blue Nile Basin in Ethiopia. Toté et al (2015) also report better performance for CHIRPS than for RFE and TARCAT, compared to independent gauge rainfall data at dekadal and total seasonal time scales in Mozambique.

Almost all studies of rainfall in northern Nigeria report great spatial variation in rainfall amounts and trends, with large differences in nearby areas, and many conflict with other studies (Buba, 2010; Mortimore, 2000; Tomlinson, 2010) for the same regions. Additionally, previous studies have been confined to data from a few climate stations, and are therefore spatially incomplete. Furthermore, these reported statistics appear in many cases to be conflicting with farmers' perceptions of rainfall trends and its effects on their lives and livelihood. This

study aims to evaluate the available sources of both spatial and temporal rainfall data over recent decades in northern Nigeria, and to assess impacts on the rural landscape and agricultural economy.

The Normalized Difference Vegetation Index (NDVI) is a normalized ratio derived using red and near-infrared band reflectance, which indicates the amount of vegetation on the ground (Tucker, 1979). The satellite-based NDVI has long been used as a major source of ecological information about arid West Africa, as it provides information about ecological conditions on the ground over wide areas, and the AVHRR GIMMS NDVI3g has been available over three decades, along with the availability of satellite-based rainfall products. During the 1972-73 drought in the Sahel, the NDVI from satellite images gave rise to concerns about human-induced desertification (Herrmann and Hutchinson, 2005; Lamprey, 1988), and the subsequent NDVI-based 'greening' of the Sahel (Anyamba and Tucker, 2005; Olsson et al., 2005) appeared to contradict this theory of human-induced degradation. Although satellite-based rainfall products are now available, and cover large areas, NDVI data indicate trends in ecological health and biomass productivity which are more directly relevant to livelihoods, than rainfall alone. Therefore in this study, both the NDVI and satellite-based rainfall products are examined, to set in context the observed trends in tree stocks and woody biomass productivity in the Sudan Zone of northern Nigeria.

3.1.1. Objectives

The specific objectives of this study are to:

- compare temporal trends in rainfall data from ground stations at daily, dekadal, monthly and annual time scales, with satellite-based estimates which use a combination of thermal infra-red and radar images, and ground station data, as satellite rainfall estimates can increase the spatial coverage if proved to be reliable,
- evaluate satellite rainfall products for retrieval of seasonal rainfall variables,

- analyse inter-annual variability and temporal trends over a 30-year period (1984-2013) from gauge-based rainfall variables,
- analyse both spatial and temporal variability (over the same 30-year period (1984-2013)) using satellite derived rainfall variables, and
- analyse long term vegetation trends across the drylands of northern Nigerian using AVHRR GIMMS3g NDVI (1982-2015) and MODIS NDVI (2000-2015).

3.2. Materials and Methods

3.2.1. Study Area

The study area covers the Sudano-Sahelian savanna ecological zone of northern Nigeria between latitude 8°-16° N and longitude 1°-17° E. This zone covers the northern states and the Federal Capital Territory Abuja of Nigeria (Figure 3.1). The landscape comprises rolling or gently undulating plains often referred to as the "High Plains of Hausaland" (Mortimore, 1965).

Most rainfall in Nigeria comes from southwesterly winds from the tropical Atlantic Ocean, thus the annual rainfall amount and duration of rainy season decreases from south to north, with greater variability northward (Anyadike, 1993; Hess et al., 1995). The more southerly Sudan zone receives more than 650 mm average annual rainfall falling to 400 mm in the Sahel zone. In the northern states of Nigeria, over 80% of the land is cultivated in the April to September rainy season. The main subsistence crops are cereals of Millet and Sorghum (Guinea corn), along with field crops of root vegetables, beans, and a few vegetables. Over the 35 years of this study, northern Nigeria has seen large increase in rural population densities (Tiffen, 2001; National Population Commission, 2006), accompanied by intensification of agriculture. Kano's rural population density was reported as 308 persons per km^2 in 2006 (National Population Commission, 2006). However as nutritional status across northern Nigeria is low, with 20 to 50 % of children showing some degree of stunting and/or underweight (Hall and Bohen, 2009), return to the drought conditions of the 1970s and 80s, could be disastrous for farming families.

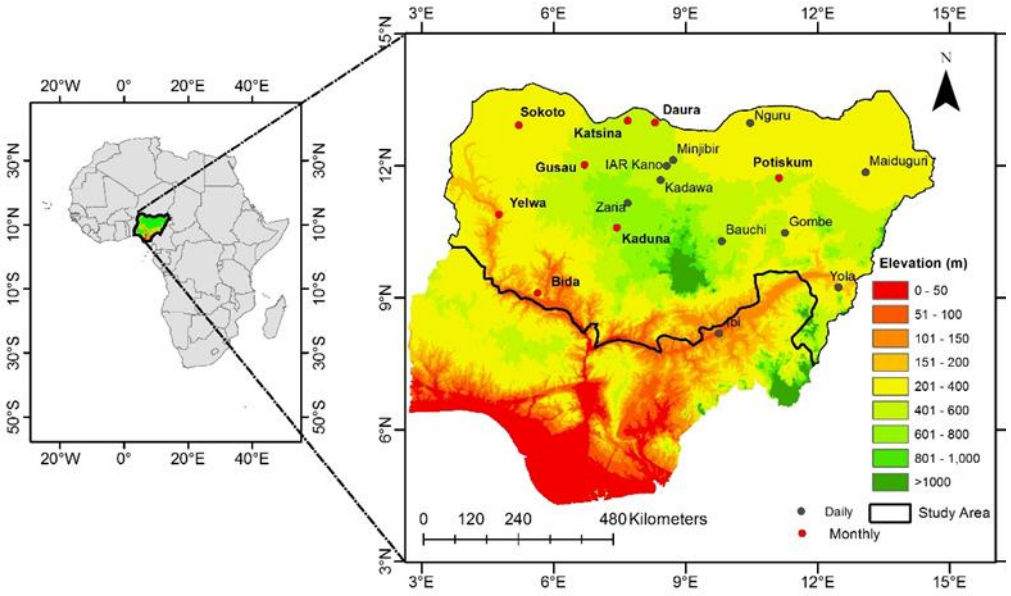

Figure 3.1 Location of northern Nigerian states and weather station rain gauges. Grey circles denote availability of daily and dekadal data, and red circles denote the location of available monthly data.

3.2.2. Datasets

In-situ gauge rainfall data

Daily rainfall data were obtained for 10 weather stations, including six (Bauchi, Gombe, Ibi, Nguru, Maiduguri, and Yola) from the Nigerian Meteorological Agency (NIMET) and four (Kadawa, Minjibir, IAR Kano, Zaria) from the Institute of Agricultural research (IAR) (Figure 3.1 and Table 3.1). The quality of daily rainfall data was checked and only stations with above 80% data availability were considered for comparison with satellite based rainfall estimates. Daily rainfall data from weather stations were accumulated to form dekadal (10 days), monthly and seasonal (Apr-Oct) rainfall for comparison with satellite based rainfall estimates. Another 8 stations (Bida, Daura, Gusau, Kaduna, Katsina, Potiskum, Sokoto and Yelwa) having only monthly rainfall data were acquired from NIMET. However, the temporal coverage of weather stations is not uniform, varying from station to station (Table 3.1).

Table 3.1 Overview of rain gauge stations.

No.	Weather station	Data availability	Temporal coverage	Latitude (° N)	Longitude (° E)	Elevation (m a.s.l)
1	Bauchi	Daily	1984-2013	10.27	9.82	584
2	Maiduguri	Daily	1984-2013	11.85	13.10	337
3	Nguru	Daily	1984-2013	12.96	10.46	343
4	Minjibir	Daily	1973-2015	12.12	8.70	429
5	IAR Kano	Daily	1998-2010	11.98	8.55	484
6	Kadawa	Daily	1984-2007	11.67	8.42	489
7	Zaria	Daily	1965-2015	11.14	7.67	660
8	Gombe	Daily	1984-2013	10.46	11.25	407
9	Yola	Daily	1984-2013	9.22	12.46	156
10	Ibi	Daily	1984-2013	8.17	9.74	107
11	Daura	Monthly	1951-2002	12.97	8.30	476
12	Bida	Monthly	1981-2015	9.10	5.63	190
13	Kaduna	Monthly	1981-2015	10.58	7.43	621
14	Katsina	Monthly	1981-2015	13.01	7.68	501
15	Sokoto	Monthly	1981-2015	12.91	5.20	307
16	Gusau	Monthly	1981-2015	12.01	6.70	508
17	Potiskum	Monthly	1981-2015	11.71	11.11	432
18	Yelwa	Monthly	1981-2015	10.88	4.75	160

Satellite based rainfall products

Satellite-based rainfall products typically exploit a combination of data from thermal infrared (TIR), passive microwave (PMW), and ground-based gauge observations, and these datatypes are often combined to create an optimal product. A variety of rainfall datasets has been produced using convective cloud top temperature by applying the cold cloud duration (CCD) technique (Maidment et al., 2014). In this study, the four satellite-based rainfall products (Table 3.2), were selected for evaluation against rainfall gauge data, because of their long time series, near-real time data availability and free access.

TAMSAT African Rainfall Climatology and Time series (TARCAT)

The TARCAT v2.0, TIR based precipitation dataset at a spatial resolution of 4 km is based on the TAMSAT (Tropical Applications of Meteorology using Satellite and ground-based observations) rainfall estimation algorithm, which was constructed by archived Meteosat TIR imagery CCD, and locally calibrated against rain gauge records. It was developed by the University of Reading, UK, for Africa only, and is available from 1983 onwards at daily, dekadal, monthly and yearly scales (Maidment et al., 2014; Tarnavsky et al., 2014).

African Rainfall Climatology Version 2 (ARC2)

The ARC v2.0 (African Rainfall Climatology Version 2) satellite based daily gridded precipitation dataset centered over Africa at a spatial resolution of 10 km is also available from 1983 onwards, and uses inputs from three sources: 1) 3-hourly geostationary thermal infrared (TIR) data from the European Organisation for the Exploitation of Meteorological Satellites (EUMETSAT), 2) data from TRMM's microwave sensors and 3) quality controlled Global Telecommunication System (GTS) gauge observations reporting 24-h rainfall accumulations over Africa (Novella and Thiaw, 2013).

Tropical Rainfall Measuring Mission (TRMM)

The Tropical Rainfall Measuring Mission (TRMM) is joint mission between National Aeronautics and Space Administration (NASA) and the Japan Aerospace Exploration Agency (JAXA) aimed at improving observations of precipitation across the globe between 45° N and 45° S. The most widely used outputs are the TRMM Multi-satellite Precipitation Analysis (TMPA) 3-hourly (3B42) product accumulated to daily and monthly (3B43) products, which are available from 1998 to 2014 at spatial resolution of 25 km (Huffman et al., 2007; Maidment et al., 2014). The TMPA product depends on input from a combination of optical, thermal and microwave sensors, as well as gauge data (Dembélé and Zwart, 2016). Daily TRMM 3B42 V7 and monthly 3B43 V7 products were used in this study.

Climate Hazards group Infrared Precipitation with Stations (CHIRPS)

The CHIRPS Version 2.0 rainfall dataset was developed by US Geological Survey (USGS) and Climate Hazard Group at the University of California, Santa Barbara. It is available from 1981 onwards at spatial resolution of 5 km.

The CHIRPS algorithm incorporates i) satellite thermal IR data to represent sparsely gauged locations, ii) blends station data to produce a preliminary information product with a latency of about 2 days and a final product with an average latency of about 3 weeks, and iii) uses a novel blending procedure

incorporating the spatial correlation structure of CCD-estimates to assign interpolation weights. CHIRPS also uses the TRMM's TMPA product, which includes several microwave sources, to calibrate global CCD rainfall estimates (Funk et al., 2015).

Satellite based NDVI products

GIMMS3g

Data of different spatial resolution and temporal coverage were used to assess vegetation changes at different levels. Coarse scale third generation Global Inventory Modeling and Mapping Studies (GIMMS3g) NDVI dataset produced with AVHRR sensor onboard NOAA satellites 7-18. GIMMS3g with its latest version (v 1.0) at 1/12° or 8-km resolution provided the only available long-term NDVI time series from 1982 to 2015 for studying long term trends. GIMMS data is bimonthly (or 15 days Maximum Value Composite (MVC)) NDVI product with corresponding quality flags, so there are total 24 images in one year. MVC method select pixel with maximum value over the 15 days, so excluding cloud affected NDVI values.

MODIS MOD13Q1

The Moderate Resolution Imaging Spectroradiometer (MODIS) with moderate resolution at 250 m provides short-term trends with higher level of spatial detail for the period 2000-2015. MOD13Q1 is a 16-days MODIS NDVI product with corresponding quality flags.

Table 3.2 Summary of satellite products used in this study.

No.	Satellite rainfall products	Temporal coverage	Data Input	Spatial Coverage	Spatial resolution	Temporal resolution
1	TARCAT Version 2.02	1983-2015	TIR, gauge	Africa	0.0375° (~4 km)	Daily
2	CHIRPS Version 2.01	1981-2015	TIR, gauge	Africa	0.05° (~5 km)	Daily
3	ARC Version 2	1983-2015	TIR, gauge, TMPA 3B42 v7	Global	0.1° (~10 km)	Daily
4	TRMM Multi-satellite Precipitation Analysis version 7 (TMPA 3B42 v7)	1998-2014	TIR, VIS, TMI, PR, gauge	Global	0.25° (~25 km)	Daily

3.3. Methods

3.3.1. Evaluation of satellite based rainfall products

Previous studies have found only weak relationships between satellites and gauge data for daily rainfall comparisons (Dembélé and Zwart, 2016; Sanogo et al., 2015). In this study we compare gauge rainfall against satellite data on daily, dekadal, monthly and seasonal time scales, for four different satellite-based rainfall products (ARC, CHIRPS, TAMSAT and TRMM). The period 1998 to 2014 was examined as TRMM data were only available for this period. Eighteen weather stations (Figure 3.1) were used, except for daily and dekadal (10 days) comparisons which were conducted for only ten weather stations which have daily rainfall data for this period (Table 3.1). Pixel values at gauge locations were extracted for comparison of gauge data with satellite rainfall estimates and accumulated into dekadal, monthly and seasonal values. For every month, the first two dekads comprise ten days with 1-10 and 11-20 dates of months, while last dekad comprises 8-11 days depending on the month.

Satellite rainfall estimates were compared with gauge rainfall using pairwise comparison statistical measures such as Pearson product-moment coefficient of linear correlation (r), Bias, Mean Error (ME) and Root Mean Square Error (RMSE).

Pearson correlation coefficient (r) measures the strength of linear relationship between satellite and gauge rainfall. Values of 'r' close to 1 indicate a perfect relationship between satellite and gauge rainfall estimates. The statistical significace of correlation (R) is represented by asterisks (** = $p < 0.01$ and * = $p < 0.05$)

$$R = \frac{\Sigma(G-\bar{G})(S-\bar{S})}{\sqrt{\Sigma(G-\bar{G})^2}\sqrt{\Sigma(S-\bar{S})^2}} \qquad \text{Equation 3.1}$$

Where G = gauge rainfall amount, $\bar{G}$= average gauge rainfall amount, S = satellite rainfall estimates, $\bar{S}$ = average satellite rainfall estimates, n = total number of data.

Bias indicates how well the average of satellite rainfall estimates corresponds with average of gauge rainfall. Its value close to 1 shows cumulative satellite rainfall estimates is closer to cumulative gauge rainfall measures. A bias value greater than 1 indicates satellite overestimates, while less than 1 indicate satellite underestimates.

$$\text{Bias} = \frac{\Sigma S}{\Sigma G} \qquad \text{Equation 3.2}$$

Mean error (ME) is the measure of average difference between satellite and gauge rainfall amounts. A positive value reflects an overestimation of satellite rainfall whereas negative indicates underestimation of satellite rainfall compared to gauge rainfall.

$$\text{ME} = \frac{1}{n}\sum_{i=1}^{n}(S - G) \qquad \text{Equation 3.3}$$

Root mean square error (RMSE) is the standard deviation of the difference between satellite rainfall estimates and gauge rainfall. A higher value of RMSE indicates large difference between satellite and gauge rainfall measures.

$$\text{RMSE} = \sqrt{\frac{1}{n}\sum_{i=1}^{n}(S - G)^2} \qquad \text{Equation 3.4}$$

According to Toté et al (2015), some statistics measures can be more useful than others depending on the specific application. For drought monitoring studies, overestimation of satellite rainfall (ME > 0) must be avoided and for hydrological and flood forecasting studies, underestimation of satellite rainfall estimate (ME < 0) should be avoided. For general purposes, rainfall products with high R and low RMSE are preferred.

3.3.2. Evaluation of seasonal rainfall variables

For analysis of changes in rainfall regime across northern Nigeria, seasonal rainfall variables were calculated based on daily rainfall events. There are several criteria for selection of onset and end of rainy season based on thresholds of rainfall amount during consecutive days (Fitzpatrick et al., 2015; Omotosho et al., 2000; Sivakumar, 1988). Fitzpatrick et al., (2015) compared 18 different definitions for onset of rainy season on regional, local and intermediate scales for

datasets of varying resolution and found that the choice of definition of rainy season depends on local pattern of the onset dates. In this study, we used the definitions of seasonal rainfall variables by (Zhang et al., 2017), as follows. Rainy season onset was defined as the first occurrence of at least 20 mm cumulative rainfall within seven consecutive days after May 1, followed by at least 20 mm rainfall in the next 20 days to avoid "false starts". Rainy season cessation was defined as the occurrence of less than 10 mm cumulative rainfall in 20 consecutive days after September 1. Length of rainy season was defined by the number of days between onset and cessation of rainy season. Season rainfall amount was defined by accumulating all daily rainfall events above 1 mm rainfall over the whole rainy season. Frequency of rainy season was defined by number of rainy days with rainfall amount ≥ 1 mm divided by the length of rainy season. Intensity of rainfall was defined as the total amount of rainfall during rainy season divided by the number of rainy days with rainfall ≥ 1 mm. The number of rainy days was calculated according to different levels of rainfall amount with 1-10, 10-20, 20-30 and >30 mm/day separately. Seasonal distribution was defined by the ratio of amount of rainfall in the first and second halves of the rainy season (calculated based on onset and length of season). Dry spells within the rainy season were defined as rainfall less than 1 mm in at least seven consecutive days. Three variables were used to characterize dry spells: firstly, the number of dry spells, secondly mean length of dry spells by number of days, and thirdly cumulative dry days was defined by the total number of dry days in each dry spell during the rainy season. Ten weather stations with long term daily rainfall were used to derive season rainfall variables (Table 3.1). Similarly, for three different satellite based rainfall gridded data (TARCAT, CHIRPS and ARC), pixel values corresponding to the location of rain gauges were extracted for the period 1984-2013 to examine the agreement between satellite and gauge based rainfall variables.

3.3.3. Temporal trends estimation from gauge based rainfall variables

To place satellite-based rainfall estimates in long term context, temporal trends in rainfall over northern Nigeria were calculated from gauge based rainfall variables for those stations which fall within Sanogo et al's (2015) definition of

the West African Sahel between latitudes 9° and 20° N, in terms of rainfall variability. Trend analysis was conducted using a non-parametric linear regression model, with the rainfall variables as the dependent variable and time as the independent variable. The output of trend analysis was a regression slope indicating the magnitude and direction of changes in rainfall variables. Normally slope is computed by least square estimates from linear regression, but the method is sensitive to outliers and assumes there is no serial autocorrelation. Since time series of season rainfall variables often do not meet parametric assumptions of normality and homoscedasticity (Hirsch et al., 1984; Horion et al., 2014), a median trend (Theil-Sen) procedure was applied to estimate the magnitude and direction of changes in seasonal rainfall variables in corresponding units per year. The Theil-Sen or Sen Slope method is a linear regression model which calculates slope using the median value of slopes from all pairs of observations in a time series (Equation 3.5). Sen Slope is known to be free from serial autocorrelation, seasonality (both inter-annual and intra-annual), non-normality and heteroscedasticity, and is also resistant to outliers and missing data within the time series (Sen, 1968). The significance of the trends in rainfall variables based on Sen Slope was assessed by a nonparametric trend test, the Mann–Kendall (MK) significance test, which accounts for the effect of serial correlation (Salmi et al., 2002; Westra et al., 2013).

The slope Q between two time periods is calculated as

$$Q = \frac{Y_j - Y_i}{t_j - t_i} \qquad \text{Equation 3.5}$$

Where Y_j and Y_i are values of time series, where j is greater than i. There will be a total of N data pairs for which j is greater than i. The Sen Slope is the median of N values of Q.

3.3.4. Calculation of standardized anomalies for studying inter-annual variability

To study inter-annual variability over the long term, the standardized anomaly was calculated for every rainfall variable using standardized rainfall index

(Agnew, 2000; Lamb, 1982). The standardized rainfall index uses average and standard deviation of long term rainfall variable to quantify rainfall variable in relation to their long term climatology. Most frequently, rainfall anomalies are computed by arithmetic mean of normalized rainfall variables recorded at several rain gauge stations over the region of interest (Hulme, 1992; Zhang et al., 2017). However, due to strong spatial variability and uneven spatial distribution of rain gauges in Sudano-Sahelian region, we applied the Standardized Precipitation Index (SPI) proposed by (Ali and Label, 2009) to all stations independently, to the rainfall variables using equation 3.6.

$$\text{SPI} = \frac{X_i - \overline{X}}{\sigma(X)} \qquad \text{Equation 3.6}$$

Where X_i= regional rainfall variable for year i, where region refers average value of all rain gauge stations over the region of interest,

$\overline{X}$ = average of the inter-annual regional rainfall variable,

$\sigma(X)$ = standard deviation of inter-annual regional rainfall variable.

3.3.5. Spatio-temporal trends for satellite rainfall variables

Based on comparison of satellite rainfall products against gauge rainfall on daily, dekadal, monthly and seasonal time scales, we selected the best satellite rainfall product (CHIRPS) to represent the per pixel spatio-temporal trends of rainfall variables for the whole of northern Nigeria. For every pixel in the study area, trends were estimated for the time period 1981-2015 using Sen slope (Sen, 1968) and the significance of these trends was assessed using the Mann–Kendall (MK) significance test which accounts for the effect of temporal autocorrelation (Westra et al., 2013).

3.3.6. Smoothing of NDVI time series using Savitzky–Golay filter

Due to cloud cover, varying atmospheric conditions, and bi-directional effects there are some disturbances in the NDVI time series. During the rainy season, clouds are a major problem and often prevail for more than two weeks. Although NDVI data sets are a MVC product (selection of maximum NDVI value over 16

days), there is still noise in NDVI time series represented by negatively biased NDVI values. To overcome this noise, a Savitsky–Golay filter was applied to smooth the NDVI time series pixel-wise and to construct high-quality NDVI time-series datasets for further analysis. The Savitsky–Golay filter is a moving filter that fits local polynomial regression to replace negatively biased NDVI values with upper an envelope of NDVI time series (Jonsson and Eklundh, 2004). For every pixel, values of quality flags were used to assign particular weights for the calculation of new NDVI time series.

3.3.7. Spatio-temporal vegetation trends using satellite based NDVI

In this study, vegetation trends were estimated using filtered NDVI time series after a applying Savitzky–Golay filter to both AVHRR GIMMS3g (1982-2015) and MODIS (2000-2015). The annual time series was divided into two seasons: wet season (May-October) and dry season (November-April). Seasonal average NDVI values were computed for both wet and dry season of each year, as autocorrelation might be present with individual images. Vegetation trends were computed using Sen Slope, and the Mann–Kendall (MK) significance test. The output of trend analysis was a regression slope indicating the magnitude and direction of change in NDVI per year.

3.4. Results

3.4.1. Evaluation of satellite rainfall estimates

In this study four satellite-based rainfall products were evaluated against gauge rainfall from weather stations (Figure 3.1), to identify the best rainfall product (in terms of closely representing rainfall patterm from gauges) for northern Nigeria at daily, dekadal, monthly and seasonal time scales. Also satellite rainfall products were evaluated for different rainy season variables to find the best product for analyzing temporal trends in rainy season characteristics over space. For all the plots (Figures 3.2-3.12), the red line is the 1:1 line, the solid blue is linear regression line between gauge and satellite estimates and the dashed blue lines are 95 % confidence intervals (CI).

Daily comparison

Comparison between satellite-based daily rainfall estimates from ARC, CHIRPS, TARCAT and TRMM and individual rain gauge stations for the period 1998-2014 shows only weak relationships, with correlation coefficient 'R' values ranging from 0.3 to 0.5 (Figure 3.2). The best performance was observed for TARCAT (R = 0.45), followed by CHIRPS (R = 0.35), ARC (R = 0.34) and TRMM (R = 0.33), although TARCAT showed the greatest bias (0.90). The lowest RMSE value was found for TARCAT (8.1 mm/daily), followed by CHIRPS (8.7 mm/daily), ARC (8.9 mm/daily) and TRMM (10.0 mm/daily). All of the satellite products show substantial overestimation of low rainfall events and underestimation of high rainfall events. This accords with Sanogo et al (2015), who also found weak relationships between daily gauge rainfall and ARC2 satellite measurements in northern Nigeria, with R values below 0.1, and Dembélé and Zwart (2016) in Burkina Faso who observed best performance for CHIRPS (R=0.47), compared to other satellite products.

Dekadal comparison

Dekadal (10 days) comparison (Figure 3.3) shows a good agreement between gauge rainfall, and CHIRPS and TARCAT satellite estimates respectively, with correlation coefficient 'R' values between 0.50 and 0.80 for the majority of weather stations. Correlation values for TRMM (0.49-0.73) and ARC (0.24-0.69) were somewhat lower. CHIRPS was also found to have the best mean bias close to one (0.79-1.10), followed by ARC (0.74-1.12), TARCAT (0.60-1.17) and TRMM (0.73-1.21). The lowest RMSE values were found for CHIRPS (35.16 mm.dekad^{-1}), followed by TARCAT (36.37 mm.dekad^{-1}), TRMM (39.53 mm.dekad^{-1}) and ARC (42.28 mm.dekad^{-1}). The superior overall performance of CHIRPS for dekadal rainfall was also noted for Ethiopia (Bayissa et al, 2017) and Mozambique (Toté et al, 2015). All of the satellite products show overestimation of low dekadal rainfall amounts, and underestimation of high rainfall amounts, with overall negative values of mean error indicative of underestimation of dekadal rainfall by satellite for the majority of weather stations.

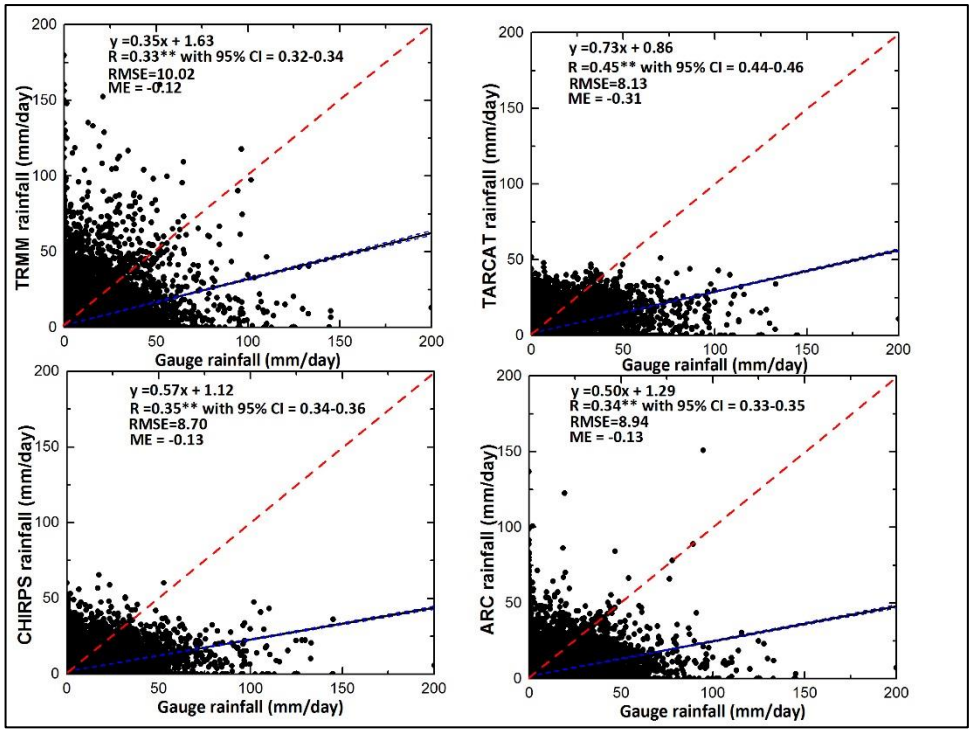

Figure 3.2 Comparison of daily rainfall, between rain gauge and satellite rainfall estimates for 1998-2014.

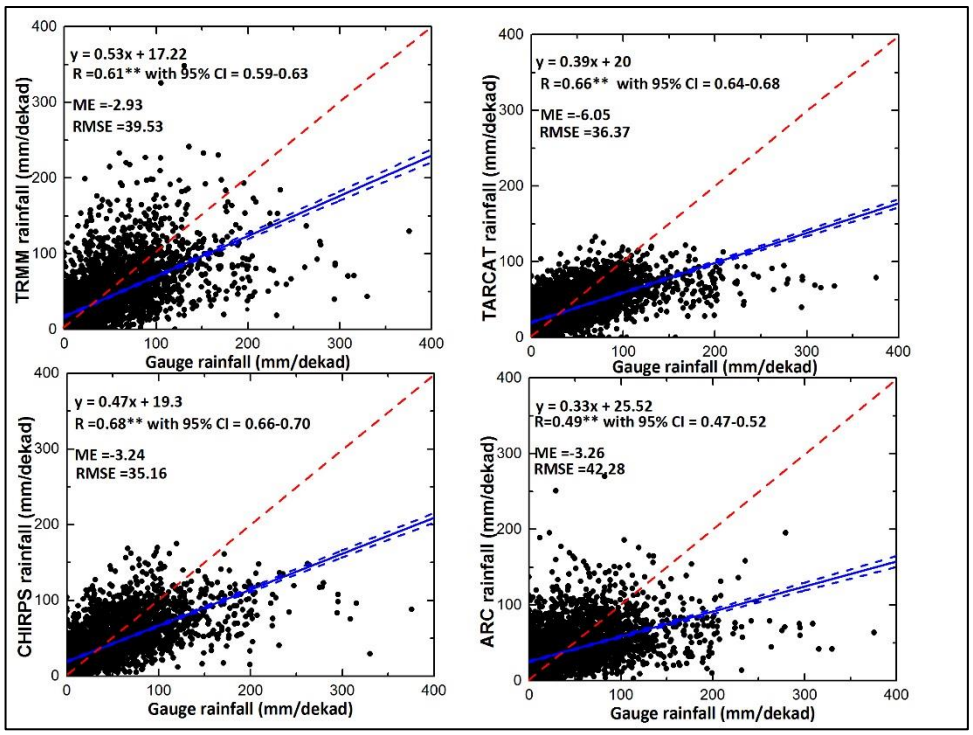

Figure 3.3 Comparison of dekadal (10 days) rainfall, between rain gauge and satellite rainfall estimates for 1998-2014.

In terms of agricultural yield prediction, such underestimation of dekadal rainfall by satellite products is not as critical as overestimation, as the major stress on the main cereal crops sorghum and millet is drought especially 15 to 20 days of no rain in mid-growing season. Thus overestimation of rainfall would tend to overlook drought periods.

Monthly comparison

Monthly satellite estimates show better performance than at daily or dekadal scales, with correlation values between 0.55-0.86 for all satellite products except for ARC (Figure 3.4). This improvement is because aggregation of daily or dekadal data into monthly values cancels out errors at daily or dekadal scales (Dembélé and Zwart, 2016). The monthly satellite estimates for all 18 weather stations for the period 1998-2014 in mm/month, compare well with gauge rainfall. Overall CHIRPS give the best results with the highest correlation value of 0.81 and lowest RMSE value of 63.47 mm/month, and for CHIRPS, the red 1:1 line is closest to the blue trend line. Lower correlation values were observed for TARCAT, TRMM and ARC of 0.77, 0.75 and 0.64 respectively. These findings are in agreement with Bayissa et al (2017) and Toté et al (2015) who reported that CHIRPS performed better than other satellite estimates at monthly scale.

Yearly comparison

Monthly rainfall data from April to October were accumulated for both satellites and gauges, to produce seasonal (yearly) rainfall totals, for the 17 years, 1998 to 2014 for the 18 weather stations. A good agreement was observed between satellite and gauge rainfall data with correlation values ranging between 0.62-0.79 (Table 3.3).

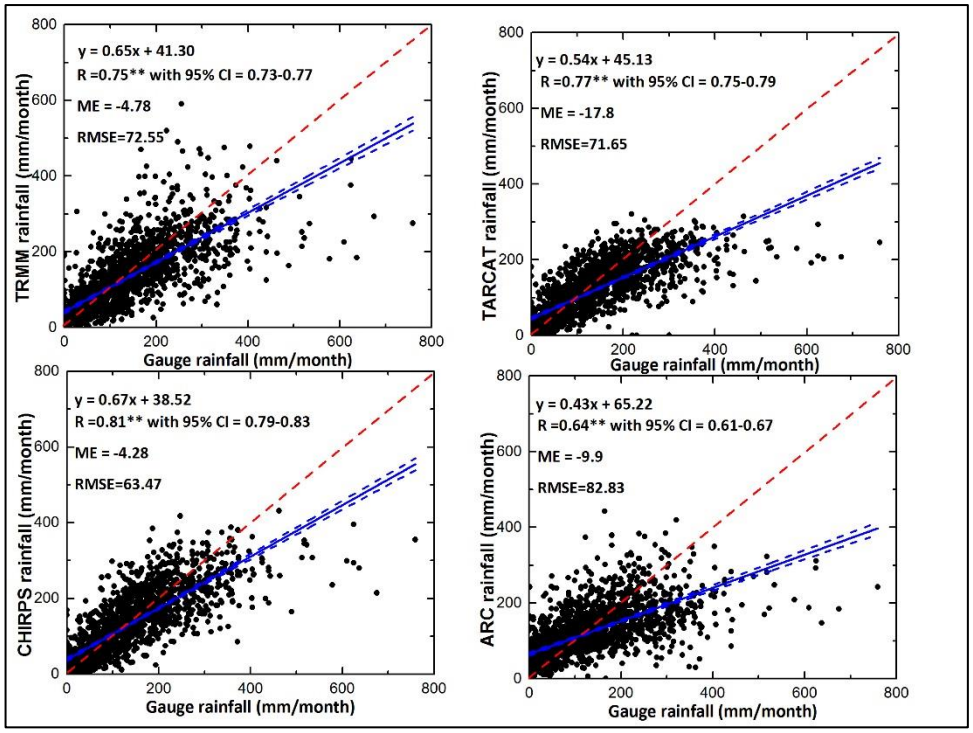

Figure 3.4 Comparison of monthly rainfall, between rain gauge and satellite rainfall estimates for 1998-2014.

Highest correlation values were observed for CHIRPS (0.79) and lowest for ARC (0.62), and a mean bias close to 1 was found both for CHIRPS and TRMM (0.97), followed by ARC (0.93) and TARCAT (0.84) respectively. The observed negative values of ME (Table 3.3) indicate that all satellite datasets underestimate seasonal rainfall compared to gauge measurements. The lowest value of mean error was observed for CHIRPS (-27.3 mm/season) followed by TRMM (-29.7 mm/season), ARC (-58.7 mm/season) and TARCAT (-141.3 mm/season) respectively. Similarly the lowest value of RMSE was found for CHIRPS (196.6 mm/season), followed by TRMM (214.3mm/season), ARC (264.4 mm/season) and TARCAT (274.3 mm/season) respectively. These findings accord with those of Bayissa et al (2017), who observed best correspondence of CHIRPS with gauge data at seasonal time scale compared to other products in Ethiopia, but disagree Dembélé and Zwarts' (2016), whose seasonal satellite indicate overestimation of annual rainfall in Burkina Faso, as our data indicate underestimation.

Table 3.3 Yearly comparison of satellite rainfall products.

	TRMM	TARCAT	CHIRPS	ARC
Correlation (R)	0.75**	0.69**	0.79**	0.62**
Bias (no units)	0.97	0.84	0.97	0.93
Mean Error (mm/season)	-29.7	-141.3	-27.3	-58.7
RMSE (mm/season)	214.3	273.9	196.6	264.4

** Statistically significant at 0.01 level.

3.4.2. Seasonal rainfall variables

A spatial correlation between three satellite datasets (TARCAT, CHIRPS and ARC) and gauge based rainfall variables for 10 weather stations was undertaken for the period 1984-2013. TRMM data are data not included as they are not available for the earlier years 1984-1997, and we observed the TRMM data quality to be consistently inferior to CHIRPS and TARCAT. For the onset and cessation of rainy season the satellite estimates compare fairly well with the gauge-based data, with correlation coefficient R values ranging between 0.53 and 0.65 for onset, and 0.59 and 0.70 for cessation, with ARC showing the lowest values (Figure 3.5).

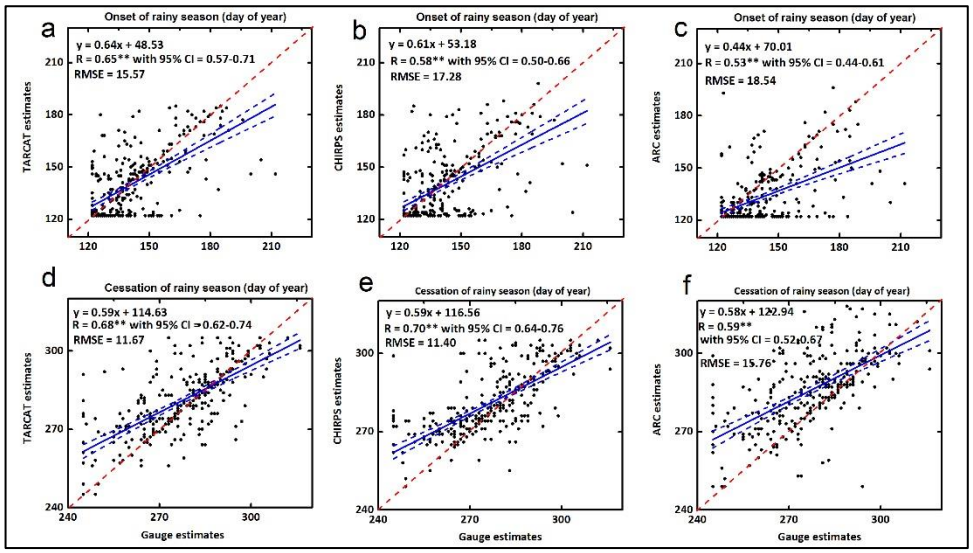

Figure 3.5 Comparison between gauge and satellite, for onset of rainy season (a-c) and cessation of rainy season (d-f) for all weather stations (1984-2013).

Similarly for length of season and amount of rainfall, a linear relationship between satellite and gauge based rainfall measures is observed with R values between 0.63 and 0.74 for season length, and 0.57 and 0.78 for rainfall amount. Again ARC indicates relatively low values of R (0.63, 0.57) for length and seasonal amount of rainfall compared to CHIRPS (0.71 and 0.78) and TARCAT (0.74 and 0.61) (Figure 3.6).

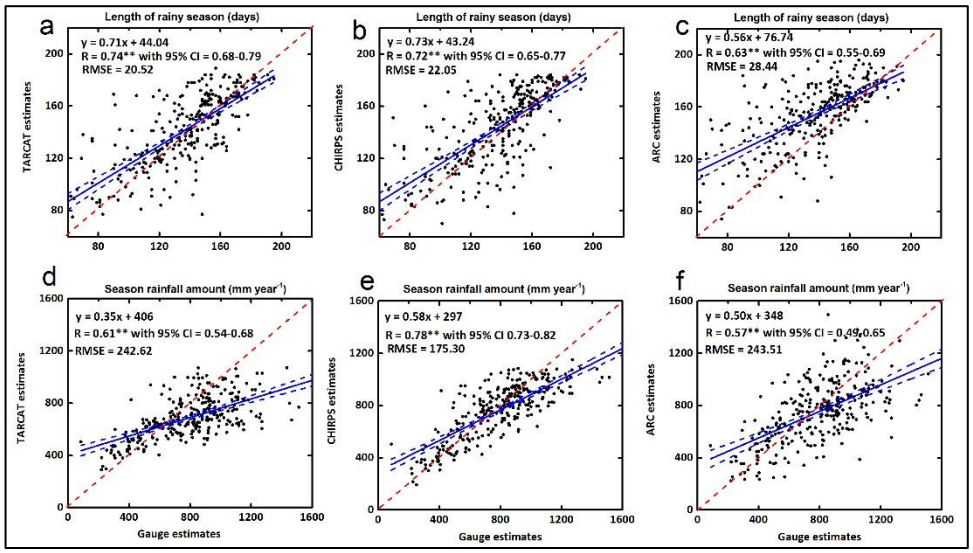

Figure 3.6 Comparison between gauge and satellite, for length of rainy season (a-c) and seasonal rainfall amount (d-f) for all weather stations (1984-2013).

For the total number of rainy days per season, a high value of R = 0.79 was observed for CHIRPS compared to ARC (0.74) and TARCAT (0.72) (Figure 3.7). However, a marked discrepancy existed for rainy days with given stepped intervals of rainfall (Figures 3.8-3.9). For rainy days with low rainfall amounts of 1-10 and 10-20 mm/day, a higher number of rainy days were observed for satellite products compared to gauge measurements (Figure 3.8), and this is in agreement with Zhang et al (2017) who also report a higher number of small rainfall events estimated by satellite compared to gauge data.

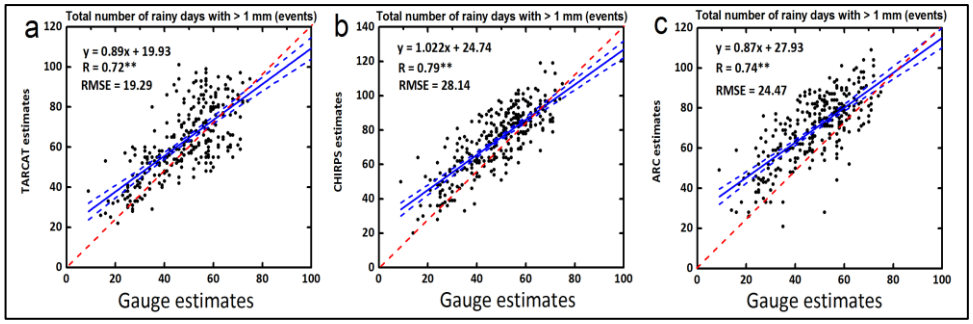

Figure 3.7 Comparison between gauge and satellite, for the total number of rainy days with at least 1 mm rainfall (a-c).

However, although rainfall variables based on single-day rainfall events may show bias due to difference in scale between point-based gauge and large pixel size of satellite data, the temporal trends in rainfall variables from satellite data are still expected to be valid. It is interesting to note that the error in satellite estimates for high rainfall events > 30 mm/day is totally reversed, with lower frequency observed for satellite measurements than for ground stations (Figure 3.9), and this is in line with the findings of Toté et al (2015), who reported large underestimation of high rainfall events by the satellite product. In this study, CHIRPS outperformed ARC and TARCAT for all stepped intervals of rainfall events, (Figures 3.8-3.9) except for the lowest class 1-10mm/day (Figure 3.8 a-c), when TARCAT obtained the lowest error..

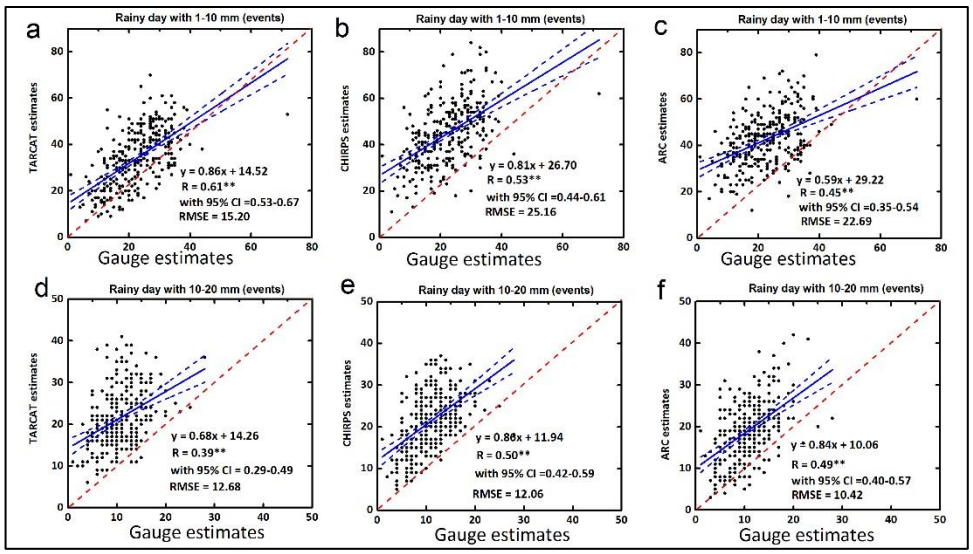

Figure 3.8 Comparison between gauge and satellite, for the number of rainy days with 1-10 mm (a-c) and 10-20 mm (d-f) for all weather stations (1984-2013).

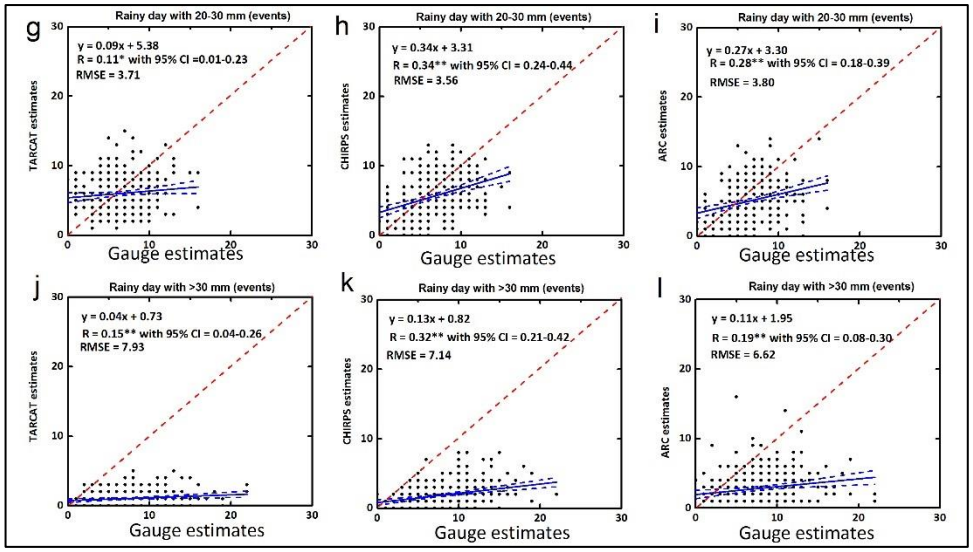

Figure 3.9 Comparison between gauge and satellite, for the number of rainy days with 10-30 mm (a-c) and >30 mm rainfall (d-f) for all weather stations (1984-2013).

Due to the higher representation of low rainfall events by satellite products, a higher total number of rainy days (Figure 3.7a-c) and higher frequency of rainfall (Figure 3.10 a-c) are observed for satellite products. Correspondingly a lower representation of intensity (Figure 3.10 d-f) of rainfall events for satellite products is observed, as Intensity is the ratio between seasonal rainfall amount and total number of rainy days per season.

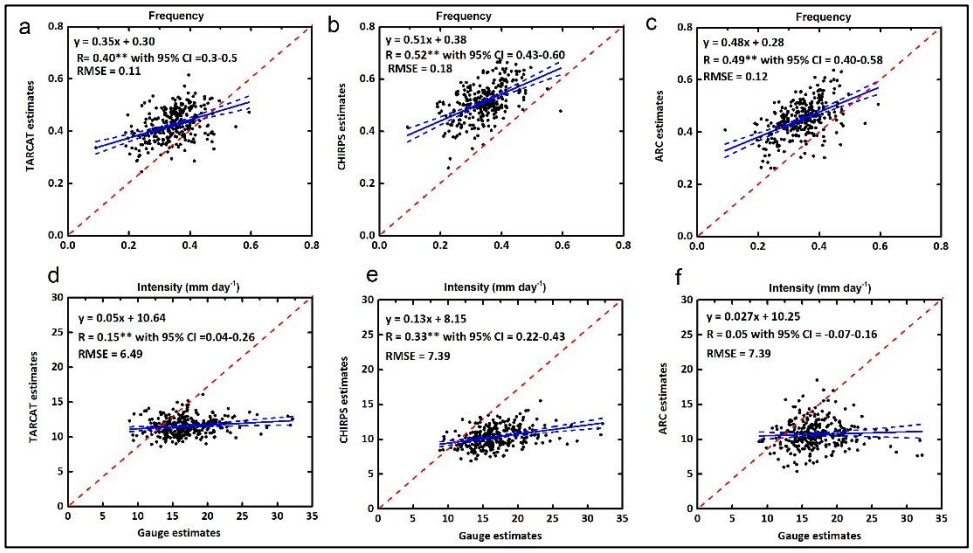

Figure 3.10 Comparison between gauge and satellite, for frequency (a-c) and intensity of rainy season (d-f) for all weather stations (1984-2013).

The higher number of low rainfall events captured by satellite products affects the estimation of dry spell variables, with a lower representation of dry spells. Thus we observe a very weak correlation for number of dry spells (0.02-0.09), mean length of dry spells (0.03-0.13) and cumulative length of dry spells (-0.005-0.03) for all of the three satellite datasets (Figures 3.11a-f and 3.12 d-f). Toté et al (2015) also found a large error in the detection of dry spells, with RFE data (only available since 2001) show the best performance compared to CHIRPS and TARCAT.

The satellite rainfall variables best representing gauge data were total annual (seasonal) rainfall, the total number of rainy days, and length of rainy season. These good results for variables measured across the whole rainy season, may be due to some extent, to positive and negative errors cancelling out.

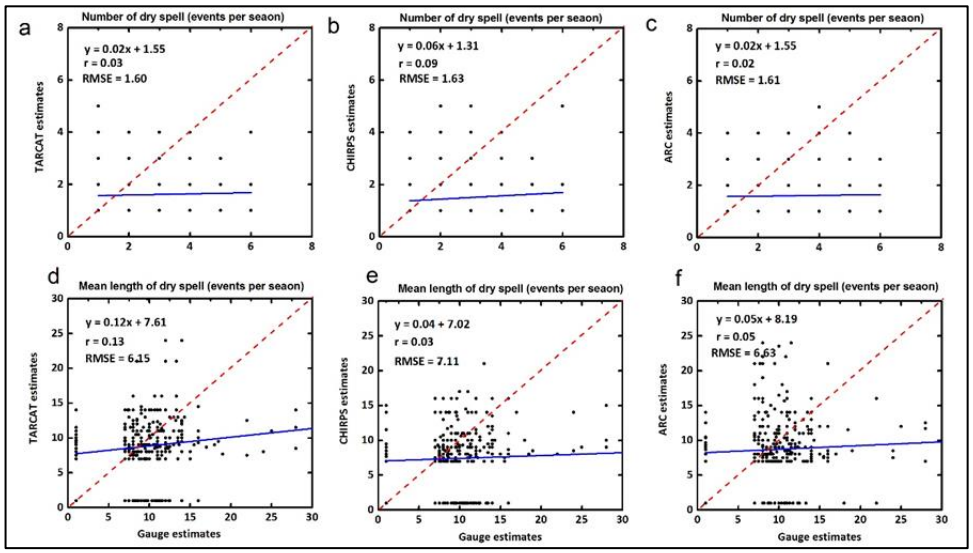

Figure 3.11 Comparison between gauge and satellite, for number of dry spells (a-c) and mean length of dry spell (d-f) for all weather stations (1984-2013).

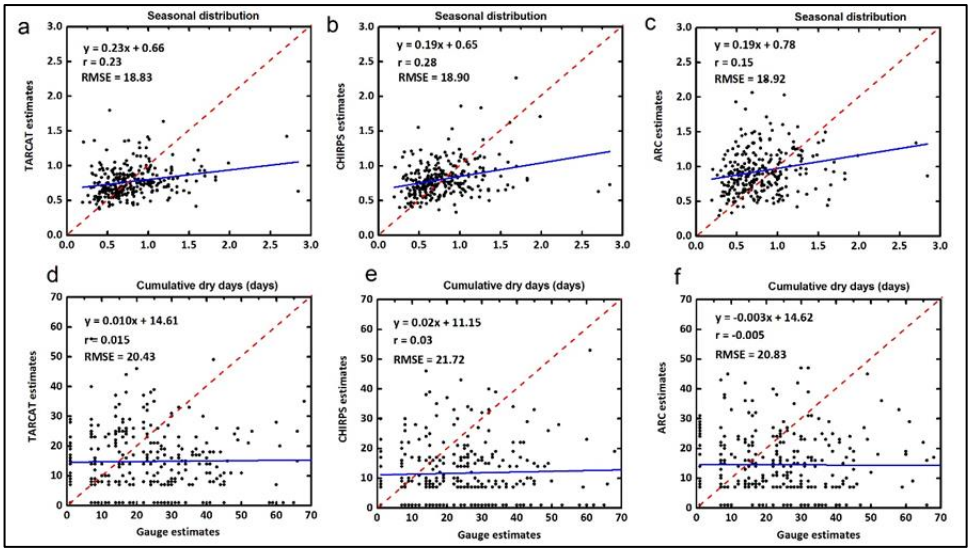

Figure 3.12 Comparison between gauge and satellite, for seasonal distribution (a-c) and cumulative dry days of all dry spells during rainy season (d-f) for (1984-2013).

The overestimation of rainy days by satellites is due to detection of low and patchy rain within a pixel, compared to a ground point where no rain has fallen. However, this is a serious shortcoming of satellite estimates, as this could suggest adequate rainfall during a drought. Notwithstanding, although rainfall variables based on single-day rainfall events may show bias due to difference in scale between point-based gauge and large area satellite data, the temporal trends in rainfall variables from satellite data are still expected to be valid.

3.4.3. Temporal trends for northern Nigeria using gauge based rainfall variables

Temporal trends over northern Nigeria were estimated over three decades, from 1984 to 2013 using the average value of all nine gauges for every year. Those stations within northern Nigeria are Nguru, Maiduguri, Minjibir, IAR Kano, Kadawa, Zaria, Gombe, Bauchi and Yola. Trends were estimated using Sen's slope (with slope expressing changes in units per year). Positive (negative) values indicate increasing (decreasing) rainfall variable trends and statistically significant changes are denoted by asterisks (+=p≤0.1, * =p≤ 0.05; ** =p≤ 0.01; *** =p ≤ 0.001) with respect to the Mann-Kendall test accounting for temporal autocorrelation. Clear significant and positive trends were observed for the seasonal rainfall amount, cessation and length, as well as for rainfall intensity,

the total number of rainy days and rainy days with more than 30 mm rainfall (Table 3.4). Our findings support those of Sanogo et al (2015), who observed similar trends from 1980 to 2010, using all gauges averaged over the West African Sahel region (Latitude 9°-20° N).

The rainy season starting date, which is critical for farming showed non-significant trends (Table 3.4), which is in agreement with Sanogo et al's (2015) gauge-based observations in the Sahel. Even during the drought decades of 1970s and 80s, no changes in rainy season onset were observed for north western Nigeria (Hess et al, 1995). We also observed significant positive trends for number of days of heavy rainfall over 30 mm, and in consecutive wet days, but insignificant trends for dry spells (Table 3.4) which accords with Sanogo et al's (2015) observations for the Sahel. This suggests that recovery of rainfall in northern Nigeria since the drought decades of 1970s and 80s is mainly related to increase in number of rainy days, a higher number of extreme rainfall events and later cessation of rainy season, rather than earlier onset of rains, or a reduction in the length or number of dry spells.

Table 3.4 Trends from 1984 to 2013 for gauge based rainfall variables (averages over all stations).

	Season rainfall variables	Gauge- trends
1	Onset of Rainy Season (day of year)	-0.18
2	Cessation of Rainy Season (day of year)	0.44*
3	Length of Rainy Season (days)	0.53*
4	Season rainfall amount (mm year^{-1})	8.2**
5	Frequency	0
6	Intensity (mm day^{-1})	0.12**
7	Number of rainy days with 1-10 mm (days)	0
8	Number of rainy days with 10-20 mm (days)	0.02
9	Number of rainy days with 20-30 mm (days)	0.02
10	Number of rainy days > 30 mm (days)	0.11**
11	Season distribution	-0.001
12	Total number of rainy days with > 1mm (days)	0.18^{+}
13	Cumulative dry days (days)	0.21
14	Length of Dry Spell (days event^{-1})	0.03
15	Number of Dry Spells (events year^{-1})	0.002

On the other hand, while Hess et al. (1995) studied rainfall trends based on three raing gauges (Daura, Maiduguri and Nguru) in northern Nigeria from 1961 to 1990, in terms of the number of rainy days per season. They found a dramatic fall in the average number of rainy days per rainy season between the 1960s and the 1980s. However our study which extends to 2015, indicates a recovery in the number of rainy days per rainy season in the last two decades (Table 3.5).

Table 3.5 Average number of rainy days per year for five different decades.

	1951-1960	1961-1970	1971-1980	1981-1990	1991-2000	2001-2010
Maiduguri		47	35	30	42	41
Nguru		36	27	20	29	27
Daura	46.7	42.4	37	29.9	35.5	

3.4.4. Spatial distribution of monthly and annual rainfall trends

Monthly rainfall data are required to investigate trends in total annual rainfall as well as its seasonal distribution. Thus the spatial aspects of trends in monthly and total annual rainfall between 1984 and 2013 were investigated based on both rain gauge data and CHIRPS data for the period 1981-2015 (Table 3.6 and Figures 3.13), as CHIRPS proved to be the most robust satellite rainfall product, and can be used to represent the typical performance of satellite rainfall datasets. CHIRPS satellite data for the 35-year period 1981 to 2015, show clear positive trends in annual rainfall over most of northern Nigeria (Figure 3.14b). The CHIRPS observations are supported by clear positive trends in annual rainfall evident at stations across northern Nigeria (Table 3.6), which confirms rainfall recovery after the droughts of the 1980s. Indeed, for the period 1984 to 2013, our gauge data indicate an increasing trend for annual rainfall by 10.2, 4.4 and 4.2 mm/year for Maiduguri, Nguru and Potiskum respectively (Table 3.6).

Our satellite and gauge-based results conflict with Sanogo et al's (2015) and Zhang et al's (2017) ARC-based estimates of rainfall trends for northern Nigeria, as they report negative but insignificant trends for areas surrounding our climate stations of Kaduna, Zaria, Kano, Minjibir and Gusau. They suggest that decline in the number of GTS ground stations for these areas explained the observed negative trends using ARC-based satellite data. The reliance of CHIRPS on multiple satellite products including visible, thermal infra-red and microwave as opposed to ARC's emphasis on ground station data may explain the better result for long-term rainfall trends from CHIRPS. Our CHIRPS satellite-based trends of increasing rainfall (Figure 3.13 and 3.14b) are in line with our gauge-based observations (Table 3.6).

Table 3.6 Trends for gauge based total annual and monthly rainfall using Sen's slope for the period 1981-2015. Statistically significant changes are denoted by asterisks (+=p≤0.1, * =p≤ 0.05; ** =p≤ 0.01; *** =p ≤ 0.001) with respect to the Mann-Kendall test accounting for temporal autocorrelation.

Station	Total Annual	April	May	June	July	August	September	October
Sokoto	5.6*	0	0.9	0.2	0.2	2.1*	0.9	0.3**
Nguru	4.4+	0	0.3	1.1+	-0.02	1.9	1.23	0.2*
Gusau	2.6	0	0.4	-0.2	0.7	1.1	-1.6	0.9*
Katsina	7.5**	0	0.3	0.9	-0.06	4.3**	0.4	0.3**
Minjibir	8.1+	0	-0.06	1.0	2.5*	3.2	1.7+	0.4*
Kano	11.2**	0	0.3	2.7*	3.1*	3.9	1.6	0.07
Maiduguri	10.2***	0	0.2	1.8	2.6	3.2	2.1	0.6
Kadawa	6	0	-0.2	-0.8	-0.3	4.8+	1.4	1.2
Potiskum	4.2	0	0.2	1.7*	1.3*	0.6	2.7*	0.1
Zaria	9.9***	0.3	0.9	-0.07	0.7	2.9	4.6**	1.4+
Yelwa	4.1	0.3	0.4	-0.002	-0.4	3.6	2.5*	0.6
Kaduna	1.7	0.07	-0.08	-0.4	0	-0.9	1.7	2.1*
Bauchi	21.4***	0.3	-0.8	3.3*	3.7	6.2*	2.3	0.8
Yola	-5.7	-0.9	-1.3+	2.2+	-3.2**	-1.3	1.1	0.9
Ibi	-1.2	0.1	-1.4	-0.1	-0.5	-3.2*	0.9	0.9
Daura	3.9+	0	0.28	1.0	1.3*	4.1**	0.5*	0.33**
Gombe	0.69	0.33	-1.4+	0.09	-1.58	1.96	0.61	1.3+
Bida	0.81	-0.75	-0.41	0.75	0.76	0.28	0.18	3.3*

Our CHIRPS satellite data observe a trend of increased rainy season length, with more rain in the months of August to October (Figures 3.13 and 3.15), and this is supported by our ground stations (Table 3.7). Based on gauge rainfall observations for the period 1984-2013, trends were also calculated for monthly regional rainfall (averaged over all stations in northern Nigeria) over the period 1984-2013 (Table 3.7). Our gauge observations indicate that the observed increase in annual rainfall is due to increases of 1-2 mm/year in each of the months August to October (Table 3.7) and these months contribute over 50% of annual rainfall amount. This observed stronger rainfall recovery in the months of August and September, supports observations by Sanogo et al (2015).

In August, the month with greatest overall increase in rainfall, distribution of the increase is extremely patchy, with large increases of over 4 mm in the northeast, but non-significant trends in many other areas. A marked decrease in September around the Federal Captal Territory in the south, is also evident. Thus CHIRPS satellite products give a better spatial representation of overall long term rainfall

trends, growing season length, and distribution of rainfall within the growing season, than ground station data.

Hess et al's (1995) gauge observations indicate a reduction in the length of rainy season in northeast Nigeria over the period 1961 to 1990. However our gauge data for the later period 1984 to 2013, for northeast Nigeria represented by Nguru and Maiduguri show a trend for increased length of rainy season by 1.33 days/year. These findings are also supported by our satellite-based CHIRPS data which confirm the trend of increased rainy season length computed from ground stations (Figure 3.15).

Table 3.7 Trends for gauge based monthly rainfall (average for all gauges in northern Nigeria) for the period 1984-2013.

Months	**March**	**April**	**May**	**June**	**July**	**August**	**September**	**October**
Trend Slope	-0.08**	-0.06	-0.07	0.74**	0.78	2.22**	1.40+	1.05**
Contribution to annual rainfall (%)	0.37	2.28	7.90	13.46	23.36	30.25	18.24	4.10

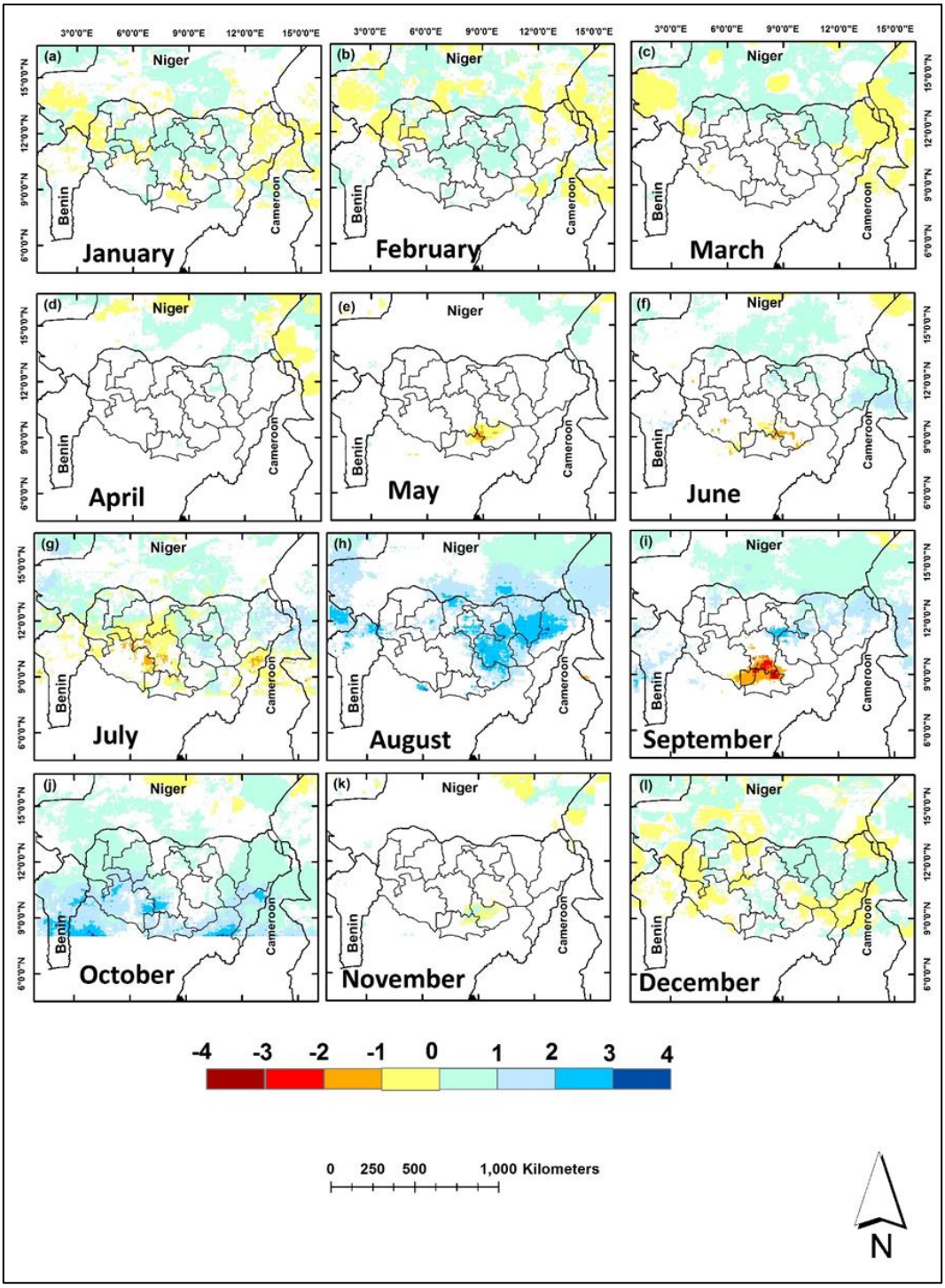

Figure 3.13 Spatial temporal trends in CHIRPS based monthly rainfall between 1981 to 2015 based on Sen's slope expressing change in monthly rainfall in mm/year. White areas showing non-significant trends at 90% confidence level with respect to the Mann–Kendall test.

3.4.5. Spatial temporal trends in CHIRPS rainfall variables (1981-2016)

In order to understand detailed spatial distribution and trends in rainfall characteristics over the whole of northern Nigeria, spatio-temporal trends of CHIRPS-based rainfall variables were calculated for those variables which showed a good agreement between satellite and gauge data. CHIRPS satellite-based observations indicate significant positive changes between 1981 and 2015 for seasonal rainfall amount, which represents the traditional May to September growing season, and these increases are most marked in northeastern and north central Nigeria (Figure 3.14) around the cities of Maiduguri and Kano, with dense rural populations dependent on agriculture. A significant but less marked increase in seasonal rainfall is also evident in the extreme northwest of Nigeria around the city of Sokoto, also with a densely settled rural hinterland. Significant positive changes across the whole region are also observed for total annual rainfall amount and the total number of rainy days (Figure 3.14). However, the distributions are extremely patchy, with some areas gaining over 9 mm annual rainfall, adjacent to areas with no gain.

The length of rainy season also showed significant positive trends over most of northern Nigeria (Figure 3.15), indicating that the rainy season has become longer in recent years, due to a late ending. The onset of rainy season shows non-significant trends in most parts of northern Nigeria, so indicating little change in the start of the rainy season, thus the longer rainy season appears mainly due to later cessation of rains.

Because discrepancies between gauge and satellite data for stepped rainfall amounts observed in section 3.4.2 and Table 3.4, (with a satellite bias towards observing a higher number of low, and lower number of high, rainfall events compared to gauge data) are consistent, and thus thought not to affect the detection of trends, these data are also considered here. Other variables which proved to have large discrepancies, namely length and number of dry spells are also considered.

The number, cumulative length and average length of dry spells (Figure 3.17) show a decreasing trend over the whole area but especially in northwestern

Nigeria. This would have favourable implications for crop production and crop security, as a non-interrupted supply of moisture throughout the growing season is essential for a good yield.

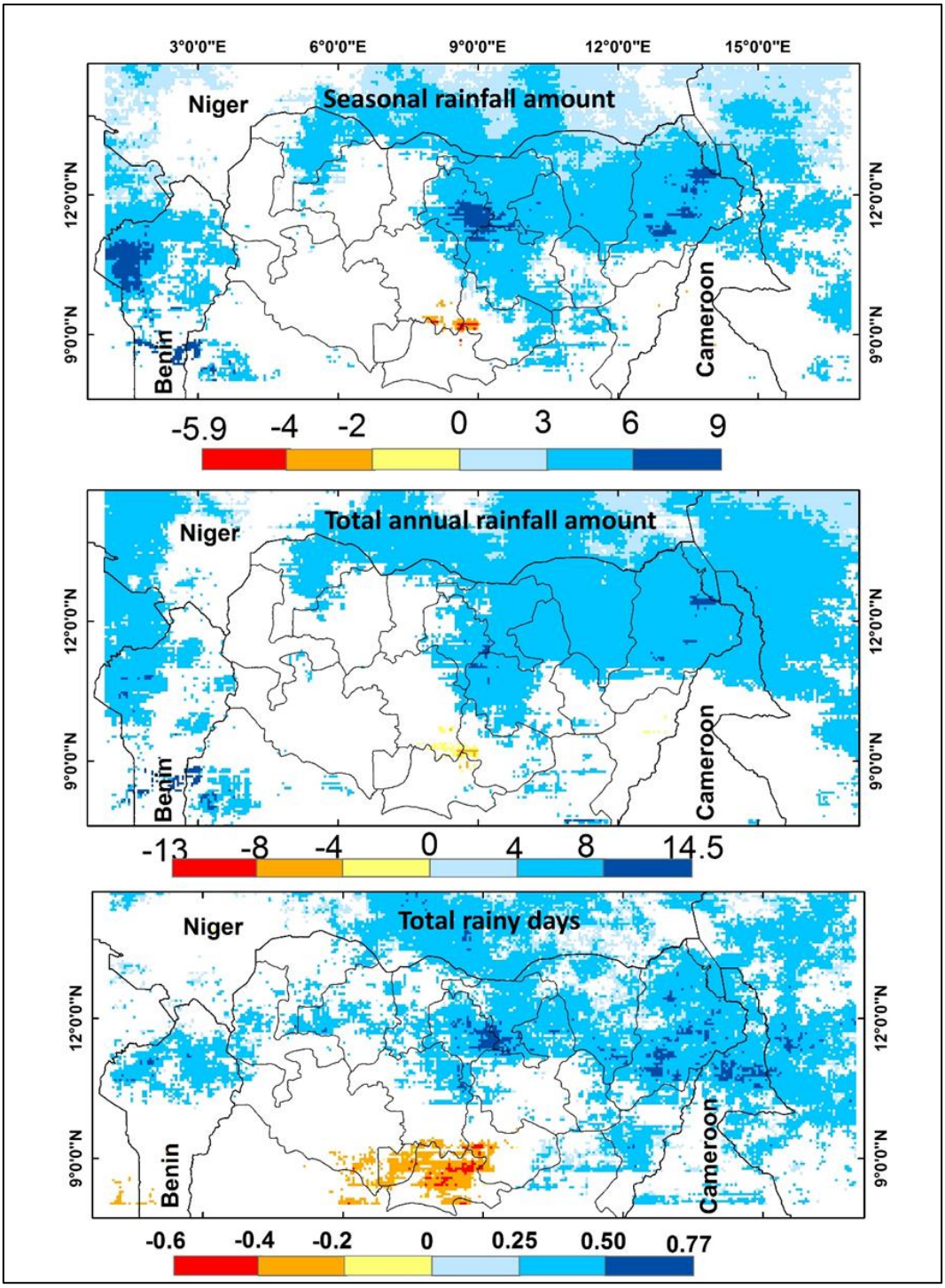

Figure 3.14 Spatial temporal trends for seasonal rainfall, total annual rainfall and number of rainy days using CHIRPS data between 1981 and 2015 based on Sen's slope.

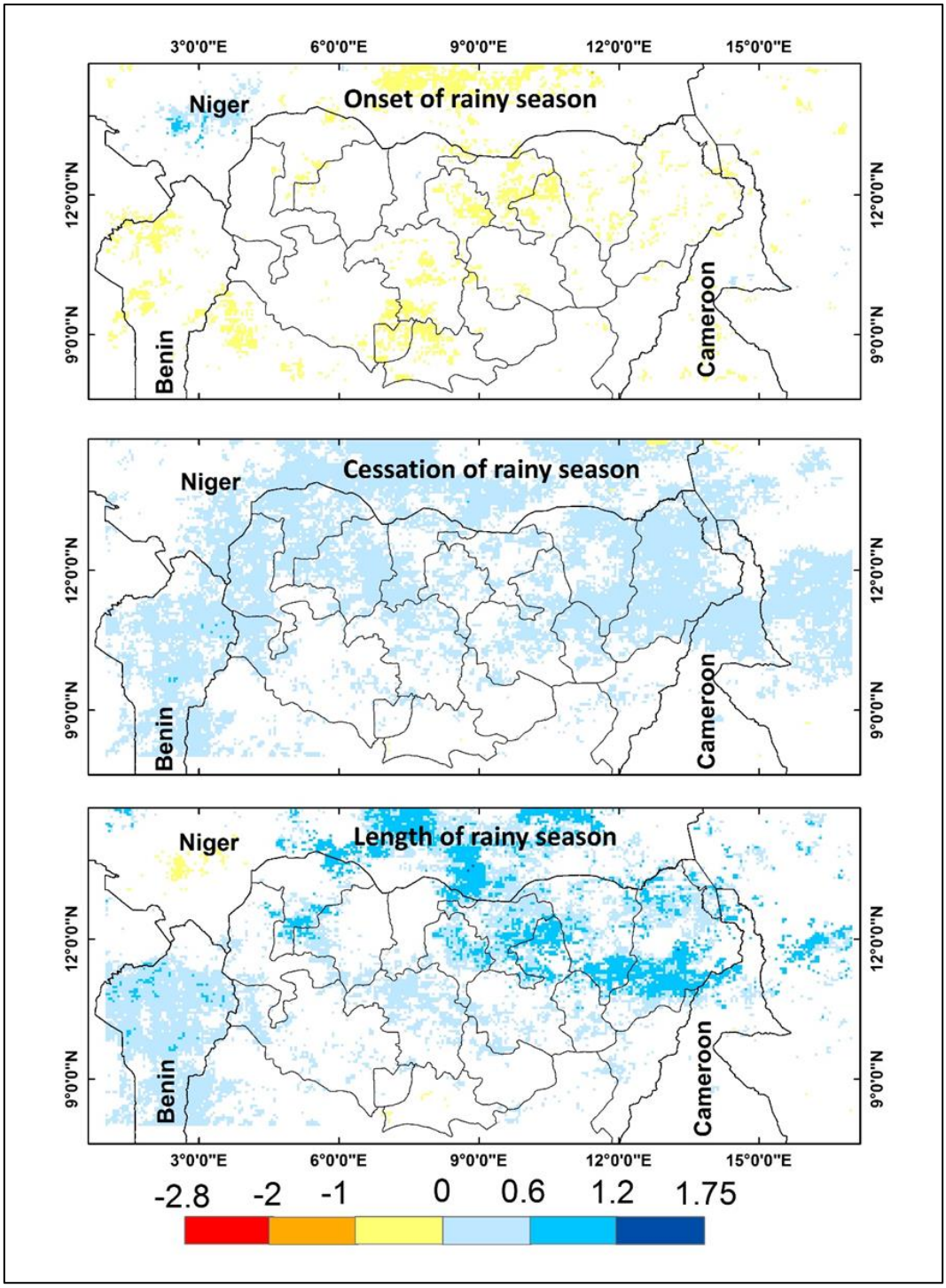

Figure 3.15 Spatial temporal trends for seasonal onset, cessation and length of rainy season using CHIRPS data between 1981 and 2015 based on Sen's slope expressing changes in days/year.

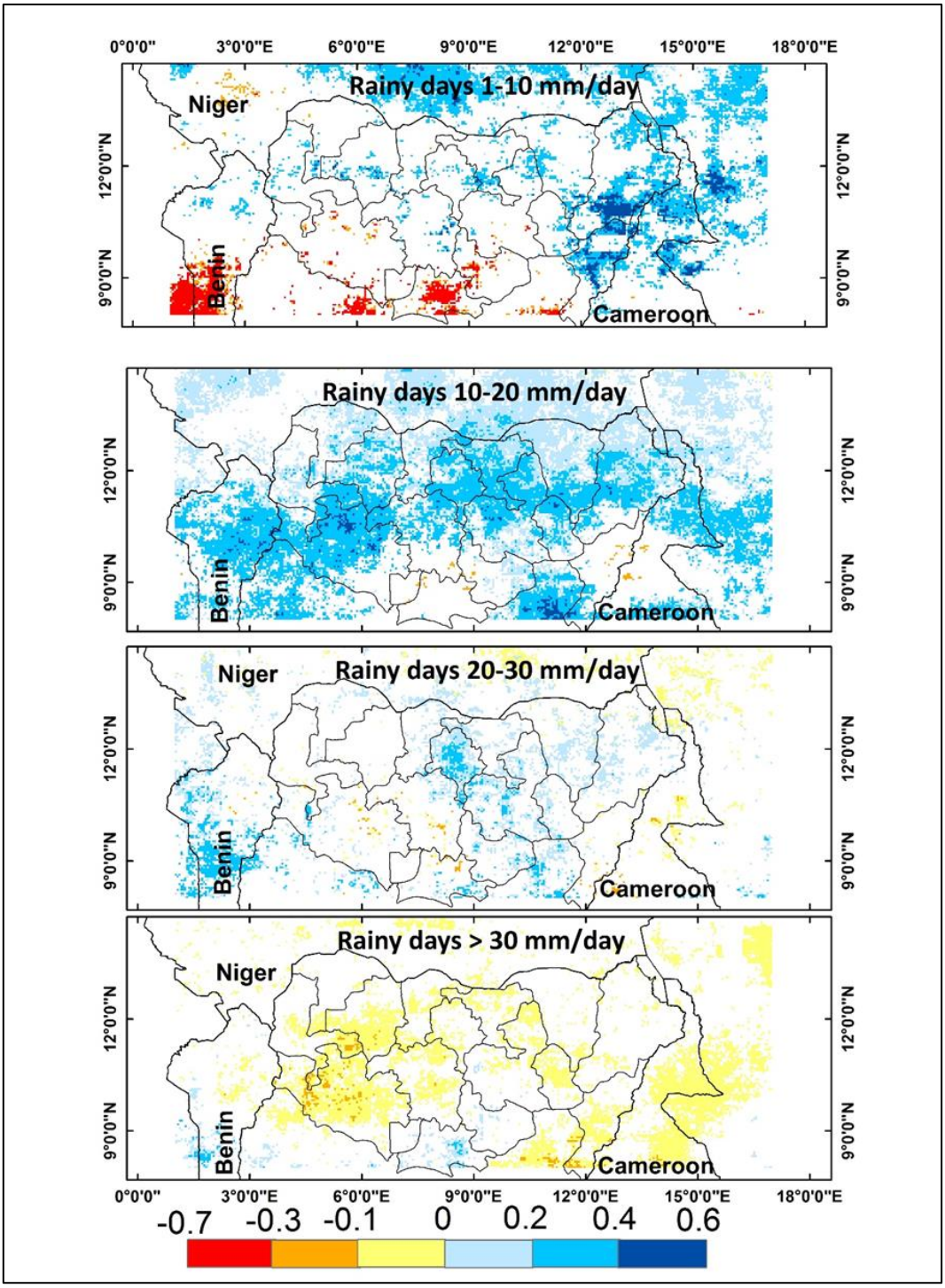

Figure 3.16 Spatial temporal trends for number of days with rainfall 1-10, 10-20, 20-30 and > 30 mm/day using CHIRPS data between 1981 and 2015 based on Sen's slope expressing changes in days/year.

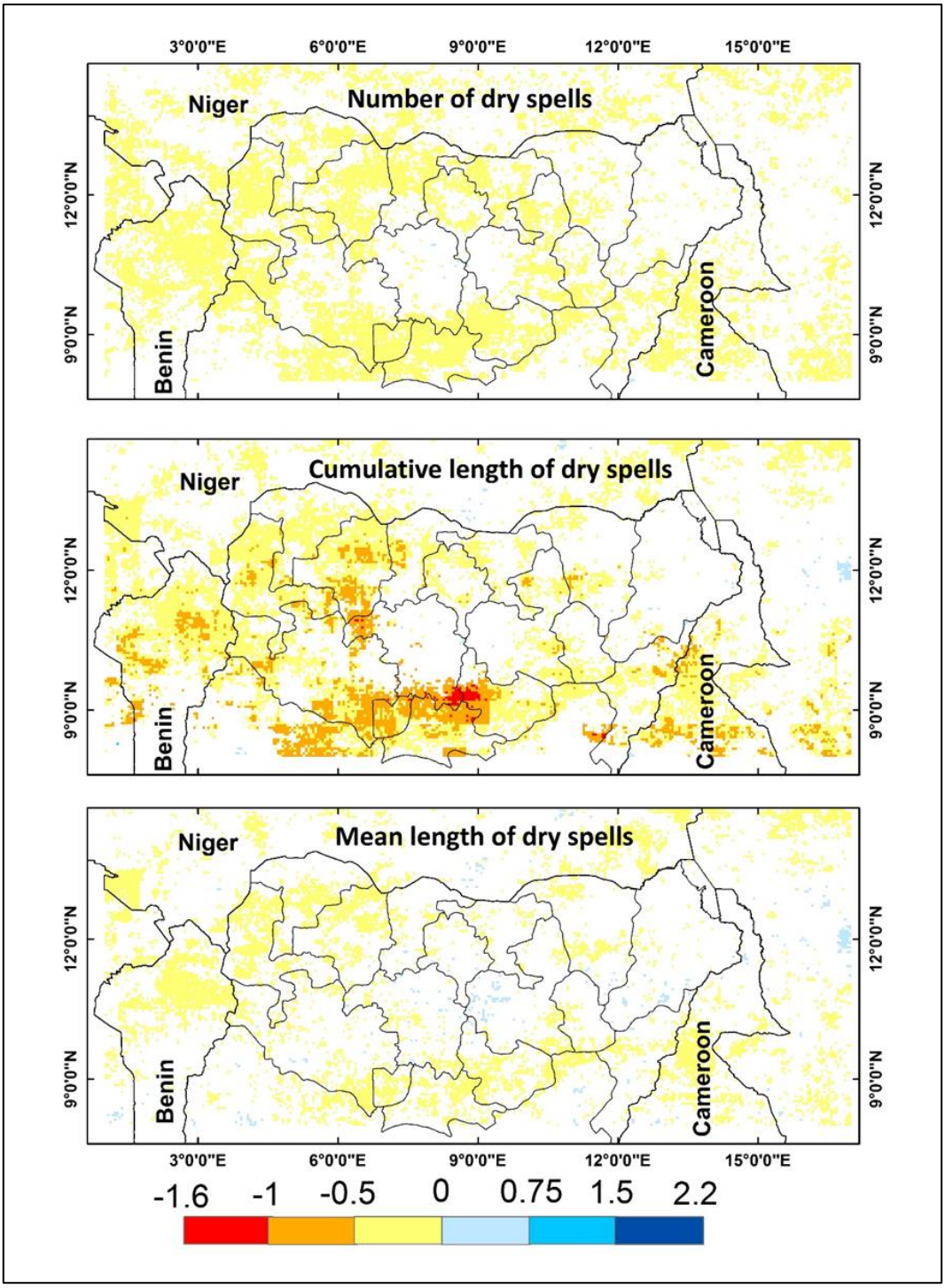

Figure 3.17 Spatial temporal trends for total number, cumulative length and mean length of dry spells using CHIRPS data between 1981 and 2015 based on Sen's slope.

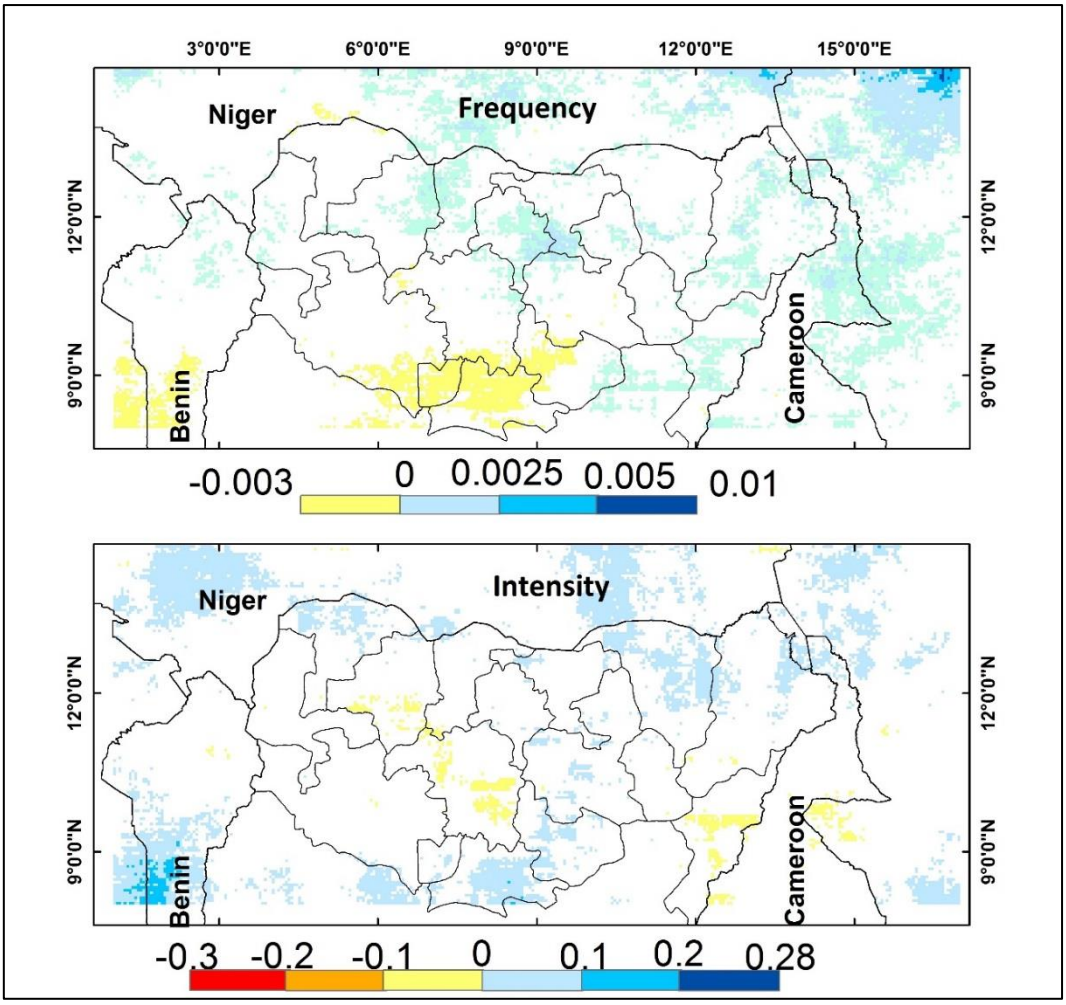

Figure 3.18 Spatial temporal trends for rainfall frequency and intensity using CHIRPS data between 1981 and 2015 based on Sen's slope.

3.4.6. Vegetation trends using NDVI

Despite widespread droughts in the 1970s and 1980s, along with dramatic reduction in rainfall during those drought decades, vegetation trends in the Sudan zone of Nigeria based on coarse resolution GIMMS 3g NDVI show significant greening for both wet (May-October) and dry (November-April) seasons over the 34 period 1982 to 2015 (Figure 3.19). A significant increase in annual rainfall during this period partly explains most of these greening trends. However, there is no close spatial correspondence between rainfall and NDVI trends (Figures 3.14 and 3.19), because the spatial pattern is controlled by human factors. According to Herrmann et al (2005), most of the observed greening in the Sahel is not only by increasing rainfall, even though there is a high correlation between vegetation and rainfall. The lack of correspondence may be

because the NDVI depends both on natural vegetation (grasses, shrubs, forest and plantations) as well as cultivated vegetation, and in northern Nigeria cultivated vegetation takes up more land space than the natural vegetation. Varying tree cover (natural regeneration and plantation program) and land cover (increase in agricultural or farmland areas due to large increase in population) also play an important role for the spatial variability in vegetation trends. Moreover due to population growth, planting of crops in the rainy season has increased and a greater percentage of land is planted and thus supporting vegetation, leading to higher NDVI over the 35-year period. So the observed pattern is not controlled by climate, but by human factors.

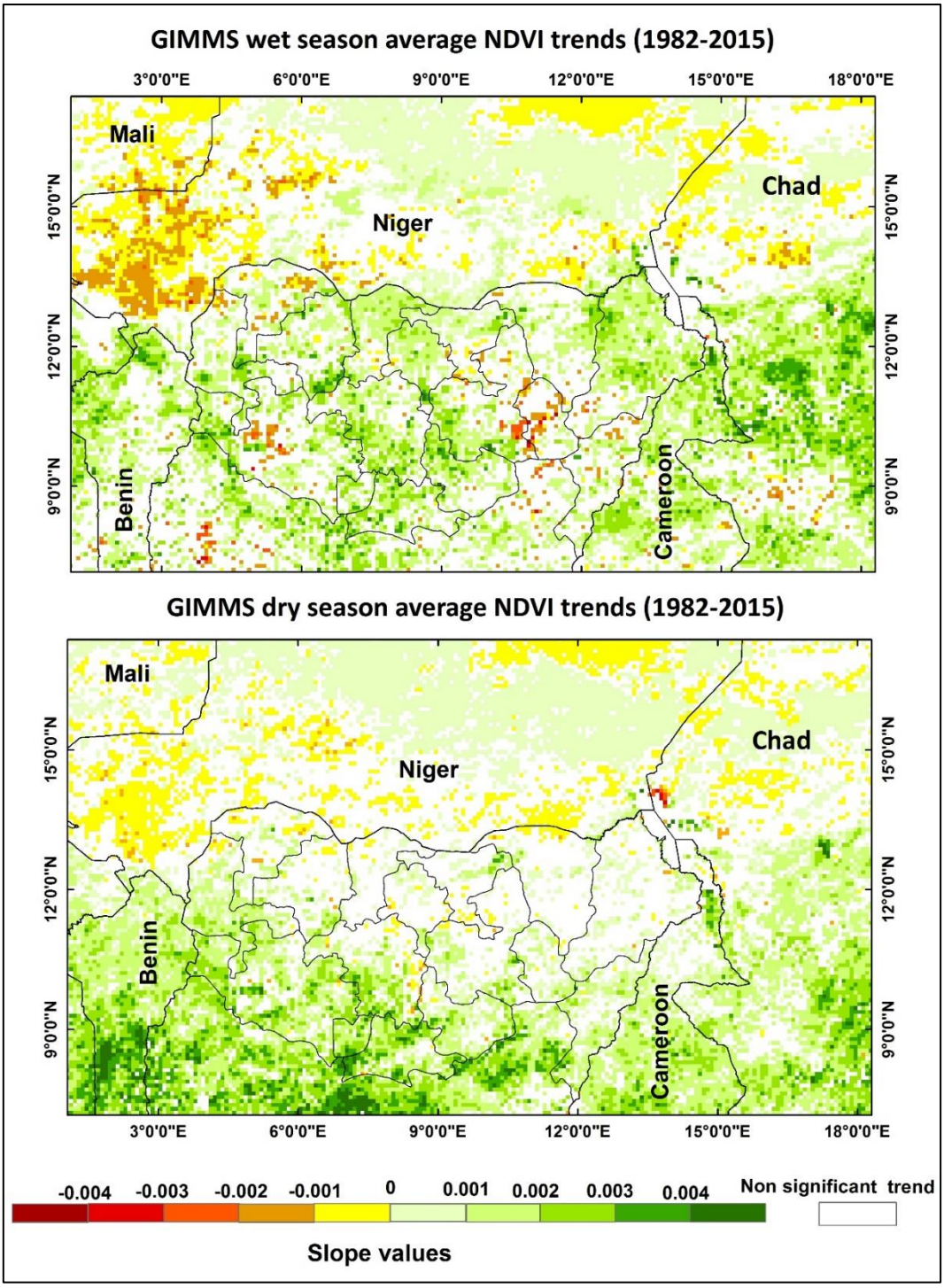

Figure 3.19 Spatial temporal trends for wet and dry season using GIMMS 3g NDVI between 1982 and 2015 based on Sen's slope expressing NDVI changes per year.

3.5. Discussion

Of the four satellite rainfall products examined, CHIRPS demonstrated the best results with consistently higher correlation, a Bias closest to 1 and lower error, when compared to ground station data. The robustness of satellite rainfall estimates increased with increasing aggregations of daily data, due to cancelling out of positive and negative errors. Thus for dekadal (monthly) data, CHIRPS, with R of 0.67 (0.81) and Bias close to 1, of 0.95 (0.98)) observed good results. The observed underestimation of dekadal rainfall by all four satellite products, with ME <1, is not as critical for agricultural yield prediction as overestimation, as the major stress on the main cereal crops of northern Nigeria, sorghum and millet is drought, especially 15 to 20 days of no rain in mid-growing season. For drought monitoring, overestimation of satellite rainfall (ME >1) should be avoided, as it would tend to overlook drought periods.

All the satellite products appear to overestimate low rainfall events, leading to overestimation of the number of rainy days in a season. This may be the result of the sensors' inability to differentiate between drizzly days and rainy days (Dembélé and Zwart, 2016; Thiemig et al., 2012; Toté et al., 2015) as their spatial scales are much larger than the point locations of rain gauges, and drizzle is likely to be more patchy than heavier rainfall. Additionally, comparing point based measurements with large area pixel values would lead to a positive bias for variables with high spatial variability like rainfall in West Africa which occurs by local convective clouds (Fensholt et al., 2006). Thus events with low rainfall of 1-10 and 10-20 mm are overestimated by satellite products due to large pixel size of the satellite product compared to point based gauge locations. Although this overestimation appears to be a serious deficiency of satellite-based estimates of drought during the growing season, with consequences for crop yields, all satellite products have the opposite tendency for high rainfall events, with underestimation. Thus for dekadal, monthly and seasonal rainfall the overall tendency is slight underestimation, and the overall estimates of rainfall amounts are good.

The satellite rainfall variables best representing gauge based data were variables which are measured across the whole rainy season, probably due to positive and

negative errors cancelling out. Thus good results were obtained for total annual (seasonal) rainfall, the total number of rainy days, and length of rainy season.

For estimating temporal trends for rainfall variables averaged over stations in northern Nigeria, our gauge data indicate recovery of rainfall in northern Nigeria since the drought decades of 1970s and 80s. This recovery, observed from both gauge and CHIRPS data between 1981 and 2015 appears to be due to increases of about 2 mm a year in the later part of the rainy season from August to October, with these months now contributing over 50% of annual rainfall. Thus both data types observed stronger rainfall recovery in the months of August and September, and CHIRPS data suggest particularly strong recovery in the northeastern states. Since sorghum enters a high water use period in the late growing season in August, this reduces the risk of late drought impeding the swelling of grain which affects dry weight production.

Furthermore, our observed significant positive trends for number of days of heavy rainfall over 30 mm, and for consecutive wet days, but insignificant trends for dry spells suggests that this recent rainfall recovery may be related to increase in number of rainy days, a higher number of extreme rainfall events and later cessation of rainy season, rather than a reduction in the length or number of dry spells. The onset of rainy season shows small negative (earlier start), but non-significant trends in most parts of northern Nigeria, so indicating little change in the start of the rainy season. Thus longer rainy season in recent years, appears to be due to a later cessation of rains.

Conversely to gauge data averaged over the whole of northern Nigeria, which indicate a slight but non-significant increase in the number and average length of dry spells, CHIRPS data indicate a significant and decreasing trend in the number and average length of dry spells in some areas, but especially in northeastern Nigeria around the city of Sokoto and in the southern part of the study areas around the cities of Jos and Abuja. This would have favourable outcomes for crop production and crop security, as a non-interrupted supply of moisture throughout the growing season is essential for a good yield. The drought tolerance of one of the main cereal staples, sorghum does not enter the high

water use period during its life cycle until August. This gives producers a better window to receive some much needed precipitation and rebuild soil moisture.

CHIRPS-based rainfall variables indicate spatial differences in the observed large increases in seasonal rainfall. The increase is especially marked in northeastern and north central Nigeria around the cities of Maiduguri and Kano, both of which have dense rural populations dependent on agricultural produce for their livelihoods. Kano's rural population density is reported as 308 persons per km^2 in 2006 (National Population Commission, 2006). The patchy nature of rainfall variables across northern Nigeria affirms the need for the spatial perspective offered by satellite observations.

3.6. Conclusion

The only other satellite-based studies of rainfall trends in West Africa (Sanogo et al, 2015; Zhang et al, 2017) were at continental scale, and used ARC satellite product, which is at a coarser (10 km) resolution, and is more reliant on the sparse network of ground stations across West Africa, than CHIRPS. The ARC products were found to be consistently inferior to CHIRPS, when compared to data from 18 rain gauges across northern Nigeria over a 30-year period, and the study did not address regional or local implications of observed trends. The CHIRPS data at 5 km resolution rely on a wider variety of satellite data inputs, as well as ground stations. The CHIRPS data were in agreement with gauge data, observing an increase in annual rainfall over the last 35 years, whereas Sanogo et al (2015) observed a slight decrease over our study area.

The study indicates that all satellite products slightly underestimate dekadal, monthly and annual rainfall. This is due to detection of a higher number of rainy days due to recording a higher number of low rainfall events than at ground stations. Consequently they also retrieve a higher number of rainy days and fewer and shorter drought spells during the growing season, than do ground stations, which may have serious implications for crop yield prediction and consequent perceptions of food security. However, since satellites tend to also underestimate high rainfall events, the over-and under-prediction cancel out

when considered at dekadal, monthly and seasonal time scales, thus the overall prediction of rainfall amounts by satellite products is good.

For trends in seasonal rainfall variables, both gauge and satellite data show increased growing season length over the last 35 years, which is due to increases in rainfall in the later part of the rainy season. This is expected to have favourable implications for local subsistence crops, especially sorghum which has lower drought tolerance at the ripening stage. Although satellite data do not show significant correlation with gauge data for number and length of dry spells, because the data are consistent among satellite products, this is not thought to affect the detection of trends. CHIRPS data indicate a decrease in the number and length of dry spells across northern Nigeria, and especially in northwest and north central Nigeria around the cities of Sokoto, Jos and Abuja, all in the densely populated Sudan zone and northern Guinea. This reduction in dry spells is potentially favorable for crop yields, and could have played a role in the increase in rural population densities over these 35 years of the study. The currently low nutritional status combined with a return to the drought conditions of earlier decades, could therefore bring severe hardship to rural households.

Chapter 04

Long term changes in tree density and species composition in ecological zones of Kano-Katsina

4.1. Introduction

In the past few decades a downward trend in rainfall and an increase of temperature in the West African Sudano-Sahelian ecological region were observed (Hulme et al., 2001; Dai et al., 2004). Also, this region was affected by severe droughts in the 1970s and 1980s that caused degradation in vegetation cover (Spiekermann et al, 2015). Besides climate change, anthropogenic activities have caused several environmental changes. Most of the natural forests have been cleared for agriculture, to meet the requirements of population and settlement growth in the region (Brandt et al., 2014a). According to Gonzalez et al. (2012), the decrease in tree density and species richness underwent several changes across the different parts of the Sahel region in the last few decades of the twentieth century. Although there is a large body of research on climate and the rural economy of the Sahel Zone of West Africa, much less attention has been paid to the more densely populated agricultural landscape and economy of the Sudan zone. The Sudan zone, with mean annual rainfall of 500-1000 mm is densely populated, with rural population densities up to 300-500 persons per square kilometer surrounding Kano.

In northern Nigeria, rural households depend mainly on subsistence agriculture, with rainy season cultivation of a limited number of cereals, root and leguminous crops, for their survival. Rural electrification is almost non-existent, thus wood fuel is widely used, and harvesting of fuelwood from rural farm trees, as well as its sale to city fuelwood merchants, provides a valuable additional income for farmers. In the face of climate change and the threat of greater climate variability and longer drought periods, the possibility of a major food and population crisis is a real threat. This study examines trends in woody vegetation and tree species composition in the Sudan zone of West Africa, using the Kano closed settled zone

of northern Nigeria as a case study. The study compares data on tree density, fuelwood production and tree species composition from fieldwork conducted in 1981 and 2016, as well as from several dates of aerial and satellite images since the 1960s. Recent satellite-based reports of greening in arid West Africa as a response to recovery from droughts in the 1970s and 1980s, are examined to explain the observed trends.

The main objective is to examine trends in woody vegetation abundance and composition in the farmed parklands of three study areas surrounding the KCSZ. Kano's status as the largest city in savanna Africa, with probably the highest rural population densities, provides a model for understanding social-ecological interactions under a scenario of climate change and population pressure.

4.2. Materials and Methods

4.2.1. Study area

The research was conducted in three study areas surrounding Kano city (Figure 4.1), which is situated at 12° N in the northern Sudan Zone of West Africa. These study areas are influenced in terms of land use and economic activities, by the proximity of Kano city. The mean annual rainfall of 750 mm at Kano, supports a natural vegetation of tree savanna, with flat-topped trees browsed by savanna fauna and livestock, when grass is unavailable during the winter dry season (Oct-Apr). Traditionally, goods were brought to Kano markets by donkey, limiting the fuelwood hinterland to around 50 km, but replacement by pickup trucks over the last two decades has expanded this to over 100 km. Questionnaires to farmers in the Kano Close Settled Zone (Maconachie et al., 2009; Maconachie and Binns, 2006; Maconachie, 2013) indicate that farmers perceive declining tree cover on farmlands, as well as reductions in tree species diversity in recent decades. Three study areas (Figure 4.1, Table 4.1) were selected within Kano's hinterland as follows. Study area 1, Kano West at 11.96° N, 8.38° E extends westwards from Kano city covering 100 km^2, and Study area 2, Kano East at 12.25° N, 8.75° is situated in the region of the Jakara river, 30 km northeast of Kano city and covers 110 km^2. These two study areas represent the long-established Kano Close Settled Zone of intensive agriculture and high rural population within a day's walking or donkey distance to the city market. They were selected based on their

geographical differences, with mainly red, well-drained sandy loam soils in Kano West, compared to Kano East dominated by the Jakara river lowlands draining into the Hadejia river and ultimately, Lake Chad. Soils in Kano East are heavier, yellow-red to grey in colour, with more clay. Study area 3, Daura, at 13.0° N, 8.25° E covering 200 km^2, was selected farther north bordering the more arid Sahel Zone, where population densities are lower and land use is somewhat less intensive. At 100 km northward from Kano, the area has become a source of rural produce by pickup truck for Kano city over the last two decades. The geographical differences between the three study areas provide a range of social-ecological conditions, within which human responses to climatic and economic pressures may differ.

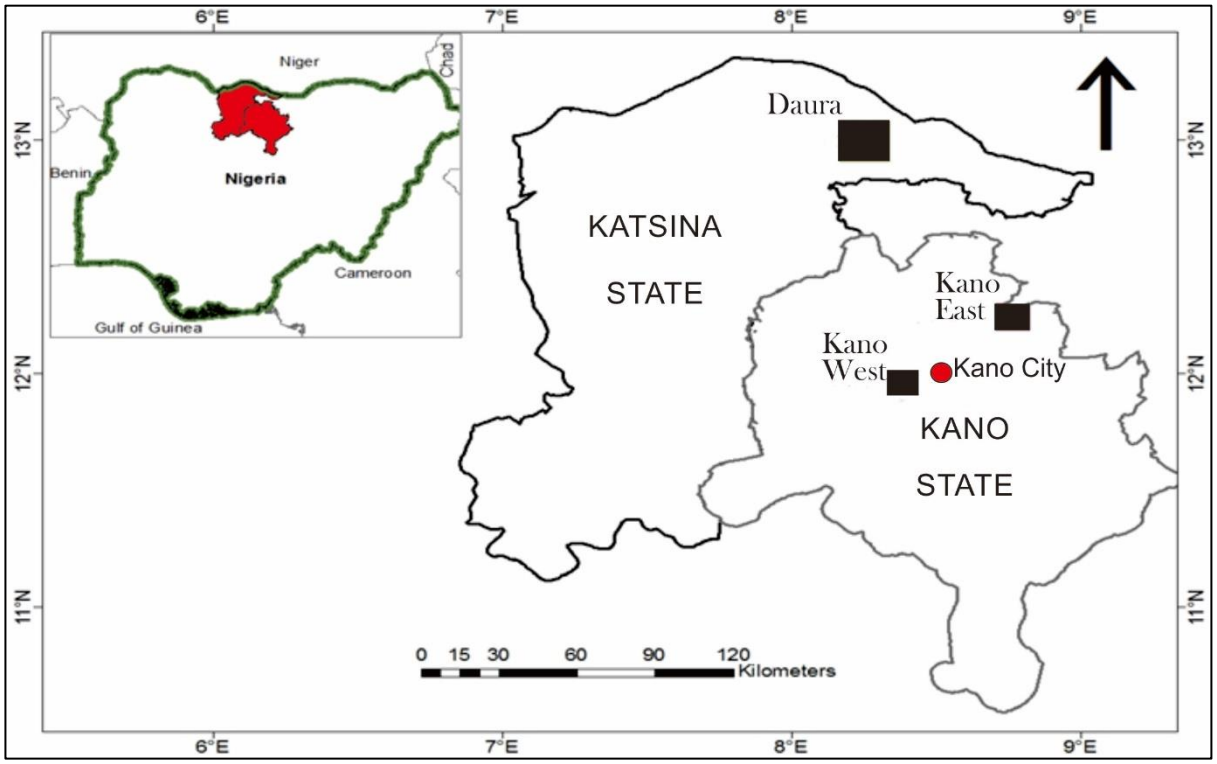

Figure 4.1 Location of the study areas surrounding Kano city.

4.2.2. Field data collection

Fieldwork conducted in the three study areas during the 2015-16 dry season provides the basis for the study, and historical trends are observed from field data collected 34 years earlier in 1981 in Study areas 1 and 3 (Nichol, 1989). Field survey quadrats in each study area (Table 4.1) were selected by stratified random sampling in order to ensure a representative range of tree densities. The

stratification was performed by dividing the study area into four classes of tree canopy cover based on an NDVI image derived from WV-2 data. Approximately even numbers of quadrats per strata were randomly selected for all study areas according to Karlson et al. (2014). Rectangular quadrats of different size were selected according to tree density variations among study areas. Field data collected included enumeration of tree numbers for trees > 5 cm in diameter, height of trees, measurement of Diameter at Breast Height (DBH), as well as species identification. For each field surveyed quadrat, the location of every individual tree was manually located on a color print of a Worldview-2 (WV-2) pan-sharpened image of 0.5 meter resolution. From this, a GIS based point shapefile of field tree locations was generated for further analysis.

Table 4.1 Image datasets and field survey.

Study areas	Population density (persons/km^2)#	Corona satellite images	Aerial photographs	Recent satellite images	Field Survey Date	Field Survey area (ha)	No. of Plots
Study Area 1	454	1967	1981	2014 (WV2)	1981, 2015-16	37	21
Study Area 2	397	NA	1972, 1981	2013 (WV2)	2015-16	137	25
Study Area 3	232	1967	1991	2015 (Google Earth)	2015-16	60	31

#(National Population Commission, 2006).

For study area 1, field survey was conducted for 21 quadrats (each 1-2 ha in area, totaling 37 ha), and these were then located on the archived images of 1967 (Corona images), 1981 (aerial photographs) and 2014 (WV-2). For study area 2, field survey was conducted for 25 quadrats (each 2-10 ha in area, totaling 137 ha), and these were then located on archived aerial images of 1972, 1981 and 2013 (WV-2). For study area 3, field survey was conducted for 31 quadrats (each 2 ha in area, totaling 62 ha), and these were then located on the archived images of 1967 (Corona), 1991 and 2015.

As the very marked increase in tree densities observed in all three study areas was surprising, especially when compared with other reports of trends in woody vegetation in West Africa, it was decided to extend the survey to a larger area outside the study area plots using images alone. Therefore, an additional 67

square plots each of 1 ha area, 35 plots of 4 ha and 20 plots of 4 ha were randomly selected for study areas 1, 2 and 3 respectively, and tree densities were calculated for three different time periods, by manual counting of trees on images.

To supplement and confirm observed trends in farmland trees, 40 questionnaires were administered to farmers in 20 different villages in each of study areas 1 and 3. Farmers selected were over the age of 40, to allow for recollection over previous decades.

4.2.3. Image datasets

Remote sensing images were used to survey areas beyond the actual field plots, as well as for years when field data were unavailable (Table 4.1). Thus for Study area 1, past tree densities were determined from Corona satellite images of September 1967, aerial photos at 1:25000 scale by Kenting Africa in 1981, and recent tree density from a WV-2 image of 2014 (panchromatic band at 0.5 m resolution and multispectral bands at 2 m). Pan-sharpened images at 0.5 m resolution were produced using the Hyperspherical Color Space (HCS) method (Padwick et al., 2010) by fusing multispectral bands at 2 m with the panchromatic band at 0.5 meter. For Study area 2, Kano East, aerial photos of March 1972 at 1:40000 scale and 1981 by Kenting Africa at 1:25000 scale, and recent WV-2 imagery of 2013 were used. For Study area 3, Daura, Corona satellite images of September 1967, aerial photographs of 1991 at 1:25000 scale acquired by Geonex during the Katsina Arid Zone Programme, and recent high resolution IKONOS satellite images in Google Earth of 2015 were available. Corona images were acquired by U.S. earth observation satellites with a ground resolution of 1.8 meter (McDonald, 1995).

As raw Corona images and aerial photographs lack positional information, these were georeferenced using Google Earth images as a reference. For each aerial photograph, 20-25 ground control points (GCP) were selected and rectification was performed with a first order affine transformation method (Hazewinkel, 2001), rounding the input cell size to 0.5 meter. As the Corona images covered a larger area, they were divided into small sections of 25 km^2, and individually georeferenced using 20-25 controls points with input cell sizes rounded to 2 m. For direct comparison between years, image-to-image registration was carried

out to an accuracy of 2-3 meters for aerial photographs, and less than 5 meters for Corona images.

4.2.4. Recording of tree densities

Tree counting on images was validated using the field plots as the reference dataset. It was observed from this, that at least 4 pixels are required for identifying a tree using the sharp contrast between the dark tree crown and its bright soil background on dry season images. Therefore on the 0.5 m resolution of the more recent (1980s to 2015) images a small tree with crown size of 4 m^2 area covers 16 pixels and can be easily identified. However, as the Corona images of 1960s used in Study areas 1 to 3, and the aerial photographs of 1972 for study area 2, had lower resolution than the more recent aerial photographs and high resolution satellite images, some undercounting of smaller trees may have occurred for the pre-drought period.

For all three study areas, Corona satellite images obtained in the 1960s and aerial photographs obtained in the 1980s and 1990s respectively, provide information on tree densities before and during the 1970s to 1980s drought, whereas recent satellite images and field data indicate post-drought conditions.

4.2.5. Timber volume and fuelwood volume

Not all species are used for fuel, for a variety of reasons from poor burning properties to local folklore. Thus it is important to distinguish between timber volume which includes all species, and fuelwood volume only those species used for fuel. For this reason, the tree *Adansonia digitata*, (Baobab), is not included with fuelwood volume (Table 4.3), as its wet and spongy wood precludes it from fuel use. The definition 'fuelwood volume' here could strictly be defined as 'potential fuelwood volume', as wood may also be used for boundary markers, fencing and furniture. However, as these are one-off uses whereas fuelwood demand is continuous, it is likely that the woody component of trees whose leaves, fruits and bark are used for medicinal, food and other purposes, would be periodically lopped and eventually felled for fuel.

Although wood volume includes canopy as well as trunk wood, since we were unable to carry out destructive sampling, volume is computed from $\pi R^2 H$ for the

volume of a cylinder, based on field measurement of DBH and tree height. This also allows direct comparison with the 1981 field data.

4.2.6. Tree species compositon

To evaluate tree species composition for trees recorded in fieldwork of 1981 and 2016, the Importance Value Index (IVI) (Kershaw, 1974) was calculated (Equation 4.1), using data from all quadrats in a study area.

IVI = (%) Basal Area + (%) Density + (%) Frequency (Equation 4.1)

Histograms of DBH size spectra by division of the total DBH values for each species into six size classes were constructed, to indicate the approximate relative age and thus the regeneration status within a study area. In many natural situations such as undisturbed woodland small trees would comprise the largest size class with an even rate of decrease to the largest class, resulting in a smooth L-shaped curve. In human disturbed situations a smooth curve is rarely seen and in farmed parkland where farmers protect trees, more large and old trees would be expected (Condit et al., 1998; Lykke, 1998).

4.3. Results

4.3.1. Tree densities

The objective of tree enumeration was to identify individual trees on time-series of images before, during and after the 1970s to 80s drought, to set recent satellite- and field-based observations of greening in context of long term climate variability. Therefore the results (Table 4.2) are grouped according to pre-drought, drought and post-drought periods.

In study area 1, fieldwork conducted during the 2015-16 dry season indicated 25 trees per ha, which represented a doubling in tree numbers since the previous fieldwork in this study area in 1981, when 12.3 trees/ha were recorded. Aerial photographs of 1980 (but from different plot locations within the study area) indicate 14.9/ha, which is a similar order of magnitude to the 1981 fieldwork. Tree density in the pre-drought year of 1967 appears similar to the 1970s to 80s

drought period (confirmed from both fieldwork and air photos), with 12 trees/ha, but again far below the 25 trees/ha recorded in the recent 2015-16 dry season. The field survey of 2015-16 shows a 31 % increase from the WV-2 image of 2014, which may represent a recent upturn in the increasing trend in tree densities (Figure 4.2).

In study area 2, tree densities have been 50% lower than in Study area 1 for all three periods, thought to be due to the heavier clay soils which are more difficult to cultivate and may prevent natural seedling regeneration. However trends in tree densities are similar in that tree numbers held constant from the 1960s up to and including the drought period, with only a 5% increase, and a doubling of tree numbers has occurred since the drought years up to the present period (Figure 4.3). As in Study area 1, the field survey of 2016 shows a marked increase in tree numbers (of 18%) since the WV-2 image of 2013, which may represent a recent upturn in the long term increasing trend in tree densities (Figure 4.2).

In Study area 3, the 25-year period from 1967 to 1991 saw a significant (approximately 35%) increase in tree density, and in the following 24 years from the post-drought period to present, a doubling of tree densities is observed. Thus the rate of increase observed between the 1960s up to the drought period, has itself substantially increased since the drought.

Table 4.2 Tree Density from field survey plots and aerial photographs.

Period	Pre-drought	Drought period		Post-drought	
	1967	1981	Field survey 1981	2014	Field Survey 2016
Study Area 1	12.5	14.9	12.3	19	25
Study Area 2	5.6 (1972)	5.9	NA	11 (2013)	13
Study Area 3	7.8	10.6 (1992)	NA	20.9 (2015)	22

The results for the additional three extended study areas surveyed on images alone, confirmed the observations of large increases in tree numbers over the study period, with similar trends of an approximate doubling in tree densities in Study areas 1 and 2, and a threefold increase in Study area 3.

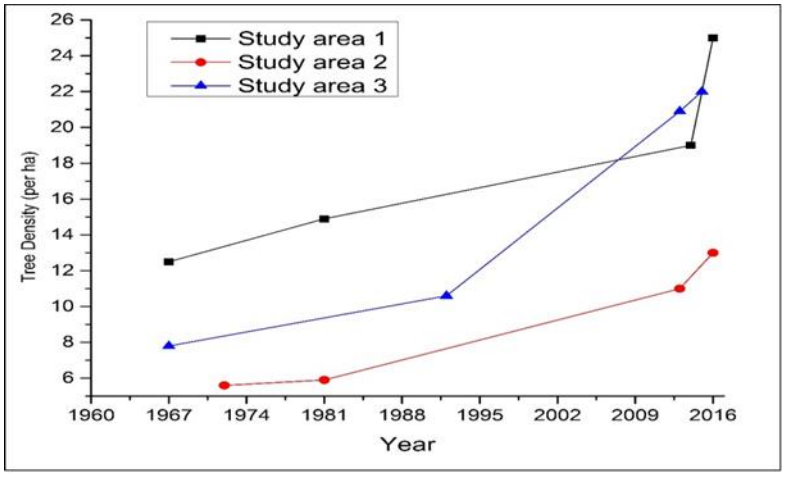

Figure 4.2 Trends in tree density for 3 study areas.

Previous reports from farm questionnaires have indicated declining tree stocks around Kano (Maconachie and Binns, 2006; Maconachie et al, 2009). Our study observed a large increase in tree numbers over the last 5 decades. To supplement and confirm observed trends in farmland trees, 40 questionnaires were administered to farmers in 20 different villages in both study areas 1 and 3. Farmers selected were over the age of 40, to allow for recollection over previous decades. Responses to questions about tree densities initially indicated that farmers perceived trees to be declining. However, typical replies to question about changes in the total numbers of trees, was mainly answered not in terms of tree numbers, but by mentioning which species had declined or disappeared. This led us to suspect that the discrepancy between our data and farmers' perceptions may, at least in part, arise from inability to distinguish between the concepts of tree numbers and tree species due to a sense of alarm at the disappearance of many valuable indigenous species such as Parkia biglobosa, Ceiba pentandra , and Adansonia digitata, given the role of trees of different species in the Hausa cultural and religious heritage (Cline-Cole, 1998; Etkin, 2002; Tomomatsu, 2014).

4.3.2. Fuelwood volume

Study area 1, with the highest tree density, also has much higher fuelwood production than the other two study areas (Table 4.3). Study area 2, with approximately half the tree density of study area 1, has correspondingly, roughly only half the timber volume, but 62% of the fuelwood volume, which may suggest the importance of wood fuel among tree products in the local economy even in an area with fewer trees.

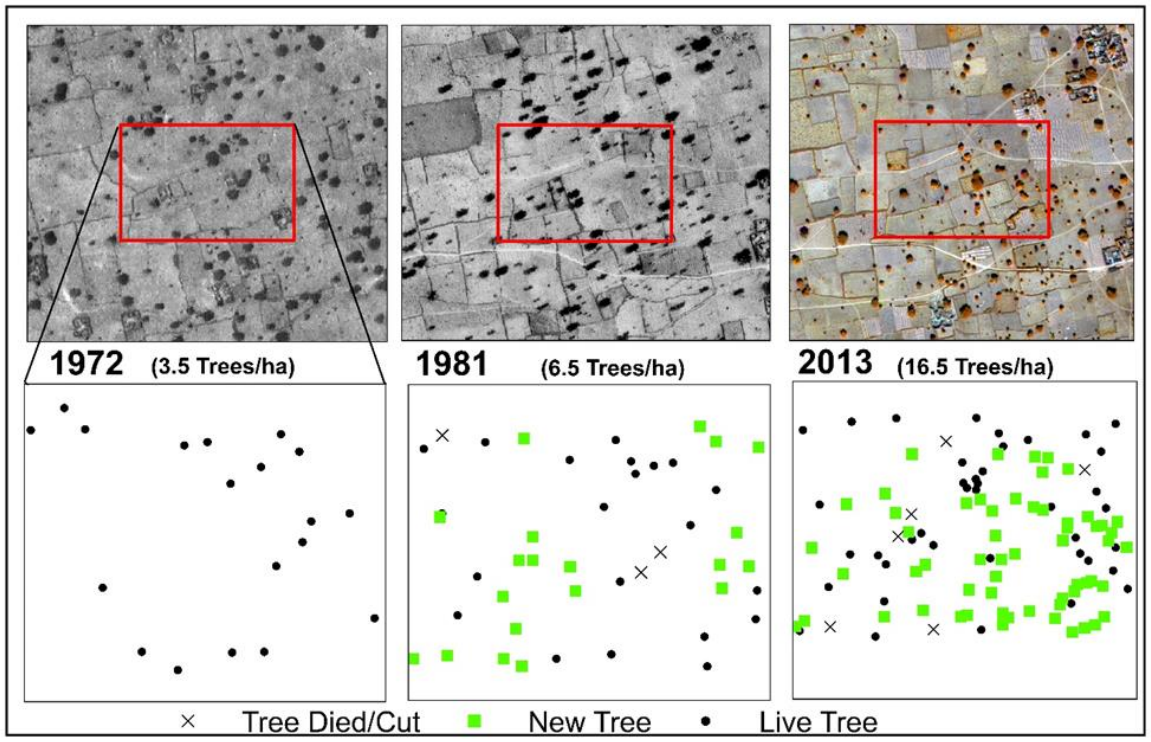

Figure 4.3 Change in tree stocks over 45-year period in Study area 2- at 1:2500 scale, size of rectangle 3 by 2 ha.

In study area 3, with similar tree densities to study area 1, both timber volume and fuelwood volume are significantly less (64% and 67% respectively) than in Study area 1, due to the smaller size of trees in this northerly study area bordering the Sahel zone. In terms of trends it is remarkable that fuelwood production has tripled since 1981 in Study area 1 and increased by 6 times in Study area 3. In 1981 study area 3 was not within the fuelwood hinterland of Kano which was then defined by donkey distance per day, but has now expanded to over 100 km with pickup trucks. Discussions with farmers indicated that they rarely purchase wood, suggesting a plentiful on-farm supply.

Table 4.3 Timber volume and Fuelwood volume (cubic meter per hectare) from fieldwork in 1981 (in brackets) and 2016.

Study areas	Timber volume	Fuelwood volume
Study Area 1: 2016 (1981)	40.3 (12)	27 (8.9)
Study Area 2: 2016	20	16.8
Study Area 3: 2016 (1981)	25.7 (5.4)*	18.2 (3.3)

* The field data reported for Study area 3 in 1981 were collected from a different location, north of Kano but at the same latitude as Study area 3.

4.3.3. Species trends

Table 4.4 shows the IVI for the ten most important tree species in each study area. The baobab tree *Adansonia digitata* appears over-represented due to its swollen trunk, thus large DBH, which is disproportionate to its crown size. It is retained in the tables due to its diverse non-fuel (including food, fibre, and medicinal) uses. Besides baobab, the common dominants in all three study areas are the exotic Neem tree, *Azadirachta indica*, and the Sudan zone species *Piliostigma reticulatum* (Appendix 1), both of which are highly valued for fuelwood use. Both species show active regeneration in all three study areas, with many trees in the lower DBH classes (Figure 4.4), and all size classes strongly represented. Table 4.5 also suggests that these two species have become dominant recently, as they were absent from the dominant species recorded in Study area 1 in 1981.

Table 4.4 Tree species dominance in farmed parkland.

No.	Study Area 1	IVI	Study Area 2	IVI	Study Area 3	IVI
1	Adansonia digitata	49.5	Parkia biglobosa	70.3	Piliostigma reticulatum*	66.5
2	Azadirachta indica*	44.8	Azadirachta indica*	39.8	Adansonia digitata	47.4
3	Piliostigma reticulatum*	24.4	Adansonia digitata	34.0	Azadirachta indica*	37.5
4	Anogeissus leiocarpus*	20.9	Piliostigma reticulatum*	16.7	Hyphaene thebaica	25.1
5	Diospyros mespiliformis*	17.3	Diospyros mespiliformis*	16.0	Diospyros mespiliformis*	20.4
6	Parkia biglobosa	16.1	Tamarindus indica*	14.5	Lannea acida	18.9
7	Faidherbia albida	15.6	Ficus platyphylla	13.1	Parkia biglobosa	13.0
8	Tamarindus indica*	15.3	Anogeissus leiocarpus*	13.1	Borassus aethiopum	7.5
9	Ceiba pentandra	10.9	Sclerocarya birrea	6.5	Anogeissus leiocarpus*	7.0
10	Butyrospermum paradoxum	5.8	Butyrospermum paradoxum	4.6	Acacia nilotica	5.9

* Species preferred for fuelwood use

The DBH spectra (Figure 4.4) show that only four of the dominant ten species in Study area 1, and three of the dominant ten species in Study are 2 are actively regenerating and all these are preferred fuelwood species Neem (*Azadirachta indica A.Juss*), Kargo (*Piliostigma reticulatum*), the African Ebony (*Diospyros mespiliformis*) and the Chewstick Tree (*Anogeissus leiocarpus*). *D. mespiliformis* has high importance and appears to be actively regenerating in all three study areas. With an IVI of 19.3 in 1981 and 17.3 in 2015-16, this preferred fuelwood species has retained its importance among tree products in the local economy. On the other hand the dominant tree in Study area 2, the African Locust Bean (*Parkia biglobosa*) used traditionally for food and fibre, comprises mainly old trees with no evident regeneration, similar to Study areas 1 and 3 where its DBH spectrum is dominated by the largest class. Similarly, the dominant species recorded in Study area 1 in 1981, *Faidherbia albida*, which is traditionally valued for its retention of leaves in the dry season, providing fodder and shade, is now only 7th in importance, with its DBH spectrum dominated by large old trees and no evident regeneration. The non-fuelwood tree *A. digitata*, although occupying 1st, 3rd and 2nd places in importance in study areas 1, 2 and 3 respectively, is heavily weighted to the largest DBH class suggesting its declining importance in recent decades. Discussions with local farmers indicated a decline in species diversity, with loss of many traditionally protected species and shift toward preferred fuelwood species Neem and *P. reticulatum*. These two species are fast-growing and well adapted to drought.

Table 4.5 Species trends (1981-2016) for Kano west area.

No.	1981	IVI	2015-2016	IVI
1	Faidherbia albida	37.5	Adansonia digitata	49.5
2	Adansonia digitata	37.4	Azadirachta indica*	44.7
3	Parkia biglobosa	29.0	Piliostigma reticulatum*	24.4
4	Diospyros mespiliformis*	19.3	Anogeissus leiocarpus*	20.9
5	Anogeissus leiocarpus*	16.7	Diospyros mespiliformis*	17.3
6	Tamarindus indica*	15.1	Parkia biglobosa	16.1

* Species preferred for fuelwood use

4.4. Discussion

Previous reports of greening in the Sahel based on NDVI, as well as increasing tree numbers since the 1970s to 80s drought period, conclude that biomass trends, whether woody or herbaceous, follow trends in rainfall. For example

Brandt et al. (2014a) observe that tree densities have recovered somewhat since the drought period but are still below those of the 1960s pre-drought period, while Hänke et al. (2016) and Brandt et al. (2017) observe recovery back to 1960s levels by 2006 and 2015 respectively. Therefore, the marked increase in tree numbers in the Kano region over the last 5 decades observed here is surprising when set in the context of recent work in West Africa.

While it is true that rainfall in Kano region generally has recovered since the 1980s, back to 1960s levels, tree densities in the farmed parkland hinterlands of Kano city, are at least double those of the 1960s. A steady increase is observed, even through the drought decades, when all other reports indicate severe decline in tree numbers and woody vegetation.

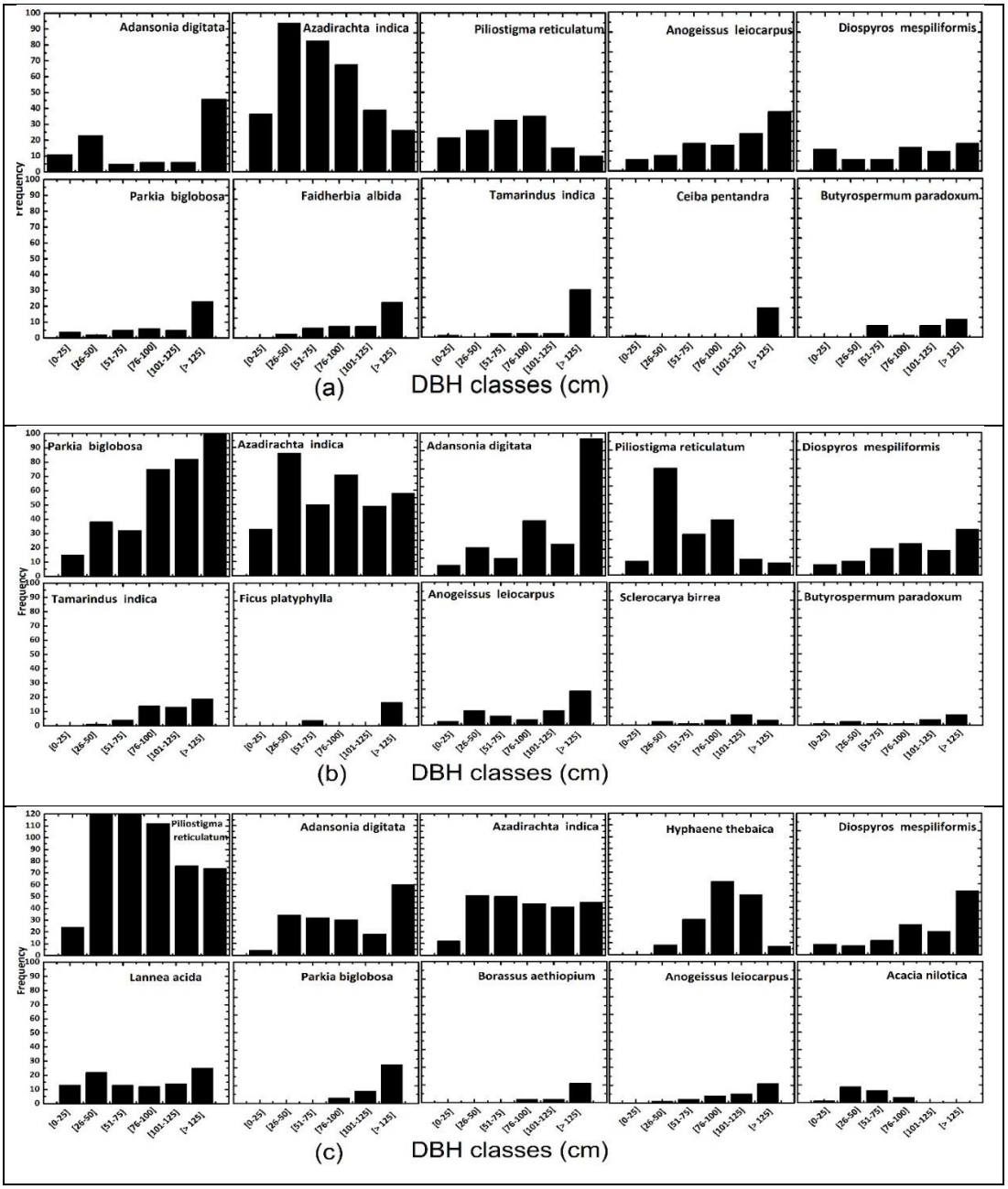

Figure 4.4 DBH spectra for ten dominant species in Study area 1 (a), Study area 2 (b) and Study area 3 (c).

Accompanying this increase in tree density has been an even greater increase in potential fuelwood production which has increased by approximately 300% in study area 1 and 600% in Study area 3, since 1981. Decline in the non-fuelwood species *Adansonia digitata* as well as other non-preferred fuelwood species, indicated by their non-regeneration in all three study areas (Figure 4.4), points to the demand for wood fuel as a likely explanation of the observed trends.

However, all similar recent studies have all been carried out in the less densely populated Sahel, rather than Sudan zone, and none in Nigeria, where government energy policies largely determine fuel options (Cline-Cole and Maconachie, 2016). Given that electricity is rare in rural areas, and kerosene prices unpredictable, a rural population of 7 million in Kano region relies on wood for cooking and heating, and the urban population now estimated at over 3.8 million (Geonames, 2017) relies on wood due to its affordability and availability. The recent rapid growth of population in Kano city and region would not have been possible without a parallel increase in the main energy source, wood fuel. The six-fold increase in fuelwood volume observed in the outer hinterlands compared to three-fold increase nearer the city since 1981, attests to the growing demand, as nearby sources would be exploited before more distant ones. The observed increased importance of preferred fuelwood species *A. indica* and *P. reticulatum*, among farmland trees has resulted in decline of other species traditionally valued for their food, fibre, fodder and medicinal uses. Cheap alternatives to products traditionally derived from trees, such as stock cubes, beverages, painkillers, petroleum jelly, foam stuffing and plastics are now available in the consumer economy, and affordable from the sustained income farmers gain from selling wood.

The on-going, apparent reduction in species diversity observed in this study, also noted by studies in the Sahel zone (Brandt et al., 2014a; Gonzalez et al., 2012; Hänke et al., 2016), has largely been attributed to a climate-induced shift towards more drought-tolerant species. Observations of higher recovery from drought nearer to houses (Hänke et al., 2016) and to villages (Brandt et al., 2014a) recognize that human factors play a role in areas where population growth has led to agricultural intensification. However, the recent concentration on species valued for fuel concurrent with rapid population growth observed in this study, strongly suggests the dominant role of socio-economic factors, possibly with climate playing a minor role.

It is also surprising that the tree surveys from fieldwork and time series of images in this study, conflict with farmers' perceptions of tree stocks, both from this study and those of previous researchers (Maconachie et al., 2009; Maconachie

and Binns, 2006). Farmers apparently perceive tree stocks on farmland to be declining, accompanied by a loss of traditional parkland species such as *P. biglobosa*, *F. albida* and *A. digitata*. However, as farmers rarely buy wood, and the rural population has doubled between 1991 and 2006, a corresponding increase in farmland tree stocks does seem inevitable. Farmers' responses may be influenced by mixed perceptions comprising insecurity in the face of current and impending climate change and increasing aridity, as well as insecurity at the disappearance of traditional trees such as *P. biglobosa*, *A. leiocarpus* and *A. albida*, which supply many free products and are part of their heritage. The practice known as *wankan jegu* whereby newly delivered mothers bathe twice daily for 40 days in scalding hot water, requiring an enormous amount of fuelwood (Maconachie and Binns, 2006), may also influence respondents' perceptions about fuelwood availability, as births in Kano region more than doubled between 1991 and 2006. Perceptions that interviewers have influence, and are thus able to alleviate long-standing frustrations at the fluctuating price of kerosene and lack of electric power supply, may also prompt farmers to indicate that trees are disappearing.

4.5. Conclusion

The findings of this study conflict with other similar work carried out in West Africa, which has mainly attributed changes in greenness and woody vegetation, to climatic fluctuations such as decadal droughts and recent global warming. Gonzalez et al. (2012) attribute their observed declining tree densities and species richness across the West African Sahel, to climatic, rather than human factors. They especially invoke global climate change, consistent with other reports of drought-induced tree dieback from around the world (Allen et al., 2010).

The reduction in species diversity noted in this study, and by others (Brandt et al., 2014a; Gonzalez et al., 2012; Hänke et al., 2016) may not be so alarming given the available supply from other sources, of traditional tree products, although market fluctuations may dictate future prices. Of greater concern is the continued overwhelming dependence on biomass for fuel by a still rapidly growing population across northern Nigeria. Return to the drought conditions of previous

decades coupled with tree death due to climate change may have serious consequences for rural households for whom the longevity of woody vegetation offers security against rainfall variability and crop failure. Urbanites' reliance on wood may be less affected, as the fuelwood hinterland of Kano has expanded with modern transport, to the more wooded Guinea zone, and has potential to expand and contract according to demand.

The Sudan zone comprises 40% of Nigeria's land area, and in view of the geographical diversity among the three study areas, it is likely that the trends in tree stocks observed here are applicable to other parts of Nigeria's Sudan zone. However, whether they are applicable to other parts of savanna Africa is probably dependent on national government energy policies, as Nigeria's continued dependence on biomass fuel is clearly both unfortunate and unusual.

Chapter 05

Mapping tree crown cover and above ground biomass using high resolution WorldView-2 imagery in the agro-forestry landscape of West Africa

5.1. Introduction

In the semi-arid Sudano-Sahelian ecological zone of West Africa, trees maintained by farmers on their farmed plots are an important element of the local livelihood (Boffa, 1999). Tree cover provides fuel wood, timber for building materials, food, fodder, fibre and medicines. Additionally, the large areal extent of farmed parkland landscapes in the Sudano-Sahelian ecological zone makes them an important component of the global climate system, as they store and sequester large amounts of carbon in the woody biomass and soils (Karlson et al., 2015; Lal, 2004). Therefore mapping and quantification of tree parameters such as tree crown cover and above ground biomass (AGB) is important for both regional socio-economic resource management, as well as terrestrial carbon accounting in environmental assessment. Tree Crown Cover (TCC) is defined as percentage of land area covered by tree crown, when viewed from above (Chidumayo and Gumbo, 2010). AGB is defined as the dry weight of all above ground live mass including wood, bark, branches, twigs and stumps (Dong et al., 2003; Zhu and Liu, 2015). Such spatial and quantitative assessments are especially urgent since climate change and intensified land use in recent decades have put increasing pressure on tree cover.

5.1.1. AGB estimation using allometric equations

Traditionally, AGB is estimated by destructive sampling, by harvesting all trees in a field plot to determine their total biomass (Henry et al., 2011). Although this method is very accurate, it is often impractical as it is time consuming, labor intensive and also destroys a large number of trees (Zhu and Liu, 2015). Alternatively a nondestructive method using allometric equations can help to determine AGB in the field. Allometric equations use dendrometric parameters

(height and Diameter at Breast Height (DBH) of individual trees), which are easy to measure in the field for estimating AGB (Henry et al., 2011). The term allometry is defined as 'the relationship between part of an organism and its whole' (West, 2009). Therefore the development of allometric equations relies on the harvesting of trees of varying sizes (for each species, or for a stand of mixed species) by selecting varying classes of DBH, for the measurement of above ground dry weight of different parts of a tree. Then a functional relationship between total dry weight of the tree and its DBH and height, is developed, using different mathematical models. In Sub-Saharan Africa, there are already developed species specific allometric equations for different countries (Henry et al., 2011). Although allometric equations provide fairly accurate estimation of AGB for the field plots, they are limited to the field plots where the DBH and height have been measured.

5.1.2. AGB estimation using Remote Sensing

In the last few years, there has been a growing interest in the use of satellite remote sensing for estimation of AGB (Karlson et al., 2015; Qazi et al., 2017; Sarker and Nichol, 2011; Schucknecht et al., 2017; Zhu and Liu, 2015), because remote sensing satellites provide timely, repetitive and large area coverage from local to global scales. However, remote sensing observations do not provide direct information about AGB, but use empirical models to relate AGB measurements on the ground, to predictor variables derived from remote sensing data. Therefore field measurement of AGB is a prerequisite for remote sensing based estimation of AGB. The empirical models range from simple parametric linear regression models (Sarker and Nichol, 2011) to complex non-parametric machine learning models like Random Forest (Karlson et al., 2015; Zhu and Liu, 2015).

For empirical models, remote sensing based predictors are derived from high and medium resolution optical images, Lidar and RADAR data. In West Africa, there are some previous studies of biomass estimation using low resolution SPOT-VEGETATION (1 km resolution) in Senegal (Diouf et al., 2015) and MODIS (250 meter) in Niger (Schucknecht et al., 2017) as well as medium resolution Landsat data (30m) in Burkina Faso (Karlson et al., 2015).

5.1.3. Tree crown extraction using high resolution imagery

Over the last few years, there has been an enormous development in the field of remote sensing with the launch of high spatial resolution commercial satellites. For high resolution satellite images, the use of traditional statistical analysis of single pixels is not appropriate as the pixel under consideration and its neighboring pixels may differ sprectrally but belong to the same land cover class (Blaschke and Strobl, 2001). The high spectral variability within the same land cover class in high resolution satellite images creates a "salt-and-pepper" effect during classification. As human beings normally recognize patterns in a landscape by their spatial relationship to neighbourhood objects, it is useful to use spatial and contextual information for characterization of land use classes, along with spectral information (Blaschke, 2010). Spatial relationships between adjacent pixels in the form of texture provide an important information for identification of individual objects, which is building blocks of original features of interest (Thomas et al., 2003). In this way, homogeneous objects based on spatially connected groups of pixels with similar spectral characteristics, can be identified. Image segmentation is the process by which homogeneous image objects are created by aggregating groups of pixels with regard to spectral and spatial characteristics. The term 'homogeneous' implies that within-object variance is low compared to that between objects, and those identified objects also contain additional information about geometry (size and shape), contextual, textural besides spectral information (Laliberte et al., 2004). These homogeneous objects reflect real-world objects of interest (Blaschke and Strobl, 2001).

5.1.4. Use of Geographic Object Based Image Analysis (GEOBIA) for tree crown delineation

Historically, panchromatic aerial photography was used to estimate tree parameters (Laliberte et al., 2004), such as crown area (m^2), tree canopy cover (%) and tree density (number of trees per hectare). However in the last 15 years, the launch of high resolution commercial satellites with pixel sizes ≤ 4 m, such as IKONOS, Quickbird, OrbView, GeoEye and WorldView, make it possible to estimate tree parameters from space using multispectral and/or panchromatic

data. In contrast to pixel based approaches, object based image analysis is very effective for classifying different objects at multiple scales. This means that tree crowns of different sizes can be delineated separately, from individual tree crowns to large-sized clusters of tree crowns. Numerous studies have found high accuracies and low error, for classification of tree species using GEOBIA as compared pixel based approaches (Bunting and Lucas, 2006; Immitzer et al., 2012).

Many studies have used high spatial resolution satellite images for tree crown delineation (Bunting and Lucas, 2006; Karlson et al., 2014; Rasmussen et al., 2011). Bunting and Lucas (2006) extracted and classified different tree crown species in Australian mixed forests using the Compact Airborne Spectrographic Imager (CASI) hyperspectral data through GEOBIA. Rasmussen et al (2011) used QuickBird imagery for extracting tree crowns in northern Senegal, and Karlson et al (2014) used WorldView-2 data for tree cover extraction in Burkina Faso using GEOBIA. In an agroforestry landscape, there is a variety of deciduous trees with varying crown sizes and ages, therefore GEOBIA is well suited for such tree crown cover mapping.

The main objectives of this study are to

- delineate tree crown cover through GEOBIA using high resolution WV-2 images in the agroforestry landscape of the Kano Closed Settle Zone of northern Nigeria,
- estimate AGB using already developed allometric equations for the reference field plots, and
- develop a linear model for AGB estimation using Crown area (CA) extracted from WV-2 data.

5.2. Study area and Datasets

5.2.1. Study area

The research was conducted in a farmed parkland area (100 km^2) surrounding Kano city in northern Nigeria (Figure 5.1), which is situated at 12° N in the northern Sudan Zone of West Africa. The mean annual rainfall of 750 mm at Kano,

supports a natural vegetation of tree savanna, with flat-topped trees browsed by savanna fauna and livestock, when grass is unavailable during the winter dry season.

5.2.2. WorldView-2 satellite data

For this study, a cloud free WorldView-2 image was acquired on 02 February, 2014. WV-2 has eight multispectral bands at 2 meter and panchromatic band at 0.5 meter resolutions (Table 5.1). For this study, pan-sharpened images at 0.5 m resolution were produced using the Hyperspherical Color Space (HCS) method (Padwick et al., 2010) by fusing multispectral bands at 2 m with the panchromatic band at 0.5 meters.

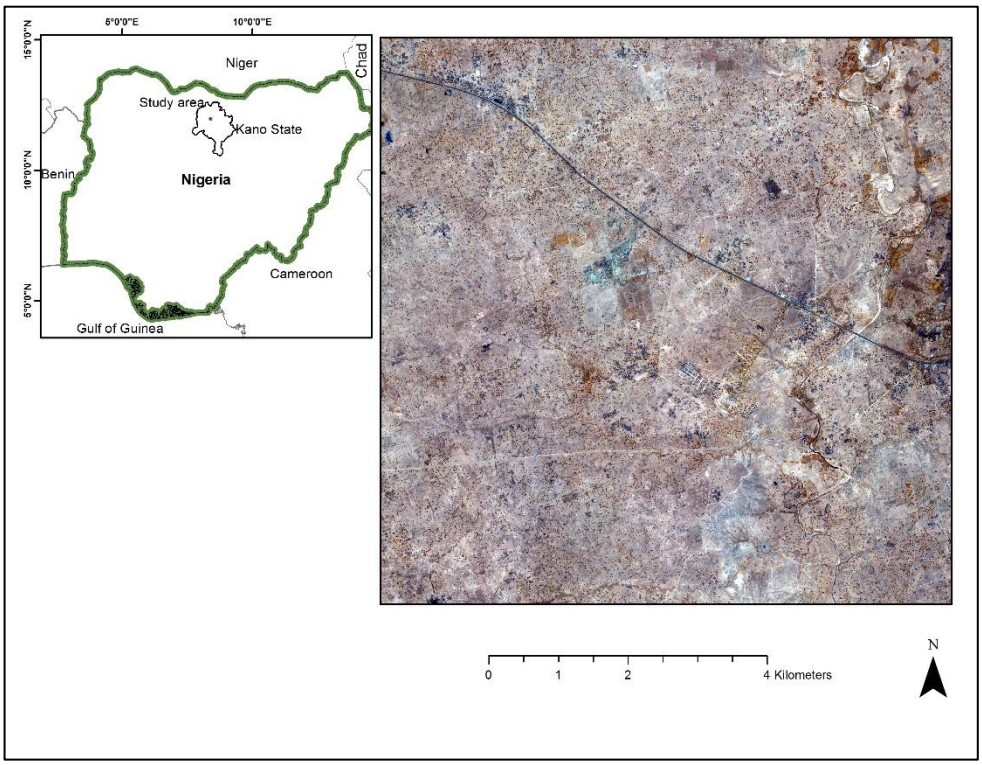

Figure 5.1 Map showing the study area located in Kano state of Nigeria (left). False colour composite image of WV-2 (right).

Table 5.1 Specifications of WorldView-2 satellite image.

Image parameters		Bands (μm)
Acquisition date	February 02, 2014	Coastal Blue (0.40-0.45)
Acquisition time	10:24:00	Blue (0.45-0.51)
Off-nadir angle	26.06	Green (0.51-0.58)
Mean sun azimuth	139.50	Yellow(0.58-0.62)
Mean sun elevation	60.40	Red (0.63-0.69)
Cloud Cover (%)	0	Red Edge (0.705-0.745)
Map projection	UTM WGS 84	NIR 1 (0.77-0.89)
Location:	(12.01, 8.34)	NIR 2 (0.86-1.04)
NW (Lat, Long)	(11.92, 8.43)	Pan (0.45-0.80)
SE (Lat, Long)		

5.2.3. Reference field inventory data

Fieldwork conducted during the 2015-16 dry season provided the reference data for AGB estimation. Fifty square plots (about 50 m × 50 m) were randomly selected for field survey. For every individual tree in a field plot, the height of trees, Diameter at Breast Height (DBH), as well as species identification were noted.

5.3. Methodology

5.3.1. Tree crown delineation in parkland using GEOBIA

In this study tree crown areas were extracted from WV-2 data using Geographic Object Based Image Analysis (GEOBIA) by modifying the method of Bunting and Lucas (2006) which they proposed for tree crown delineation in Australian mixed species forests. Their method was adapted for tree characteristics found in the parklands of Nigeria.

First image objects were created and vegetation areas were masked using an NDVI threshold to separate them from non-vegetation areas (bare soil, settlements and water). The value of NDVI threshold was based on field data of trees. All of the spatially connected objects in the vegetation areas were merged for further analysis. As there were some patches of shrubs and grass in the vegetation masked objects, size and standard deviation of NIR band were used as object features, to exclude patches of shrubs and grasses from the masked vegetation areas. Since the reflectance of a tree crown is derived from both

photosynthetic materials (green leaves) and non-photosynthetic materials (branches), they have high variation in NIR reflectance compared to homogeneous features like patches of background soil, grass and shrubs (Karlson et al., 2014). In next step, we delineated shadows from non-vegetation areas based on thresholding the Blue band, and their relative border with masked vegetation areas, these shadows of individual trees used for separating trees from shrubs. In the next step, multi resolution segmentation was applied to vegetation objects to generate homogeneous objects for subsequent classification into tree crowns. We used field data for defining the scale parameter in multi resolution segmentation according to size of trees, by a trial and error approach. Geometric object features of roundness and elliptical fit were used to identify those objects of vegetation areas approximately circular in shape, to represents individual tree crowns or grouped tree crown clusters. These resulting objects were considered as potential candidates for tree crown delineation in the next step.

A local maxima algorithm was used to identify a pixel within every potential candidate object for tree crown based on NDVI. These pixels are referred as seed pixels, and are assumed to be the top of the tree crown. A region growing process was used to expand the seed into its neighboring pixels based on NDVI and NIR thresholds. The values of NDVI and NIR thresholds were selected based on the difference between seed pixels and adjacent pixels. After completing the first step of the region growing process, a new seed was generated, and expanded into neighboring pixels. These two processes of seed identification and region growing were iterated until a realistic and reasonable form of individual or group of tree crowns was delineated.

As some shrubs were also included in the final tree crown objects, these shrubs were excluded using shadow information, as trees have distinct shadows according to their size and height. The size and relational border between the shadow and tree crown were used as features to separate shrubs from trees. Individual tree crowns were separated from crown clusters using geometric features of roundness, ratio of length to width, elliptical fit and size of objects. Normally individual tree crowns has circular shape with values of roundness

close to zero and relatively small sizes, while crown clusters have elongated shape with high value of roundness and ratio of length to width with large size of object. For crown cluster objects, a morphological watershed segmentation method was applied to separate crown clusters into individual tree crowns based on shape characteristics, and further refinement were made using geometric and contextual information. In the final step, manual editing was performed to remove false detection of tree crowns. Crown cover in percentage was calculated in 50 m grid by cumulating the CA of individual trees divided by size of 50 m grid.

5.3.2. AGB estimation using allometric equations

Tree level above ground biomass (AGB) was calculated using already developed species specific allometric equations. These equations were derived within similar climatic zones as the current study areas (Table 5.2). These allometric equations used height and Diameter at Breast Height (DBH) of trees for calculation of AGB in tons per hectare. In cases, where species specific allometric equations were not available, generalized equations were used from (Mbow et al., 2014, 2013).

The AGB of individual trees lying within a 50 m plot were accumulated to determine the total AGB per 50 m plot.

Table 5.2 Summary of allometric equation used for tree computing tree level AGB, DBH- Diameter at breast height, H – Height of tree.

Tree Species	Input variables	Location	Source
Vitellaria paradoxa, Anogeissus leiocarpus, Parkia biglobosa	DBH	Nigeria	(Jibrin and Abdulkadir, 2015)
Tamarindus indica	DBH	Madagascar	(Ranaivoson et al., 2015)
Balanites aegyptiaca	DBH	Senegal	(Poupon, 1980)
Ceiba pentandra, Diospyros mespiliformis	DBH, H	Benin	(Guendehou et al., 2012)
Faidherbia albida, Piliostigma reticulatum	DBH	Niger	(Larwanou et al., 2010)
Sclerocarya birrea, Commiphora africana	DBH, H	South Africa	(Colgan et al., 2013)
Combretum glutinosum, Combretum micrantum, Entada africana	DBH, H	Burkina Forest	(Sawadogo et al., 2010)
Azadirachta indica	DBH, H	India	(Kumar and Tewari, 1999)
Others	DBH, H	Senegal	(Mbow et al., 2014, 2013)

5.3.3. AGB estimation using CA – Modelling and Validation

A simple linear regression model was used to relate the AGB from field survey plots to the CA derived from WV-2 data. The significant correlation obtained between AGB and crown area allowed modelling of AGB based on crown area. AGB was modelled using simple linear regression, with crown area as the predictor variable. A total of 50 plots was randomly divided into two groups: of 30 (for model training) and 20 (for model testing). Finally the AGB was estimated for the whole WV-2 image over a 50 m grid using the model developed using CA as the predictor variable.

5.4. Results and discussion

For the accuracy assessment of tree crown area delineated using WV-2 data through GEOBIA, an independent reference tree crown area measured during field survey was compared with satellite image based crown area by a linear regression line. A significant value of R^2 of 0.88 was found (Figure 5.2). Tree

crowns delineated using the satellite image tended to underestime the tree crown area measured in the field. This is in line with the findings of Karlson et al (2014) for tree crowns delineated in the parklands of Burkina Faso. Underestimation of small tree crown area from satellite image appears to be affected by the time difference between acquisition of the satellite image (February 02, 2014) and field survey (January 2016), as tree crown may be expected to have grown during about 2 years period between image acquisition and field survey.

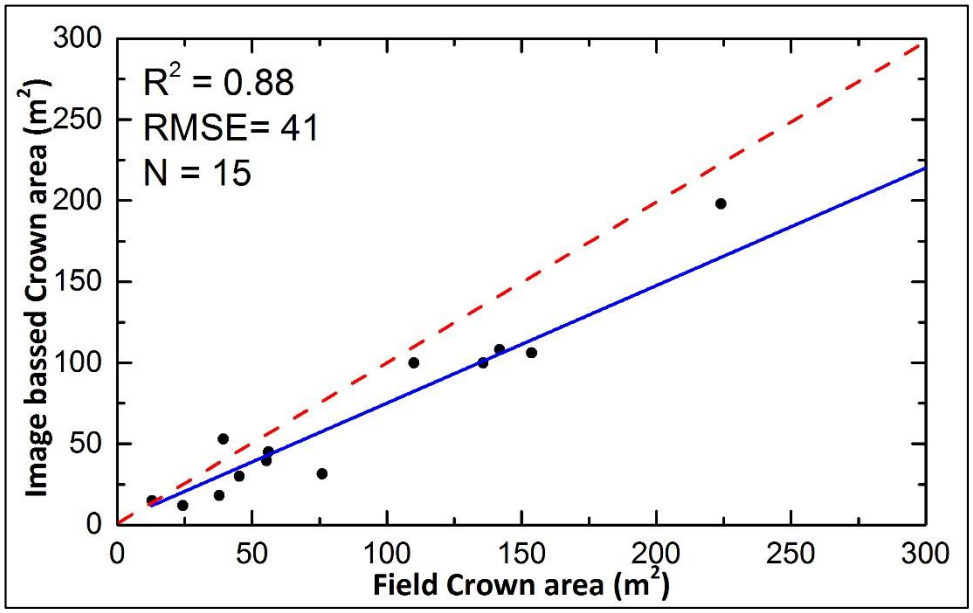

Figure 5.2 Linear correlation between field-based and image-based crown area (m^2).

Figure 5.3 shows results of observed and predicted AGB from linear model for both model training and testing. A good linear relationship was found between observed and predicted AGB ($ton.ha^{-1}$) for both training (left) and training (right) with R^2 values of 0.72 and 0.69 respectively. Finally tree crown area was calculated for the whole area of WV-2 satellite image based on a 50 m grid, and similarly AGB ($ton.ha^{-1}$) was computed for the whole image using crown area extracted from the high resolution WV-2 image as the predictor variable.

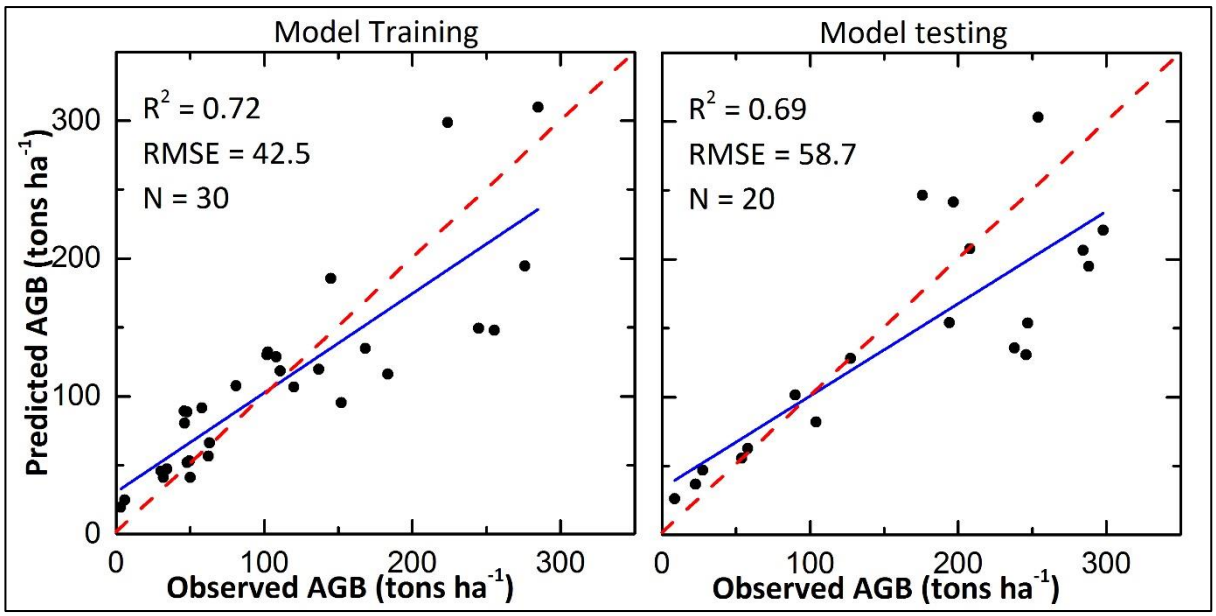

Figure 5.3 Observed versus predicted AGB (ton.ha^{-1}) from a simple linear regression model for model training (left) and model testing (right).

Highest tree cover and AGB are found in the East and NE areas where there are densely populated settlements compared to the sparsely populated western and SE areas (Figure 5.4). This agrees with the findings of Herrmann et al (2013) of highest tree cover in the densely population western portion of Senegal. Highest values of AGB were found in areas where dense Mangoes tree orchards are planted. However, there was overestimation of tree cover in some low lying valley areas where dry season agriculture is common, causing inclusion of some agriculture fields along with the tree crowns, due to similar reflectance.

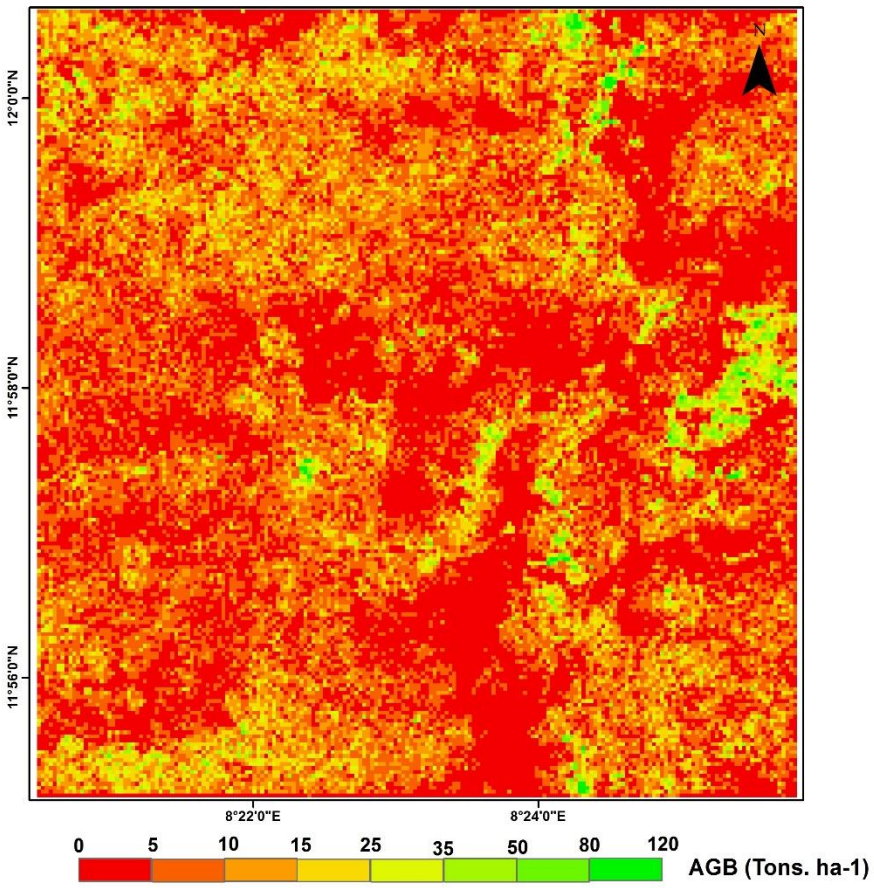

Figure 5.4 Map of above ground biomass in tons per ha estimated using tree crown cover extracted from WV2 satellite image.

5.5. Conclusion

Tree crown mapping using high spatial resolution WV-2 satellite imagery through GEOBIA shows acceptable accuracy and therefore has potential for automated delineation of tree crowns in the agroforestry landscape of the Sudano-Sahelian zone. GEOBIA can be successfully used for tree cover extraction in other similar dryland environments which exist throughout many African savanna regions. However the quality of tree cover extraction depends on many factors, including acquisition time of the satellite imagery, phenology, type of trees, and complexity of the landscape. In our study area of Kano west, a WV-2 imagery was available during the peak dry season when the majority of trees have full leaf, except for *Adansonia digitata*. Although our study area is flat, the accuracy of tree crown extraction could be further increased using tree structure information like Digital Surface Model (DSM) data from LIDAR in areas where agricultural activities during the dry season makes it difficult to discriminate trees from background agricultural fields.

A map of AGB (ton.ha^{-1}) for agroforestry landscape in KCSZ was produced by tree crown area extracted with GEOBIA using a WV-2 satellite imagery. A high value of AGB was observed in areas with densely populated settlements. The proposed method of AGB modelling based on tree crown area can be helpful for locating areas of high and low AGB in drylands of the Sudan zone, and provide a guide to promote integration of different trees species in the agricultural farms. However the cost of high spatial resolution satellite images from commercial satellites along with large volume for processing limits their potential for large geographic areas. Mapping of AGB at high spatial resolution (50 m) provides a baseline for monitoring long term changes due to extreme events like drought in future. It can also be helpful for evaluation of afforestation projects. In addition to the fact that field trees are an integral part of traditional farmed parklands and they have multiple benefits to local people, increasing or maintaining tree cover in agriculture fields will help to strengthen resilience to climate change in the future.

Chapter 06

Summary and Conclusions

Rainfall and its variability drive the rural economies across the Sudano-Sahelian zone of northern Nigeria, where drought strategies largely determine crop yields and woody vegetation productivity. The increasing scarcity of rain gauges in West Africa generally limits assessments of the degree and spatial extent of hardship arising from rainfall deficiency. However, the improved availability and robustness of satellite-based rainfall products since the early 1980s, offers an alternative source of rainfall data which is spatially, and often temporally, more complete than rain gauges.

The consistency between gauge and satellite based derived rainfall variables trends suggest that change in rainfall regime analysis can be done in other similar dryland environments of the world, where rainfall has profound impacts on local livelihoods. The study indicates that after the severe droughts of 1970s and 1980s, both gauge and satellite rainfall showed an increasing rainfall. This increasing rainfall was supported by greening trends over the last 35 years derived using GIMMS 3g NDVI datasets. The increase in annual rainfall is due to increase of length of rainy season, total number of rainy days and extreme rainfall events. The study also indicates that increase in rainfall in the later part of rainy season, especially marked in northern and northeastern states of Nigeria. This is expected to have favourable implications for local subsistence crops, especially sorghum which has lower drought tolerance at the ripening stage.

From a policy point of view, the extended late rainy season may offer farmers flexibility to reduce risk in planting too early, as planting too early would be subject to failure and crop loss if the early rains are not sustained. It may be possible that the increase in the total number of rainy days and consequent reduction in dry spells in recent decades evident from the CHIRPS data, is one factor underlying the vast increase in both urban and rural populations in Kano

region. If so, a return to the drought conditions of earlier decades would be disastrous.

Since satellite rainfall products over northern Nigeria have been shown to be robust, with high accuracies especially for deckadal, monthly and seasonal products, they can be used to evaluate growing conditions, including drought across the northern agricultural regions. This would give insight into potential crop failures and exposure of rural households to economic hardship in the following months. The use of satellite rainfall products at government level would therefore permit early intervention by government and NGOs, given that the droughts of 1972-1974 and 1983-1985 entailed severe food shortages, and loss of human life and livestock (Mortimore, 2000).

As the satellite-based long term NDVI datasets of West Africa have coarse resolution (8 km) and cover heterogeneous land cover types within a single pixel, this study used fine resolution old aerial photographs, recent satellite images and field data. The study of long term trends in tree density and species composition indicated that tree densities in the hinterland of Kano city have at least doubled since drought period, and no decline, rather a slight increase was observed during the drought decades. This contradicts reports of woody vegetation trends from the more arid and less densely populated Sahel zone, which generally observed decline during the drought years and current recovery to pre-drought levels.

Most studies across the West African Sahel zone (Gonzalez et al., 2012) have attributed their observed declining tree density and species composition to climatic change rather than human factors. But in the Sudan zone of northern Nigeria, government energy policies and growing population cause farmers to grow more trees in the farmlands according to their household fuel requirements, as well as for sale. The remarkable increase in tree numbers in Kano region is accompanied by increasing fuelwood production as evidenced from greater concentration by farmers on tree species highly valued for fuel (e.g., *Azadirachta indica*), at the expense of other traditional species. In case of Nigeria, climate is thought to play only a minor role in explaining increasing trends in tree density and fuelwood productivity, rather human factors play a major role.

The observed increase in tree densities in the face of massive population growth, supports work in Kano region over three decades ago (Cline-Cole et al., 1990), which challenged long-held attitudes that farmers caused land degradation through loss of plant productivity. As this study shows, since trees are an integral part of farm livelihoods and the only source of energy for most households it appears inevitable that as population grows, so must the supply of wood fuel to meet increased demand. The study's observations of increased concentration on a few fast-growing species at the expense of a large number of traditional species supplying a wide range of 'free' products is however a cause for concern. The last two decades in northern Nigeria have seen high population growth rates accompanied by high rainfall levels, giving rise to a potential Malthusian situation. Thus in an era of increasing global temperatures which IPCC expects to be above average in arid west Africa, coupled with periodic drought typical of the region, continued dependence on biomass productivity for both food and fuel appears dangerous, given the present high rural population levels.

In the face of changing climate and intensified land use in recent decades that have put increasing pressure on tree cover, automated mapping of the crown cover area of individual trees and biomass, can enable understanding of the viability of the farmed parkland system over large areas, as tree are essential components of the farming system. In this study, the application of GEOBIA to high spatial and spectral resolution WV-2 imagery shows good accuracy (R^2 = 0.88) for automated delineation of tree crown cover. Above Ground Biomass (AGB) at high resolution (50 m) was estimated using crown area with R^2 value of 0.70 and shows pockets of high tree cover in farmlands in and around densely populated rural areas. This further supports our overall conclusion that increase in tree densities is a response to population growth. The proposed method for AGB estimation based on tree crown area can be successfully used in other similar dryland environments. However, tree crown mapping using a single panchromatic band aerial photographs shows unsatisfactory results, because of the inability to distinguish shadows and agricultural fields from the tree canopy using a single band. This would restrict the ability to detect trends in tree canopy

cover and biomass to the last two decades since 2000 when high resolution multispectral satellite images have been available.

In view of the continued intra- and inter-annual rainfall variability across northern Nigeria, and amid rapid rural population growth recently, a return to the rainfall levels of the drought decades, would require informed response at government level, because the majority of rural and urban population in northern Nigeria still rely on wood fuel and agricultural products for basic subsistence. The study suggests that greater use of remote sensing including satellite rainfall estimates, and tree density monitoring, can offer such information, especially since we observed high spatial variability in rainfall distributions and trends, as well as in tree densities. Accurate monitoring of trends in rainfall, crop productivity and tree stocks is now possible using remote sensing datasets, and is potentially executable from Nigeria's Remote Sensing Centre established at Abuja in 1999. Although Nigeria's own satellite NIGERIASAT-2 With 2.5 m for panchromatic (and 5 m for multispectral) spatial, spectral (4 Multispectral bands) and 2 days temporal resolutions may not be capable of providing rainfall and tree density estimates, the rainfall products used in this study are largely free of charge and can be downloaded in near-real time For tree density monitoring across the northern Nigerian states, although the required fine resolution satellite images are expensive, an update every five years would provide the necessary insights into trends in woody biomass.

Appendices

Appendix 1 Field inventoried tree species, families, abundance and their ecological zone.

Tree species	Family	Ecological Zone	Study Area 1 (37 ha)	Study Area 2 (137 ha)	Study Area 3 (60 ha)
Acacia albida	Mimosaceae	Sudan	38	10	8
Acacia nilotica	Mimosaceae	Sahel	14	7	17
Acacia seyal	Mimosaceae	Sahel	6	0	0
Acacia sieberiana	Mimosaceae	Guinea	8	0	6
Acacia senegal	Mimosaceae	Sahel	0	0	3
Adansonia digitata	Bombacaceae	Sudan	94	157	166
Albizia chivalieri	Mimosacea	Sahel	3	0	15
Anacardium occidentali	Anacardiaceae	Sudan	0	0	3
Anogeissus leiocarpus	Combretacea	Guinea	84	51	21
Anona senegalensis	Annonaceae	Guinea	0	1	0
Azadirachta indica	Meliacea	Exotic	236	338	212
Balanites aegyptiaca	Balanitaceae	Sahel	5	3	5
Bauhinia rufescens	Caesalpiniaceae	Sudan	0	1	0
Bombax costatum	Bombacaceae	Guinea	1	0	0
Borassus aethiopum	Arecaceae	Sudan	4	5	16
Boswellia dalzielli	Burseraceae	Sudan	0	24	0
Calotropis procera	Asclepiadaceae	Guinea	3	1	1
Carica papaya	Caricaceae	Guinea	0	2	4
Cassia sieberiana	Caesalpiniaceae	Guinea	0	0	34
Cassia singueana	Leguminosae	Guinea	1	0	0
Ceiba pentandra	Malvaceae	Guinea	16	11	0
Combretum glutinosum	Combretaceae	Sudan	1	11	0
Combretum micranthum	Combretaceae	Sudan	3	2	4
Commiphora africana	Burseraceae	Sahel	8	17	0
Detarium microptera	Caesalpiniaceae	Guinea	2	1	3
Dichrostachys cinerea	Mimosaceae	Sudan	4	0	0
Diospyros mespiliformis	Ebenaceae	Guinea	60	93	65
Entada africana	Mimosaceae	Guinea	7	4	0

Euphorbia kamerunica	Euphorbiaceae	Sahel	0	0	1
Ficus sycomorus	Moraceae	Sudan	6	1	7
Ficus glumosa	Moraceae	Sudan	0	3	0
Ficus iteophylla	Moraceae	Sudan	3	4	1
Ficus platyphylla	Moraceae	Guinea	1	16	1
Ficus polita	Moraceae	Guinea	0	1	0
Ficus populifolia	Moraceae	Sudan	2	0	0
Ficus thonningii	Moraceae	Guinea	15	3	0
Gardenia erubescens	Rubiaceae	Guinea	1	2	0
Hyphaene thebaica	Arecaceae	Sahel	10	9	118
Ipomoea argentaurata	Convolvulaceae	Sudan	1	0	0
Jatropha curcas	Euphorbiaceae	Sudan	1	0	0
Khaya senegalensis	Meliaceae	Guinea	0	0	15
Lannea acida	Anacardiaceae	Guinea	2	19	75
Mangifera indica	Anacardiaceae	Sudan	17	37	7
Moringa oleifera	Moringaceae	Sudan	0	1	7
Parkia biglobosa	Mimosaceae	Guinea	43	435	31
Phoenix dactilifera	Arecaceae	Sahel	1	2	0
Piliostigma reticulatum	Caesalpiniaceae	Sudan	116	114	431
Sclerocarya birrea	Anacardiaceae	Sudan	18	20	10
Steriospermum kunthianum	Bignoniaceae	Guinea	0	1	0
Strychnos spinosa	Loganiaceae	Guinea	0	4	0
Tamarindus indica	Caesalpiniaceae	Sudan	32	50	7
Terminalia macroptera	Combretaceae	Guinea	2	5	0
Viteralleria paradoxa	Sapotaceae	Sudan	19	16	1
Vitex doniana	Verbenaceae	Guinea	8	11	1
Ziziphus spina-cristi	Rhamnaceae	Sudan	3	9	1
Zizyphus mauritiana	Rhamnaceae	Sahel	1	0	0

References

Abdi, A., 2017. Primary production in African drylands: Quantifying supply and demand using earth observation and socio-ecological data. Ph.D. Thesis, Department of Physical Geography and Ecosystem Science, Lund University, Sweden.

Agnew, C.T., 2000. Using the SPI to Identify Drought. Drought Netw. News 12, 6–12.

Ali, A., Lebel, T., 2009. The Sahelian standardized rainfall index revisited. Int. J. Climatol. 29, 1705–1714.

Allen, C.D., Macalady, A.K., Chenchouni, H., Bachelet, D., McDowell, N., Vennetier, M., Kitzberger, T., Rigling, A., Breshears, D.D., Hogg, E.H. (Ted), Gonzalez, P., Fensham, R., Zhang, Z., Castro, J., Demidova, N., Lim, J.H., Allard, G., Running, S.W., Semerci, A., Cobb, N., 2010. A global overview of drought and heat-induced tree mortality reveals emerging climate change risks for forests. For. Ecol. Manage. 259, 660–684. doi:10.1016/j.foreco.2009.09.001

Anyadike, R.N.C., 1993. Seasonal and annual rainfall variations over Nigeria. Int. J. Climatol. 13, 567–580.

Anyamba, A., Tucker, C.J., 2005. Analysis of Sahelian vegetation dynamics using NOAA-AVHRR NDVI data from 1981-2003. J. Arid Environ. 63, 596–614. doi:10.1016/j.jaridenv.2005.03.007

Audu, E., 2013. Fuel wood consumption and desertification in Nigeria. Int. J. Sci. Technol. 3, 1–5.

Bayissa, Y., Tadesse, T., Demisse, G., Shiferaw, A., 2017. Evaluation of Satellite-Based Rainfall Estimates and Application to Monitor Meteorological Drought for the Upper Blue Nile Basin, Ethiopia. Remote Sens. 9, 1–17. doi:10.3390/rs9070669

Behnke, R., Mortimore, M., 2016. The end of desertification? Disputing environmental change in the drylands, Springer Earth System Sciences, London., 560pp.

Blaschke, T., 2010. Object based image analysis for remote sensing. ISPRS J. Photogramm. Remote Sens. 65, 2–16. doi:10.1016/j.isprsjprs.2009.06.004

Blaschke, T., Strobl, J., 2001. What's wrong with pixels? Some recent developments interfacing remote sensing and GIS. GIS - Zeitschrift für Geoinformationssysteme 14, 12–17.

Boffa, J.M., 1999. Agroforestry Parkland in Sub-Saharan Africa: FAO Conservation Guide 34. FAO, Rome.

Bose, M.M., Abdullah, A.M., Kasim, I., Harun, R., Mande, K.H., Abdullahi, A.C., 2015. Rainfall Trend Detection in Northern Nigeria over the Period of 1970-2012. J. Environ. Earth Sci. 5, 94–99.

Brandt, M., Romankiewicz, C., Spiekermann, R., Samimi, C., 2014a. Environmental change in time series - An interdisciplinary study in the Sahel of Mali and Senegal. J. Arid Environ. 105, 52–63. doi:10.1016/j.jaridenv.2014.02.019

Brandt, M., Tappan, G., Diouf, A., Beye, G., Mbow, C., Fensholt, R., 2017. Woody vegetation die off and regeneration in response to rainfall variability in the West African Sahel. Remote Sens. 9, 39. doi:10.3390/rs9010039

Brandt, M., Verger, A., Diouf, A.A., Baret, F., Samimi, C., 2014b. Local vegetation trends in the sahel of mali and senegal using long time series FAPAR satellite products and field measurement (1982-2010). Remote Sens. 6, 2408–2434. doi:10.3390/rs6032408

Buba, L.F., 2010. Evidence of Climate Change in Northern Nigeria: Temperature and Rainfall Variations. Ph.D. Thesis, Bayero University, Kano, Nigeria.

Bunting, P., Lucas, R., 2006. The delineation of tree crowns in Australian mixed species forests using hyperspectral Compact Airborne Spectrographic Imager (CASI) data. Remote Sens. Environ. 101, 230–248. doi:10.1016/j.rse.2005.12.015

Capecchi, V., Crisci, A., Lorenzo, G., Maselli, F., Vignaroli, P., 2008. Analysis of NDVI trends and their climatic origin in the Sahel 1986–2000. Geocarto Int. 23, 297–310. doi:10.1080/10106040801950492

Cline-Cole, R., 1998. Knowledge claims and landscapes: alternative views of thefuelwood-degradation nexus in northern Nigeria. Environ. Plan. D Soc. Sp. 16, 311–346. https://doi.org/10.1068/d160311

Chidumayo, E.N., Gumbo, D.J., 2010. The dry forests and woodlands of Africa: Managing for products and services, Earth Scan. doi:10.4324/9781849776547

Cline-Cole, R., Maconachie, R., 2016. Wood energy interventions and development in Kano, Nigeria: A longitudinal, "situated" perspective. Land Use Policy 52, 163–173. doi:10.1016/j.landusepol.2015.11.014

Colgan, M.S., Asner, G.P., Swemmer, T., 2013. Harvesting tree biomass at the stand level to assess the accuracy of field and airborne biomass estimation in savannas. Ecol. Appl. 23, 1170–1184. doi:10.1890/12-0922.1

Condit, R., Sukumar, R., Hubbell, S., Foster, R.B., 1998. Predicting population trends from size distributions : a direct test in a tropical tree community. Am. Nat. 152, 495–509. doi:10.1086/286186

Dai, A., Lamb, P.J., Trenberth, K.E., Hulme, M., Jones, P.D., Xie, P., 2004. The recent Sahel drought is real. Int. J. Climatol. 24, 1323-1331.

Dembélé, M., Zwart, S.J., 2016. Evaluation and comparison of satellite-based rainfall products in Burkina Faso, West Africa. Int. J. Remote Sens. 37, 3995–4014. doi:10.1080/01431161.2016.1207258

Diouf, A.A., Brandt, M., Verger, A., El Jarroudi, M., Djaby, B., Fensholt, R., Ndione, J.A., Tychon, B., 2015. Fodder biomass monitoring in Sahelian rangelands using phenological metrics from FAPAR time series. Remote Sens. 7, 9122–9148. doi:10.3390/rs70709122

Dong, J., Kaufmann, R.K., Myneni, R.B., Tucker, C.J., Kauppi, P.E., Liski, J., Buermann, W., Alexeyev, V., Hughes, M.K., 2003. Remote sensing estimates

of boreal and temperate forest woody biomass: Carbon pools, sources, and sinks. Remote Sens. Environ. 84, 393–410. doi:10.1016/S0034-4257(02)00130-X

Etkin, N.L., 2002. Local knowledge of biotic diversity and its conservation in rural Hausaland, northern Nigeria. Econ. Bot. 56 (1), 73–88. https://doi.org/10.1663/0013-0001(2002)056[0073:lkobda]2.0.co;2

Falake, A.A., Akangbe, J.A., Iyilade, A.O and Olowosegun, T., 2010. Small scale farmers' perception and adaptation to climate change in Nasarawa state, Ngeria. Agrosearch 11, 49–61. https://doi.org/Http://dx.doi.org/10.4314/agrosh.v11i1.6

Fensholt, R., Sandholt, I., Rasmussen, M.S., Stisen, S., Diouf, A., 2006. Evaluation of satellite based primary production modelling in the semi-arid Sahel. Remote Sens. Environ. 105, 173–188. doi:10.1016/j.rse.2006.06.011

Fink, A.H., Schrage, J.M., Kotthaus, S., 2010. On the Potential Causes of the Nonstationary Correlations between West African Precipitation and Atlantic Hurricane Activity. J. Clim. 23, 5437–5456. doi:10.1175/2010JCLI3356.1

Fitzpatrick, R.G.J., Bain, C.L., Knippertz, P., Marsham, J.H., Parker, D.J., 2015. The West African monsoon onset: A concise comparison of definitions. J. Clim. 28, 8673–8694. doi:10.1175/JCLI-D-15-0265.1

Funk, C., Peterson, P., Landsfeld, M., Pedreros, D., Verdin, J., Shukla, S., Husak, G., Rowland, J., Harrison, L., Hoell, A., Michaelsen, J., 2015. The climate hazards infrared precipitation with stations—a new environmental record for monitoring extremes. Sci. Data 2, 150066. doi:10.1038/sdata.2015.66

Geonames, 2017. http://www.geonames.org/2335204/kano.htm. Accessed May, 2017

Gonzalez, P., Tucker, C.J., Sy, H., 2012. Tree density and species decline in the African Sahel attributable to climate. J. Arid Environ. 78, 55–64. doi:10.1016/j.jaridenv.2011.11.001

Guendehou, G., Lehtonen, A, Moudachirou, M., Mäkipää, R., Sinsin, B., 2012. Stem biomass and volume models of selected tropical tree species in West Africa. South. For. a J. For. Sci. 74, 77–88. doi:10.2989/20702620.2012.701432

Hall, A., Bohen, C., 2009. A review of malnuutrtition in Nigeria and potential role of homestead agriculture to imporove the nutritional status and income of poor rural people.

Hänke, H., Börjeson, L., Hylander, K., Enfors Kautsky, E., 2016. Drought tolerant species dominate as rainfall and tree cover returns in the West African Sahel. Land Use Policy 59, 111–120. doi:10.1016/j.landusepol.2016.08.023

Hazewinkel, M., 2001, Affine transformation, Encyclopedia of Mathematics, Springer.

Henry, M., Picard, N., Trotta, C., Manlay, R.J., Valentini, R., Bernoux, M., Saint-Andre, L., 2011. Estimating tree biomass of sub-saharan african forests: a reveiw of availbe allometric equations. Silva Fenn. 45, 447–569. doi:10.1055/s-2002-20437

Hess, T.M., Stephens, W., Maryah, U.M., 1995. Rainfall trends in the North East Arid Zone of Nigeria 1961-1990. Agric. For. Meteorol. 74, 87–97. doi:10.1016/0168-1923(94)02179-N

Herrmann, S.M., Hutchinson, C.F., 2005. The changing contexts of the desertification debate. J. Arid Environ. 63, 538–555. doi:10.1016/j.jaridenv.2005.03.003

Herrmann, S.M., Tappan, G.G., 2013. Vegetation impoverishment despite greening: A case study from central Senegal. J. Arid Environ. 90, 55–66. doi:10.1016/j.jaridenv.2012.10.020

Hiernaux, P., Diarra, L., Trichon, V., Mougin, E., Soumaguel, N., Baup, F., 2009. Woody plant population dynamics in response to climate changes from 1984 to 2006 in Sahel (Gourma, Mali). J. Hydrol. 375, 103–113. doi:10.1016/j.jhydrol.2009.01.043

Hirsch, R.M., Slack, J.R., Geological, U.S., 1984. A Nonparametric Trend Test for Seasonal Data With Serial Dependenc 20, 727–732.

Horion, S., Fensholt, R., Tagesson, T., Ehammer, A., 2014. Using earth observation-based dry season NDVI trends for assessment of changes in tree cover in the Sahel. Int. J. Remote Sens. 35, 2493–2515. doi:10.1080/01431161.2014.883104

Huffman, G.J., Bolvin, D.T., Nelkin, E.J., Wolff, D.B., Adler, R.F., Gu, G., Hong, Y., Bowman, K.P., Stocker, E.F., 2007. The TRMM Multisatellite Precipitation Analysis (TMPA): Quasi-Global, Multiyear, Combined-Sensor Precipitation Estimates at Fine Scales. J. Hydrometeorol. 8, 38–55. doi:10.1175/JHM560.1

Hulme, M., 1992. Rainfall changes in Africa: 1931–1960 to 1961–1990. Int. J. Climatol. 12, 685–699. doi:10.1002/joc.3370120703

Hulme, M., Doherty, R., Ngara, T., New, M., Lister, D., 2001. African climate change: 1900-2100. Climate Research 17, 145-168.

Immitzer, M., Atzberger, C., Koukal, T., 2012. Tree species classification with Random forest using very high spatial resolution 8-band worldView-2 satellite data. Remote Sens. 4, 2661–2693. doi:10.3390/rs4092661

Ingram, K.T., Roncoli, M.C., Kirshen, P.H., 2002. Opportunities and constraints for farmers of west Africa to use seasonal precipitation forecasts with Burkina Faso as a case study. Agric. Syst. 74, 331–349. doi:10.1016/S0308-521X(02)00044-6

IPCC, 2014. Climate Change 2014 Impacts, Adaptation, and Vulnerability Part B: Regional Aspects. Contribution of Working Group II to the Fifth Assessment Report of the Intergovernmental Panel on Climate Change. Cambridge, United Kingdom and New York, NY, USA. doi: 10.1007/s13398-014-0173-7.2

Jibrin, A., Abdulkadir, A., 2015. Allometric Models for Biomass Estimation in Savanna Woodland Area, Niger State, Nigeria. Int. J. Environ. Chem. Ecol. Geol. Geophys. Eng. 9, 270–278.

Jönsson, P., Eklundh, L., 2004. TIMESAT - a program for analysing time-series of satellite sensor data. Computers and Geosciences, 30, 833-845.

Karlson, M., Reese, H., Ostwald, M., 2014. Tree crown mapping in managed woodlands (Parklands) of semi-arid West Africa using WorldView-2 imagery and geographic object based image analysis. Sensors (Switzerland) 14, 22643–22669. doi:10.3390/s141222643

Karlson, M., Ostwald, M., Reese, H., Sanou, J., Tankoano, B., Mattsson, E., 2015. Mapping tree canopy cover and aboveground biomass in Sudano-Sahelian woodlands using Landsat 8 and random forest. Remote Sens. 7, 10017–10041. doi:10.3390/rs70810017

Karlson, M., Ostwald, M., 2016. Remote sensing of vegetation in the Sudano-Sahelian zone: A literature review from 1975 to 2014. J. Arid Environ. 124, 257–269. doi:10.1016/j.jaridenv.2015.08.022

Kershaw, K.A.,1974. Quantitative and dynamic plant ecology, Elsevier, 308pp.

Knauer, K., Gessner, U., Dech, S., Kuenzer, C., 2014. Remote sensing of vegetation dynamics in West Africa. Int. J. Remote Sens. 35, 6357–6396. doi:10.1080/01431161.2014.954062

Kumar, V.S.K., Tewari, V.P., 1999. Above ground biomass tables for Azadirachta indica A. juss. Int. For. Rev. 1, 109–111.

Lal, R., 2004. Carbon sequestration in dryland ecosystems. Environ. Manage. 33, 528–544. doi:10.1007/s00267-003-9110-9

Laliberte, A.S., Rango, A., Havstad, K.M., Paris, J.F., Beck, R.F., McNeely, R., Gonzalez, A.L., 2004. Object-oriented image analysis for mapping shrub encroachment from 1937 to 2003 in southern New Mexico. Remote Sens. Environ. 93, 198–210. doi:10.1016/j.rse.2004.07.011

Lamb, P.J., 1982. Persistence of Subsaharan drought. Nature 299, 46–48.

Lamprey, H.F., 1988. Report on desert encroachment reconnaissance in Northern Sudan. Desertification Control Bull. 17, 1-7.

Larwanou, M., Yemshaw, Y., Saadou, M., 2010. Prediction models for estimating foliar and fruit dry biomasses of five Savannah tree species in the West African Sahel. Int. J. Biol. Chem. Sci. 4, 2245–2256. doi:10.4314/ijbcs.v4i6.64943

Lykke, A.M., 1998. Assessment of species composition change in savanna vegetation by means of woody plants' size class distributions and local information. Biodivers. Conserv. 7, 1261–1275. doi:10.1023/A:1008877819286

Maconachie, R.A., Binns, T., 2006. Sustainability Under Threat ? the Dynamics of Environmental Change and Food Production in Peri-Urban Kano, Northern Nigeria 171, 159–171.

Maconachie, R., Tanko, A., Zakariya, M., 2009. Descending the energy ladder? Oil price shocks and domestic fuel choices in Kano, Nigeria. Land Use Policy 26, 1090–1099. doi:10.1016/j.landusepol.2009.01.008

Machonachie, R., 2013. Urban pressure and tree cover. Chapter 26 in A.I. Tanko and S.B. Momale (eds) Geography of the Kano Region, Adonis and Abbey publishers, UK., 551pp.

Maidment, R.I., Grimes, D.I.F., Allan, R.P., Greatrex, H., Rojas, O., Leo, O., 2013. Evaluation of satellite-based and model re-analysis rainfall estimates for Uganda. Meteorol. Appl. 20, 308–317. doi:10.1002/met.1283

Maidment, R.I., Grimes, D., Allan, R.P., Tarnavsky, E., Stringer, M., Hewison, T., Roebeling, R., Black, 2014. The 30 year TAMSAT African Rainfall Climatology And Time series (TARCAT) data set. J. Geophys. Res. Atmos. 119, 10619–10644. doi:10.1002/2014JD021927.

Mbow, C., Chhin, S., Sambou, B., Skole, D., 2013. Potential of dendrochronology to assess annual rates of biomass productivity in savanna trees of West Africa. Dendrochronologia 31, 41–51. doi:10.1016/j.dendro.2012.06.001

Mbow, C., Verstraete, M.M., Sambou, B., Diaw, A.T., Neufeldt, H., 2014. Allometric models for aboveground biomass in dry savanna trees of the Sudan and

Sudan-Guinean ecosystems of Southern Senegal. J. For. Res. 19, 340–347. doi:10.1007/s10310-013-0414-1

McDonald, R.A., 1995. CORONA: success for space reconnaissance, a look into the Cold War, and a revolution for intelligence. Photogramm. Eng. Remote Sens. 61, 689–720.

Mishra, N.B., Crews, K.A., Neeti, N., Meyer, T., Young, K.R., 2015. MODIS derived vegetation greenness trends in African Savanna: Deconstructing and localizing the role of changing moisture availability, fire regime and anthropogenic impact. Remote Sens. Environ. 169, 192–204. doi:10.1016/j.rse.2015.08.008

Mortimore, M., 2000. Profile of rainfall change and variability in the Kano-Maradi region, 1960–2000, Drylands Research Working Paper 25, Drylands Research, Crewkerne, Somerset.

Mortimore, M.J., Adams, W.M., 2001. Farmer adaptation, change and crisis in the Sahel. Glob. Environ. Chang. 11, 49–57. doi:10.1016/S0959-3780(00)00044-3

Mortimore, M., Wilson, J., 1965. Land and people in the Kano close-settled zone; a survey of some aspects of rural economy in the Ungogo District, Kano Province: A report to the Greater Kano Planning Authority.

Naibbi, A.I., Healey, R.G., 2013. Northern Nigeria's Dependence on Fuelwood: Insights from Nationwide Cooking Fuel Distribution Data. Int. J. Humanit. Soc. Sci. 3, 160–173.

National Bureau of Statistics, 2011. Annual Abstract of Statistics. Published by the Federal Republic of Nigeria, Table 111.

National Population Commission, 2006. Federal Republic of Nigeria 2006 Population and Housing Census, Priority Tables Vol. VII, Abuja, Nigeria.

Nicholson, S.E., 2000. The nature of rainfall variability over Africa on time scales of decades to millenia. Glob. Planet. Change 26, 137–158. doi:10.1016/S0921-8181(00)00040-0

Nichol, J.E., 1989. Ecology of fuelwood production in Kano, Northern Nigeria. J. Arid Environ. 16, 347–360.

Novella, N.S., Thiaw, W.M., 2013. African rainfall climatology version 2 for famine early warning systems. J. Appl. Meteorol. Climatol. 52, 588–606. doi:10.1175/JAMC-D-11-0238.1

Olaniran, O.J., 1991. Evidence of climatic change in Nigeria based on annual series of rainfall of different daily amounts, 1919-1985. Clim. Change 19, 319–340. doi:10.1007/BF00140169

Olaniran, O.J., 1988. The distribution in space of rain-days of rainfall of different amounts in the tropics: Nigeria as a case study. Geoforum 19, 507–520. doi:10.1016/S0016-7185(88)80021-6

Olsson, L., Eklundh, L., Ardö, J., 2005. A recent greening of the Sahel - Trends, patterns and potential causes. J. Arid Environ. 63, 556–566. doi:10.1016/j.jaridenv.2005.03.008

Omotosho, J.B., Balogun, A.A., Ogunjobi, K., 2000. Predicting monthly and seasonal rainfall, onset and cessation of the rainy season in West Africa using only surface data. Int. J. Climatol. 20, 865–880. doi:10.1002/1097-0088(20000630)20:8<865::AID-JOC505>3.0.CO;2-R

Padwick, C., Scientist, P., Deskevich, M., Pacifici, F., Smallwood, S., 2010. WorldView-2 pan-sharpening, in: ASPRS 2010. pp. 26–30.

Poupon, H. Structure et Dynamique de la Strate Ligneuse d'une Steppe Sahélienne au Nord du Sénégal; ORSTOM: Paris, France, 1980; p. 351.

Qazi, W.A., Baig, S., Gilani, H., Waqar, M.M., Dhakal, A., Ammar, A., 2017. Comparison of forest aboveground biomass estimates from passive and active remote sensing sensors over Kayar Khola watershed, Chitwan district, Nepal. J. Appl. Remote Sens. 11, 26038. doi:10.1117/1.JRS.11.026038

Ranaivoson, T., Brinkmann, K., Rakouth, B., Buerkert, A., 2015. Distribution, biomass and local importance of tamarind trees in south-western

Madagascar. Glob. Ecol. Conserv. 4, 14–25. doi:10.1016/j.gecco.2015.05.004

Rasmussen, M.O., Göttsche, F.M., Diop, D., Mbow, C., Olesen, F.S., Fensholt, R., Sandholt, I., 2011. Tree survey and allometric models for tiger bush in northern Senegal and comparison with tree parameters derived from high resolution satellite data. Int. J. Appl. Earth Obs. Geoinf. 13, 517–527. doi:10.1016/j.jag.2011.01.007

Salmi, T., Maatta, A., Anttila, P., Ruoho-Airola, T., Amnell, T., 2002. Detecting Trends of Annual Values of Atmospheric Pollutants by the Mann-Kendall Test and Sen's Solpe Estimates the Excel Template Application MAKESENS, Finnish Meteorological Institute, Air Quality Research.

Sanogo, S., Fink, A.H., Omotosho, J.A., Ba, A., Redl, R., Ermert, V., 2015. Spatio-temporal characteristics of the recent rainfall recovery in West Africa. Int. J. Climatol. 35, 4589–4605. doi:10.1002/joc.4309

Sarker, L.R., Nichol, J.E., 2011. Improved forest biomass estimates using ALOS AVNIR-2 texture indices. Remote Sens. Environ. 115, 968–977. doi:10.1016/j.rse.2010.11.010

Sawadogo, L., Savadogo, P., Tiveau, D., Dayamba, S.D., Zida, D., Nouvellet, Y., Oden, P.C., Guinko, S., 2010. Allometric prediction of above-ground biomass of eleven woody tree species in the Sudanian savanna-woodland of West Africa. J. For. Res. 21, 475–481. doi:10.1007/s11676-010-0101-4

Schucknecht, A., Meroni, M., Kayitakire, F., Boureima, A., 2017. Phenology-Based Biomass Estimation to Support Rangeland Management in Semi-Arid Environments. Remote Sens. 9, 463. doi:10.3390/rs9050463

Seetharama, N., Mahalakshmi,V., Bidinger, F.R., Singh, S., 1984. Response of sorghum and millet to drought stress in semi-arid India. ICRISAT (International Crops Research Institute for the Semi-Arid Tropics). 1984 Agrometeorology of Sorghum and Millet in the Semi-Arid Tropics: Proceedings of the International Symposium, 15-20 Nov 1982, ICRISAT Center, India. Patancheru, A.P. 502324, India: ICRISAT.

Sen, P.K., 1968. Estimates of the regression coefficient based on Kendall's tau. J. Am. Stat. Assoc. 63, 1379-1389.

Sivakumar, M.V.K., 1988. Predicting rainy season potential from the onset of rains in Southern Sahelian and Sudanian climatic zones of West Africa. Agric. For. Meteorol. 42, 295–305. doi:10.1016/0168-1923(88)90039-1

Spiekermann, R., Brandt, M., Samimi, C., 2015. Woody vegetation and land cover changes in the Sahel of Mali (1967-2011). Int. J. Appl. Earth Obs. Geoinf. 34, 113–121. doi:10.1016/j.jag.2014.08.007

Tappan, G.G., Sall, M., Wood, E.C., Cushing, M., 2004. Ecoregions and land cover trends in Senegal. J. Arid Environ. 59, 427–462. doi:10.1016/j.jaridenv.2004.03.018

Tarhule, A., Woo, M., 1998. Changes in rainfall characteristics in northern Nigeria. Int. J. Climatol. 18, 1261–1271. doi:10.1002/(SICI)1097-0088(199809)18:11<1261::AID-JOC302>3.3.CO;2-Q

Tarnavsky, E., Grimes, D., Maidment, R., Black, E., Allan, R.P., Stringer, M., Chadwick, R., Kayitakire, F., 2014. Extension of the TAMSAT satellite-based rainfall monitoring over Africa and from 1983 to present. J. Appl. Meteorol. Climatol. 53, 2805–2822. doi:10.1175/JAMC-D-14-0016.1

Thiemig, V., Rojas, R., Zambrano-Bigiarini, M., Levizzani, V., De Roo, A., Thiemig, V., Rojas, R., Zambrano-Bigiarini, M., Levizzani, V., Roo, A. De, 2012. Validation of Satellite-Based Precipitation Products over Sparsely Gauged African River Basins. J. Hydrometeorol. 13, 1760–1783. doi:10.1175/JHM-D-12-032.1

Thomas, N., Hendrix, C., Congalton, R.G., 2003. A Comparison of Urban Mapping Methods Using High-Resolution Digital Imagery. Photogramm. Eng. Remote Sens. 69, 963–972. doi:10.14358/PERS.69.9.963

Thornton, P., Jones, P., Owiyo, T., Kruska, R., Herrero, M., Kristjanson, P., Notenbaert, a, Bekele, N., Omolo, a, 2006. Mapping climate vulnerability and poverty in Africa. Rep. to Dep. Int. Dev. ILRI PO Box 30709, 171. doi:http://www.dfid.gov.uk/research/climate-change.asp.

Tiffen, M., 2001. Profile of demographic change in the Kano-Maradi region, 1960–2000, Drylands Research Working Paper 24.

Timberlake, J., Chidumayo, E., Sawadogo, L., 2010. Distribution and Characteristics of African Dry Forests and Woodlands, The dry forests and woodlands of Africa: Managing for products and services. doi:10.4324/9781849776547

Tomlinson, J., 2010. Observed trends in rainfall: northern Nigeria, Miscellaneous Report to the British Hydrological Society, 2010, 12pp.

Tomomatsu, Y., 2014. Parkia biglobosa-dominated cultural landscape: an ethnohistory of the Dagomba political institution in farmed parkland of northern Ghana. J. Ethnobiol. 34(2), 153-174. https://doi.org/10.2993/0278-0771-34.2.153

Toté, C., Patricio, D., Boogaard, H., van der Wijngaart, R., Tarnavsky, E., Funk, C., 2015. Evaluation of satellite rainfall estimates for drought and flood monitoring in Mozambique. Remote Sens. 7, 1758–1776. doi:10.3390/rs70201758

Tucker, C.J., 1979. Red and photographic infrared linear combinations for monitoring vegetation. Remote Sens. Environ. 8, 127–150

UNEP, 2007. Freshwater Resources, Sudan Post-Conflict Environmental Assessment.

UNICEF, 2014. Generation 2030|Africa, IGARSS 2014. doi:10.1007/s13398-014-0173-7.2

Vincke, C., Diédhiou, I., Grouzis, M., 2010. Long term dynamics and structure of woody vegetation in the Ferlo (Senegal). J. Arid Environ. 74, 268–276. doi:10.1016/j.jaridenv.2009.08.006

West, P.W., 2009. Tree and Forest Measurement, 2nd edition. Springer-Verlag Berlin Heidelberg, Germany.

West, C.T., Roncoli, C., Ouattara, F., 2008. Local perceptions and regional climate trends of the Central Plateau of Burkina Faso. L. Degrad. Dev. 20, 587–588.

Westra, S., Alexander, L. V., Zwiers, F.W., 2013. Global increasing trends in annual maximum daily precipitation. J. Clim. 26, 3904–3918. doi:10.1175/JCLI-D-12-00502.1

Zhang, W., Brandt, M., Guichard, F., Tian, Q., Fensholt, R., 2017. Using long-term daily satellite based rainfall data (1983–2015) to analyze spatio-temporal changes in the Sahelian rainfall regime. J. Hydrol. 550, 427–440. doi:10.1016/j.jhydrol.2017.05.033

Zhu, X., Liu, D., 2015. Improving forest aboveground biomass estimation using seasonal Landsat NDVI time-series. ISPRS J. Photogramm. Remote Sens. 102, 222–231. doi:10.1016/j.isprsjprs.2014.08.014